

R-98-59

Partitioning and transmutation

Annual report 1998

Å Enarsson, A Landgren, J-O Liljenzin, L Spjuth

Department of Nuclear Chemistry
Chalmers University of Technology

December 2007

Svensk Kärnbränslehantering AB

Swedish Nuclear Fuel
and Waste Management Co
Box 5864

SE-102 40 Stockholm Sweden

Tel 08-459 84 00
+46 8 459 84 00

Fax 08-661 57 19
+46 8 661 57 19



Partitioning and transmutation

Annual report 1998

Å Enarsson, A Landgren, J-O Liljenzin, L Spjuth

Department of Nuclear Chemistry
Chalmers University of Technology

December 1998

This report concerns a study which was conducted for SKB. The conclusions and viewpoints presented in the report are those of the author(s) and do not necessarily coincide with those of the client.

CONTENTS

	Page
1. INTRODUCTION	3
2. SOLVENT EXTRACTION RESEARCH	3
2.1 Oligopyridines and triazines	3
2.2 Malonamides	6
2.3 Redox kinetics of tetravalent actinides	8
3. COLLABORATIONS	9
4. MEETINGS AND LECTURES	10
5. REFERENCES	11

APPENDICES

Articles/Reports

- I L. Spjuth, J.O. Liljenzin, M. Skålberg, M.J. Hudson, G.Y.S. Chan, M.G.B. Drew, M. Feaviour and C. Madic, "Coextraction of Actinides and Lanthanides from Nitric Acid Solution by Malonamides", *Radiochimica Acta*, 78, 39-46, 1997
- II Jonas Halvarsson "Extraction and Synthesis of a Dipyrityltriazine", *Diploma Thesis, Department of Nuclear Chemistry, Chalmers University of Technology, April 1998*
- III Å. Enarsson, A. Landgren, J.O. Liljenzin, M. Skålberg, and L. Spjuth, Progress report on "Partitioning Experiments and Waste Minimisation", *Contract NEWPART (FI41-CT-96-0010), May 1998*
- IV M.G.B. Drew, M.J. Hudson, P.B. Iveson, M.L. Russell, J.O. Liljenzin, M. Skålberg, L. Spjuth and C. Madic "Theoretical and experimental studies of the protonated terpyridine cation. Ab initio quantum mechanics calculations, and crystal structures of two different ion pairs formed between protonated terpyridine cations and nitratolanthanate(III) anions", *J. Chem. Soc. Dalton Trans.*, 2973, 1998
- V G. Källvenius, J.O. Liljenzin, and L. Spjuth, Progress report on "Partitioning Experiments and Waste Minimisation", *Contract NEWPART (FI41-CT-96-0010), November 1998*
- VI G. Källvenius, "Basicity and Extraction Studies of Ligands for Actinide/Lanthanide Separation", *Diploma Thesis, Department of Nuclear Chemistry, Chalmers University of Technology, November 1998*

Travelling Reports

- VII UK Macrocyclic and Supramolecular Chemistry Group Conference, Nottingham, January 5-6, 1998.
- VIII Visit to Reading January 4 - March 31, 1998

1. INTRODUCTION

The research on partitioning and transmutation at the Department of Nuclear Chemistry, Chalmers, is focused on separation of actinides from spent nuclear fuel using solvent extraction. An efficient separation of actinides from fission products is necessary prior to transmutation to avoid parasitic neutron absorption by the fission products. This would otherwise cause a low transmutation rate.

There is no “supermolecule” known today that can extract all elements intended for transmutation in one single step from high nitric acid concentration. Instead, the actinides and lanthanides are considered to be coextracted in a first step, from high nitric acid concentration. The extracted elements are thereafter stripped back to an aqueous solution of low nitric acid concentration whereafter the separation of trivalent actinides and lanthanides is performed at this lower nitric acid concentration.

Extractants for both actinide extraction and trivalent actinide/lanthanide separation are studied at Chalmers. A criteria for these extractants is that they should only contain the elements carbon (C), hydrogen (H), oxygen (O) and nitrogen (N), the so called CHON-principle, to be completely incinerable and don't contribute to the secondary waste.

2. SOLVENT EXTRACTION RESEARCH

2.1 Oligopyridines and triazines

It has been shown that extractants that coordinate to the metal ion with a nitrogen atom have a higher selectivity for trivalent actinides over lanthanides than extractants that coordinate with an oxygen atom. Several new nitrogen-containing extractants has therefore been studied in order to achieve the best separation between actinides and lanthanides at as high nitric acid concentration as possible. An optimal molecular structure is still not found so many different structures are being tested to get information about their separation ability, e.g. oligopyridines and substituted triazines.

Terpyridine, which is commercially available, has been used as a reference molecule in synergy with 2-bromodecanoic acid (HA) in *tert*-butylbenzene to learn more about the synergistic extraction mechanism with these group of extractants. It was shown that there is a maximum in metal extraction at intermediate concentrations of HA when the concentration of terpyridine was held constant, see Figure 1. Too much HA decreases the metal extraction, but on the other hand, the separation factor show a steady increase when the concentration of HA is increased implying that a very high ratio between HA and terpyridine concentrations are needed to achieve the best separation.

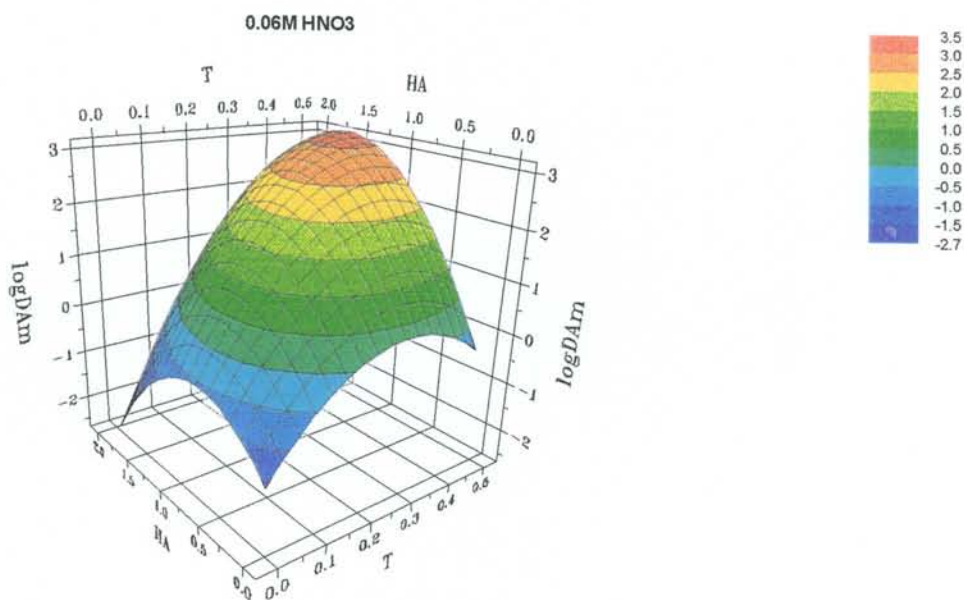
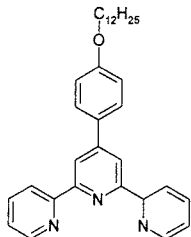
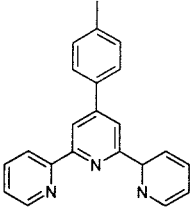
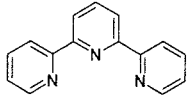
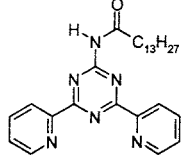
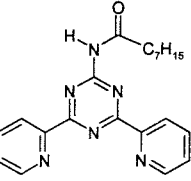
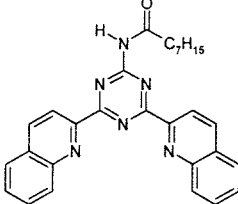
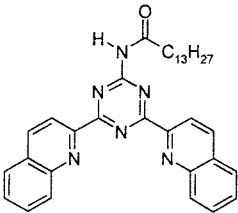


Figure 1. Extraction of Am(III) with different concentrations of terpyridine (T) and 2-bromodecanoic acid (HA) in *tert*-butylbenzene from 0.06M HNO₃ (PLS model used).

Since protons and metal cations are competing for the same binding site in the extractant, the basicity of the extractant is important. A low basicity of an extractant gives a higher metal extraction because the protonation is less severe than for a more basic ligand, at a certain pH. The basicities of different extractants were determined by titration in acetonitrile media in order to study the effect of basicity on the metal extraction. The method has previously been used for titration of amines [1]. The HNP, the potential at the half-neutralisation volume, was used as a measure for basicity. The higher the HNP, the lower the basicity. The relative order of basicity was basically in the same order as the metal extraction ability; the lower the basicity the better the metal extraction (Table 1), except for the quinolinyl-derivatives (OADQTZ and TADQTZ) which showed the lowest basicity but also the lowest metal extraction (D-values less than 1). Molecular modelling showed that the bulky quinolinyl-groups induce a strain in the molecule which inhibit co-ordination to the metal cation. However, the separation factor doesn't seem to be influenced by the basicity. The method for measuring basicity will be used for new ligands to verify the relation between metal extraction and basicity.

M.Sc. student Jonas Halvarsson finished his diploma work in April 1998. His work concerned synthesis and extraction studies of a dipyridyltriazine (Appendix II). A second M.Sc. student, Göran Källvenius, studied the extraction and basicity of ligands for separation of trivalent actinides and lanthanides and his diploma work was finished in November 1998 (Appendix VI).

Table 1. Extraction with 0.02M oligopyridine/1M HA in TBB from 0.01M HNO₃. Basicity (HNP) measured by titration in acetonitrile.

Extractant	Name	HNP(mV)	D _{Am(III)}	SF
	Dodoxy	137±2	4.2	7.7
	Tolpy	143±1	2.8	8.3
	Terpy	154±3	13	7.2
	TADPTZ	195±1	359	7.5
	OADPTZ	198±1	287	10
	OADQTZ	233±3	0.09	3.5
	TADQTZ	234±3	0.16	3.0

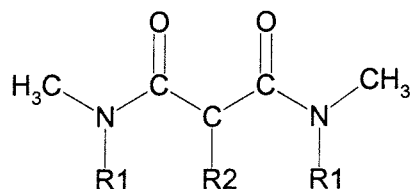
2.2 Malonamides

Malonamides have been suggested as the extractant used in the DIAMEX-process for co-extraction of actinides and lanthanides in an advanced reprocessing process prior to transmutation. To be able to understand the extraction mechanism with these extractants, the chemical behaviour must be thoroughly investigated. It has previously been shown that both the structure of the malonamide molecule and the electroinductive effects around the binding site are important factors for the metal extraction.

A study of how the basicity of the malonamides influence the metal extraction was performed and *ab initio* methods were used in order to investigate if the relative order of basicity could be calculated accurately. As mentioned earlier, a low basicity is considered to give a high metal extraction. The basicity was determined by titration with HClO₄ in acetic acid using acetonitrile as the titration media. The higher the HNP (half-neutralisation potential) the lower the basicity. The listed HNP-values in Table 2 are ordered from the least basic to the most basic molecule and as can be seen, the 4-chlorophenyl- and phenyl substituted malonamide are the least basic molecules. They also show the highest metal extraction, Figure 2. The butyl- and cyclohexyl substituted malonamides have the highest basicity and as seen in Figure 2 they show a decrease in metal extraction at high nitric acid concentration as a result of the competition between metal ions and protons. The malonamides which have an alkoxy-group substituted on the central carbon chain show lower basicity than the malonamides substituted with alkyl groups on the central carbon if they have the same nitrogen substituents.

Table 2. The basicity (HNP) of the different malonamides investigated.

R ₁	R ₂	Ligand	HNP(mV)
4-chlorophenyl	-C ₁₄ H ₂₉	DMDCIPHTDMA	529±6
phenyl	-C ₁₄ H ₂₉	DMDPHTDMA	490±4
octyl	-C ₂ H ₄ OC ₆ H ₁₃	DMDOHEMA	356±6
butyl	-C ₂ H ₄ OC ₁₂ H ₂₅	DMDBDEMA	352±3
butyl	-C ₃ H ₆ OC ₁₁ H ₂₃	DMDBUDOPMA	346±1
cyclohexyl	-C ₁₄ H ₂₉	DMDCHTDMA	332±5
butyl	-C ₁₄ H ₂₉	DMDBTDMA	332±3



Ab initio calculations were carried out in order to investigate if calculated gas-phase basicities could be related to the experimentally determined basicities. Gas-phase basicity is defined as the negative of Gibbs free energy for the protonation reaction; $L + H^+ \rightleftharpoons LH^+$, where L is the ligand. The more negative ΔG the more basic molecule. The method for calculating the free energies for the protonation reaction is well established [2-4];

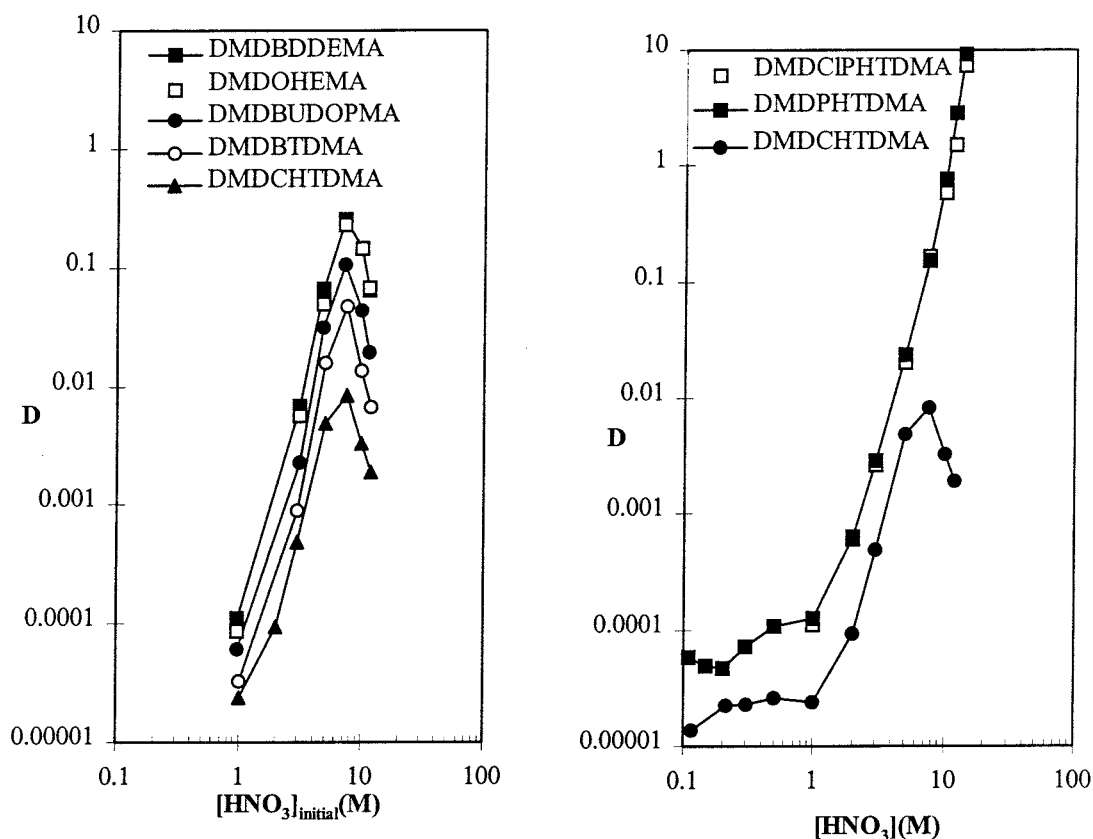


Figure 2. Extraction of Am(III) with 0.1M of the different malonamides studied in *tert*-butylbenzene.

$$\Delta G_R = \Delta H_R - T\Delta S_R \quad (1)$$

The ΔH_R and ΔS_R terms can be obtained from frequency calculations preceded by geometry optimisation, using the Gaussian 94 software. The ΔG_R -data in Table 3 are ordered from the least basic to the most basic structure (the one with most negative ΔG_R). The long carbon chain at the central carbon ($-C_{14}H_{29}$) was replaced by a hydrogen to minimise the computation time.

Table 3. The difference in Gibbs free energy for the protonation reaction of some different substituted malonamides (Gaussian94, full geometry optimisation).

R_1	R_2	$\Delta G_R(\text{kcal/mol})$
4-chlorophenyl	H	-215.30
phenyl	H	-228.56
2,6-dichlorophenyl	H	-229.35
cyclohexyl	H	-230.71

The order of basicity using the calculated data is consistent with the experimentally determined basicities presented in Table 2. More calculations and measurements on new malonamides, e.g. with alkoxy groups on the central carbon, are in progress and are needed to verify the correlation between calculated and experimental basicity and the relation between basicity and extraction.

2.3 Redox kinetics of tetravalent actinides

Previous experiments within this project have been performed in order to study the extraction behaviour of tetravalent actinides in the Aliquat-336/nitric acid system. The results show a high extraction of tetravalent actinides in this system. However, since some of the actinides (uranium, plutonium and neptunium) may not be stable as tetravalent species under the experimental conditions, an investigation of the oxidation kinetics is important. A relevant and, to the first approximation, simple system would be the U(IV)/U(VI) redox couple. It was shown that the oxidation mechanism of U(IV) with molecular oxygen in perchlorate media may be of the first order, with respect to U(IV) [5]. However, a rate law for the oxidation in chloride or nitrate media has not been found in literature. The scope of the present study is to find the rate law corresponding to the equation;

$$-\frac{d[U(IV)]}{dt} = f([U]_{\text{tot}}, pO_2, [H^+], [X], I, T) \quad (2)$$

where $[U]_{\text{tot}}$ is the total uranium concentration, pO_2 the partial pressure of oxygen, $[H^+]$ the hydrogen ion concentration, $[X]$ the concentration of any anion, I the ionic strength, and T the temperature. The experimental technique utilises spectrophotometry to follow the reaction. The results will be used to verify that only the tetravalent species are present during the extraction experiments.

Figure 3 shows the decrease in U(IV) concentration when hydrogen ion- and chloride concentrations were held constant. In contradiction to perchlorate media, no first order behaviour with respect to the total uranium concentration was observed. This may indicate a different reaction mechanism and/or competing reactions.

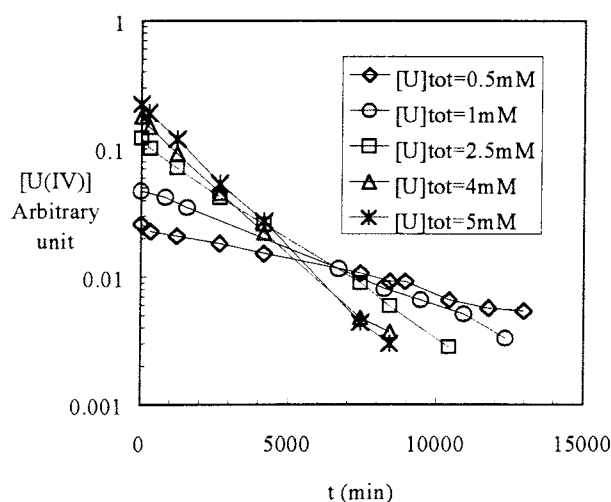


Figure 3. The oxidation of U(IV) with oxygen at different total uranium concentrations. $[H^+]=0.1M$, $[Cl^-]=0.1M$ and $I=0.5M$.

The influence of the hydrogen ion concentration is given in Figure 4. The result shows that U(IV) is stabilised with the hydrogen ion concentration. Furthermore, the non-

linear behaviour of the curves in the plot indicate a deviation from a first order reaction.

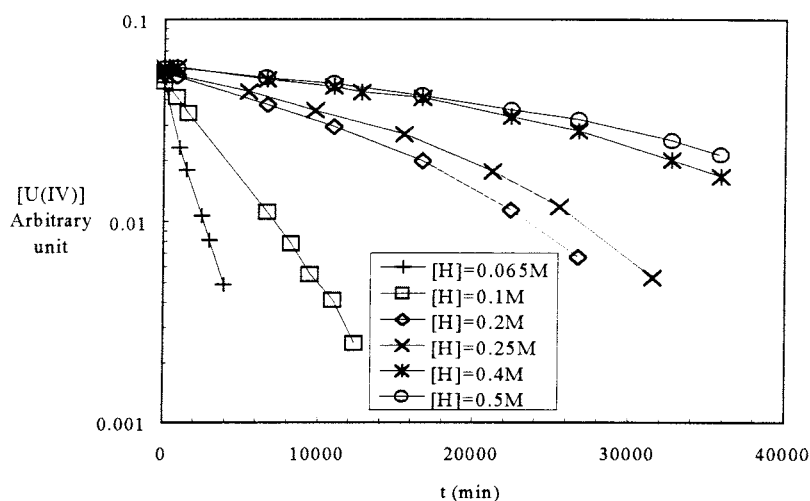


Figure 4. The oxidation of U(IV) with oxygen at different hydrogen ion concentrations. $[U]_{\text{tot}}=1.0\text{mM}$, $[Cl^-]=0.1\text{M}$ and $I=0.5\text{M}$.

Since nitric acid is used in the Aliquat-336 extraction system, the oxidation behaviour in nitrate media will be studied as well. The main scope of the project is to find out the oxidation mechanism, and furthermore to model the oxidation according to Equation 2.

This work is done in cooperation with the SKB/CTH Fuel Program.

3. COLLABORATIONS

Sweden

The Swedish Spallator Network (SSN) is a national network with the objective to inform internally and externally about Swedish and international research concerning accelerator-driven transmutation systems. The group participated in "Energimässan" at Svenska Mässan, Göteborg, in April 1998. The network consists of representatives from different universities and institutes;

- * Chalmers University of Technology, Göteborg
- * Royal Institute of Technology, Stockholm
- * Uppsala University
- * Lund University

Europe

A three-year European contract started in May 1996 concerning new partitioning techniques within the Nuclear Fission Safety program (NEWPART CT FI4I-CT96-0010). There are seven participating institutes from five different countries; Department of Nuclear Chemistry, Chalmers (Sweden), CEA (France), University of Reading (UK), Transuranium Institute (Germany), Forschungszentrum Karlsruhe (Germany), Forschungsanlage Jülich (Germany) and ENEA (Italy). The project has so far been very successful and a proposal for the next Fifth Framework Programme is under preparation. Project meetings are held every 6 months.

England

The University of Reading has an important role in the European contract as a "supplier" of new extractants. The department also performs co-ordination chemistry and molecular modelling of these new ligands. Several new extractants from Reading have been investigated at Chalmers during the year and one Ph.D. student, Lena Spjuth, spent 3 months at the University of Reading to study molecular modelling and synthesis, see Appendix VII.

France

There has been a lot of contacts between the CEA laboratory in Marcoule and Chalmers since the work performed at the two laboratories are closely connected. There is a continuous exchange of new ligands and discussions of new results.

U.S.A.

An informal collaboration was initiated in 1992 between the Los Alamos National Laboratory (LANL) and the Department of Nuclear Chemistry, CTH. The collaboration involves exchange of information and results within aqueous based partitioning processes.

Japan

A collaboration was initiated in 1993 between the Department of Nuclear Chemistry, CTH and the Department of Fuel Cycle Safety Research at Japan Atomic Energy Institute (JAERI). It was agreed to exchange information, results and personnel between CTH and JAERI.

4. MEETINGS AND LECTURES

Except for the meetings and conferences presented in the travelling reports (Appendix VI-VII), several other meetings were attended during the year and several invited lectures were held.

The Swedish Spallator Network (SSN) had a meeting at Chalmers on April 27 where problems concerning separation techniques were discussed. The SSN-group also participated in "Energimässan" at Svenska Mässan, Göteborg, in the end of April.

Two progress meetings within the European collaboration (NEWPART) were held, in Sellafield, UK, in May and in Karlsruhe, Germany, in November (Appendix III, V).

Jan-Olov Liljenzin gave a lecture entitled “Accelerator-driven kärnenrgi - fantasi eller verklighet?” in the seminar series about energy arranged by Energitekniskt Centrum and Göteborg Energi AB.

On the 28:th of April Jan-Olov Liljenzin gave a public seminar entitled “Transmutation - avfallsfrågor” in Oskarshamn

At the seminar “Blick på kärnteknik inom EU - ett svenskt perspektiv” on the 6:th of May, arranged by KTC, Jan-Olov Liljenzin talked about projects within nuclear chemistry.

At a seminar on the 3:rd of November at the Department of Chemistry, Chalmers, Jan-Olov Liljenzin gave a lecture about “Liquid-liquid extraction as a method for separation of metal ions”

Jan-Olov Liljenzin and Anders Landgren gave an invited lecture about P&T arranged by SKB in Stockholm, December 4, 1998.

Lena Spjuth gave an invited lecture about P&T for WIN (Women in Nuclear) at Ringhals, December 16, 1998

5. REFERENCES

- [1] STREULI, C.A., *Anal. Chem.*, **30(5)**, 997, (1958)
- [2] ZHANG, K., ZIMMERMAN, D.M., CHUNG-PHILLIPS, A., AND CASSADY C.J., *J. Am. Chem. Soc.*, **115**, 10812, (1993)
- [3] JEBBER, K.A., ZHANG, K., CASSADY, C.J., AND CHUNG-PHILLIPS, A., *J. Am. Chem. Soc.*, **118**, 10515, (1996)
- [4] ZHANG, K., CASSADY C.J., AND CHUNG-PHILLIPS, A., *J. Am. Chem. Soc.*, **116**, 11512, (1994)
- [5] HALPERN, J., AND SMITH, J.G.: *Can. J. Chem.*, **34**, 1419 (1956)

Appendix

I

Extraction of Actinides and Lanthanides from Nitric Acid Solution by Malonamides*

By L. Spjuth, J. O. Liljenzin, M. Skålborg

Department of Nuclear Chemistry, Chalmers University of Technology, S-41296 Göteborg, Sweden

M. J. Hudson, G. Y. S. Chan, M. G. B. Drew, M. Feaviour, P. B. Iveson

Department of Chemistry, University of Reading, Box 224, Whiteknights, Berkshire RG6 6AD, UK

and C. Madic

CEA-Valrhô, Marcoule, BP 171, 30207 Bagnols-sur-Cèze, Cédex, France

(Received November 26, 1996; accepted in revised form February 8, 1997)

Actinides / Extraction / Malonamides / Lanthanides / Nitric acid

Summary

Solvent extraction from nitric acid solutions by three different malonamides; N,N'-dimethyl-N,N'-dibutyloctadecyl malonamide, N,N'-dimethyl-N,N'-diphenyltetradecyl malonamide and N,N'-dimethyl-N,N'-dicyclohexyltetradecyl malonamide, dissolved in *tert*-butylbenzene, has been investigated. The dependence on nitric acid concentration, nitrate concentration and malonamide concentration on the extraction of U, Th, Am, Eu, Tb and HNO₃ is described. The influence of the different malonamide structures on the extraction behaviour is discussed. The phenylsubstituted malonamide, DMDPHTD, is able to extract metal species even from high nitric acid concentrations. The experimental data indicate both a coordination mechanism and an ion-pair extraction mechanism depending on the nitric acid concentration.

Introduction

In an advanced reprocessing process of nuclear fuel not only uranium and plutonium have to be separated, but also neptunium, americium and curium. The transmutation of the separated actinides (An) to short-lived nuclides by neutron irradiation can then be considered. To achieve an efficient transmutation process all actinides have to be effectively separated from the remaining waste, including the large amount of lanthanides (Ln). One separation route is to coextract the actinides and lanthanides in a first stage and then separate the trivalent actinides from the lanthanides in a second stage. In order to be able to design extractant molecules for such a process we need systematic data on the effect of structure on extraction power and selectivity. The present work is part of an effort to understand the importance of different substituents on the behavior of malonamide derivatives as extractants.

Malonamides are considered to be interesting actinide-lanthanide coextractants, leaving the rest of the

fission products in the aqueous phase [1–13]. These extractants do not generate incombustible waste (in contrast to the phosphorus-containing extractants), since they only contain carbon, hydrogen, oxygen and nitrogen and thus are completely incinerable. The degradation products formed by radiolysis and hydrolysis of malonamides are less of a problem in the stripping of An(III) and Ln(III) than the degradation products formed by phosphorus-containing extractants, e.g. CMPO [14–15].

The structure of the malonamide has a great influence on the metal extraction. Solubilities, electronic effects and steric hindrances together influence the degree of extraction. To minimize the steric hindrance and to increase the metal extraction one of the substituents on the nitrogen atoms should be a methyl group. The other nitrogen substituent has to be a long carbon chain to make the molecule lipophilic. A lengthening of the carbon chain on the methylene carbon also enhances the extraction ability and an oxyalkyl substituent increases the extraction even more [16]. IR measurements indicate that the metal is coordinated to the carbonyl oxygen atoms in the malonamide rather than to the nitrogen [5].

Experimental

The two new malonamides, N,N'-dimethyl-N,N'-diphenyltetradecyl malonamide (DMDPHTD) and N,N'-dimethyl-N,N'-dicyclohexyltetradecyl malonamide (DMDCHTD), were synthesized and purified at the University of Reading, UK. N,N'-dimethyl-N,N'-dibutyloctadecyl malonamide (DMDBOD) was synthesized and purified by Synthelec AB, Sweden. The purities of the new malonamides were checked by elemental analysis, high resolution electron impact mass spectroscopy and 400 MHz ¹H-NMR and was determined to be over 99%. *Tert*-butylbenzene, in the purity of 99%, was used as diluent and was provided by Aldrich and Co. All experiments were performed at ambient temperature.

* Presented at the Fourth International Conference on Nuclear and Radiochemistry, Saint Malo, September 1996.

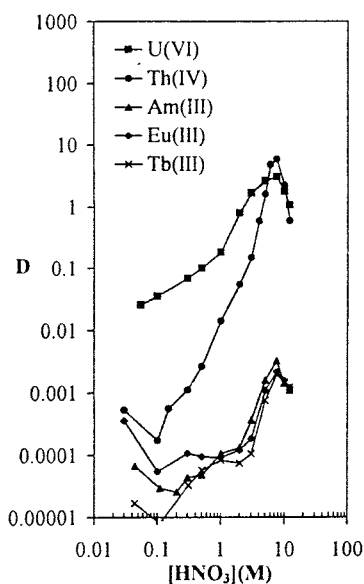


Fig. 1. Extraction of metal cations by 0.1 M DMDBOD in *tert*-butylbenzene.

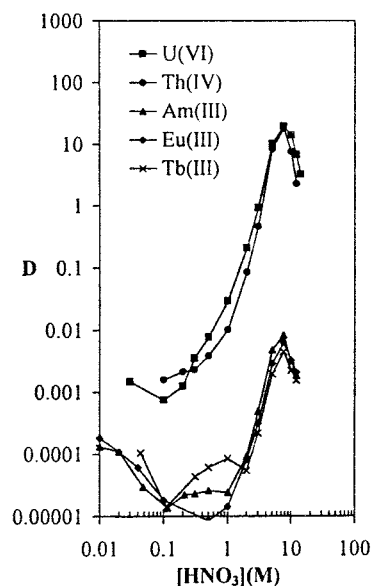


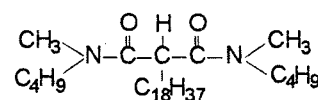
Fig. 2. Extraction of metal cations by 0.1 M DMDCHTD in *tert*-butylbenzene.

Procedure and apparatus

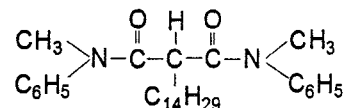
The malonamide, dissolved in *tert*-butylbenzene, was vigorously shaken for five minutes with the nitric acid or LiNO_3 solutions, preequilibrated with the tracer. After phase separation by centrifugation at 4500 rpm, aliquots of each phase were withdrawn and the distribution ratio was determined by radiometric analysis. The γ -energies at 59.6 keV, 121.8 keV and 879.4 keV from ^{241}Am , ^{152}Eu , and ^{160}Tb , respectively, were measured using a HPGe detector. For the α - and β -emitters (^{233}U , ^{241}Am , and ^{234}Th) a LKB Wallac 1219 Rackbeta liquid scintillation counter was used. The distribution of nitric acid between the aqueous and organic phases was determined by pH-metric titration using a Mettler DL20 Compact Titrator. The titrations were performed in ethanolic media.

Results

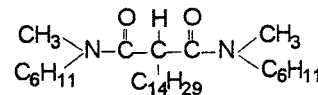
The three investigated malonamides all have one methyl group substituted to each nitrogen atom which minimize the steric hindrance. The second nitrogen substituents in DMDBOD are butyl groups. DMDPHTD and DMDCHTD have as second nitrogen substituents phenyl and cyclohexyl groups, respectively. One of the objectives of this study was to compare the extraction behaviour of the different malonamide structures. A concentration of 0.1 M malonamide was used in the main part of the metal extractions due to the limited amounts available of the newly synthesized malonamides. Distribution ratios are therefore quite low. However, higher concentrations of malonamide will give higher distribution ratios, which is also shown in this work.



N,N'-dimethyl-N,N'-dibutyloctadecyl malonamide (DMDBOD)



N,N'-dimethyl-N,N'-diphenyltetradecyl malonamide (DMDPHTD)



N,N'-dimethyl-N,N'-dicyclohexyltetradecyl malonamide (DMDCHTD)

Metal extraction

In almost the whole range of nitric acid concentration investigated, metal extraction decreases in the order $\text{U(VI)} \geq \text{Th(IV)} \gg \text{M(III)}$ as is seen in Figs. 1–3. Na^+ and Ba^{2+} were used as analogues for monovalent and divalent cations, respectively, and their extraction ability was at least one order of magnitude lower than for the trivalent cations. Metal extraction increases when the nitric acid concentration is increased. For DMDBOD and DMDCHTD a maximum in the metal extraction is reached at about 7–8 M HNO_3 . This is not seen for DMDPHTD which shows a constant increase in extraction with increasing nitric acid concentrations. The decrease in extraction at high nitric acid concentration, observed for DMDBOD and DMDCHTD, may be explained by the competition from nitric acid extraction. At low nitric acid concentrations, below 0.1 M, the metal extraction increases slightly indicating a change in the dominating extraction mechanism.

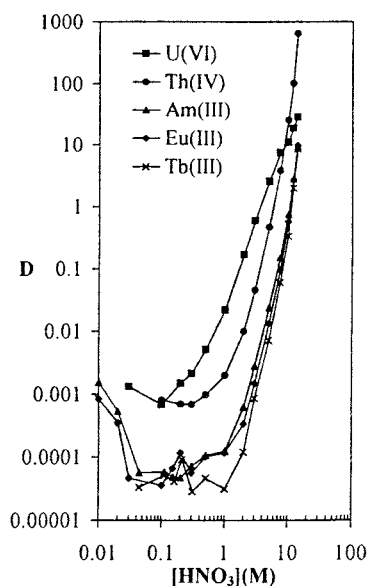


Fig. 3. Extraction of metal cations by 0.1 M DMDPHTD in *tert*-butylbenzene.

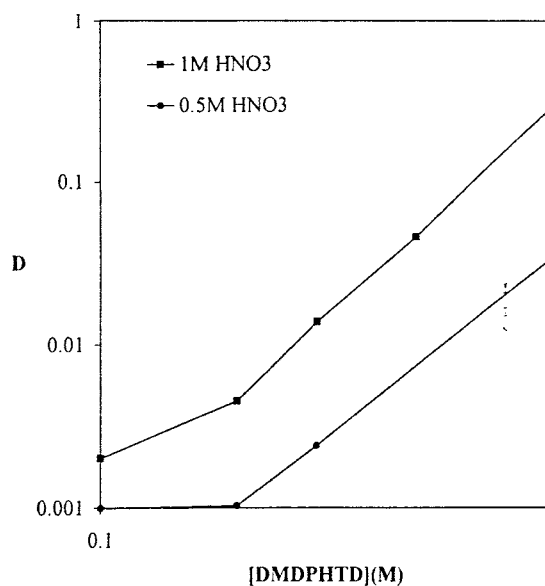


Fig. 5. Extraction of Th(IV) by DMDPHTD in *tert*-butylbenzene at two different nitric acid concentrations.

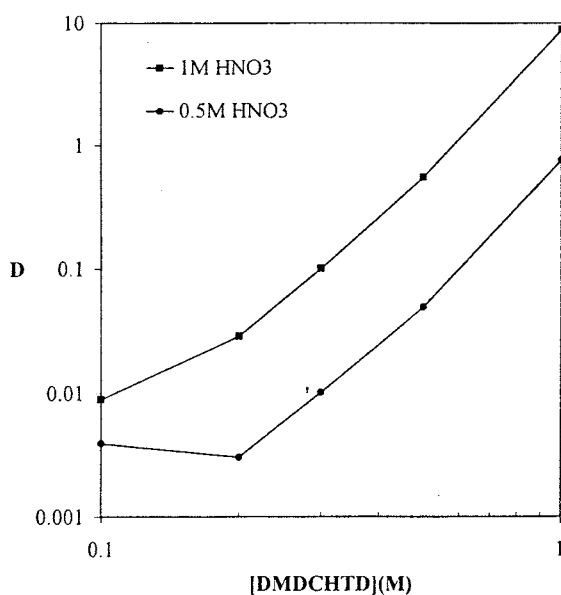


Fig. 4. Extraction of Th(IV) by DMDCHTD in *tert*-butylbenzene at two different nitric acid concentrations.

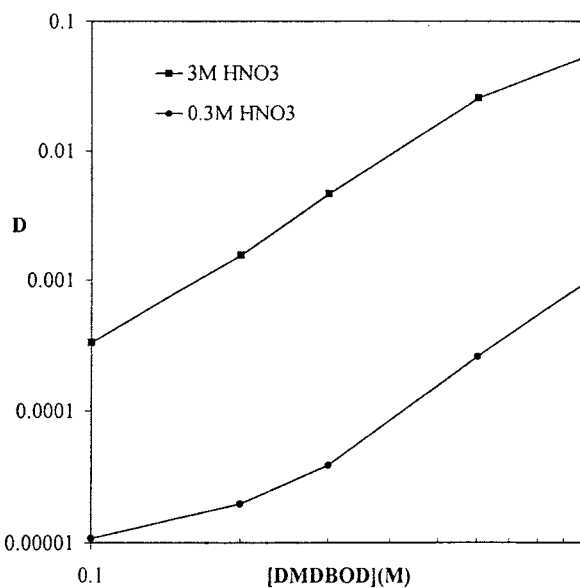


Fig. 6. Extraction of Am(III) by DMDBOD in *tert*-butylbenzene at two different nitric acid concentrations.

Metal extraction is increased when the concentration of the extractant is increased. Figs. 4 and 5 show the dependence on malonamide concentration of the extraction of Th(IV) with DMDCHTD and DMDPHTD at different nitric acid concentrations. In Figs. 6–8, values are given for Am(III) extracted with different concentrations of the malonamides. The extraction dependence is non-linear at nitric acid concentrations below 1 M and low malonamide concentrations. This may be explained by a change in the extraction mechanism at these conditions.

Detailed structural and molecular modelling studies have been carried out on a range of malonamides

in the free state and complexed to lanthanide metals. Results for the unsubstituted parent malonamides (without the tetradecyl group) are reported elsewhere [17]. In crystals the phenyl malonamides exhibit a very different conformation from the cyclohexyl malonamide in that the $O=C\dots C=O$ torsion angle is found to be 57.2° compared to 179.5° . Conformational analysis show that these conformations found in crystals are indeed the lowest energy conformations of these malonamides. This clearly indicates that the phenyl malonamides are more likely to complex a metal, or form an ion-pair, than the cyclohexyl malonamide because only a small conformational change is required

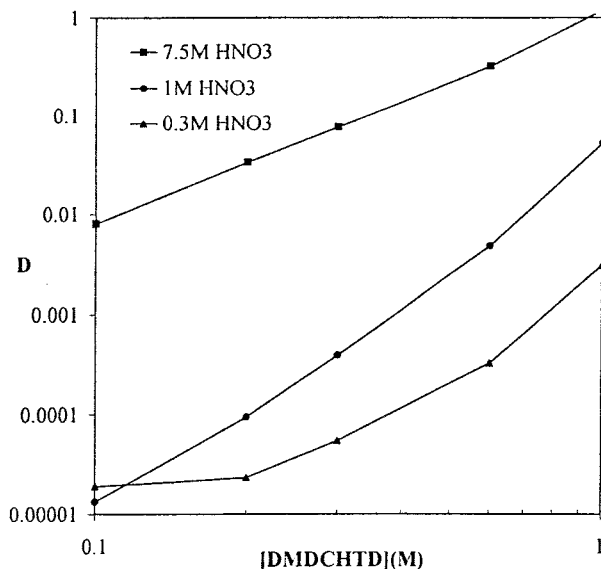


Fig. 7. Extraction of Am(III) by DMDCHTD in *tert*-butylbenzene at three different nitric acid concentrations.

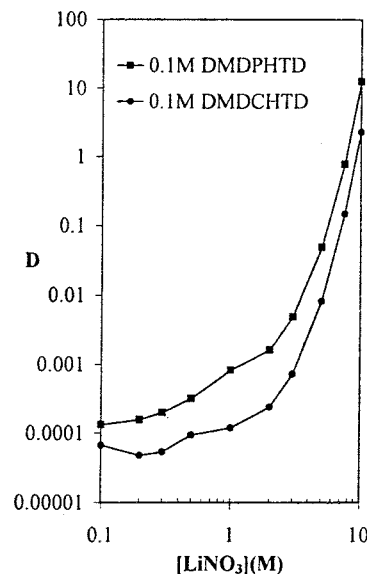


Fig. 9. Extraction of Am(III) at different concentrations of LiNO_3 by 0.1 M malonamide in *tert*-butylbenzene.

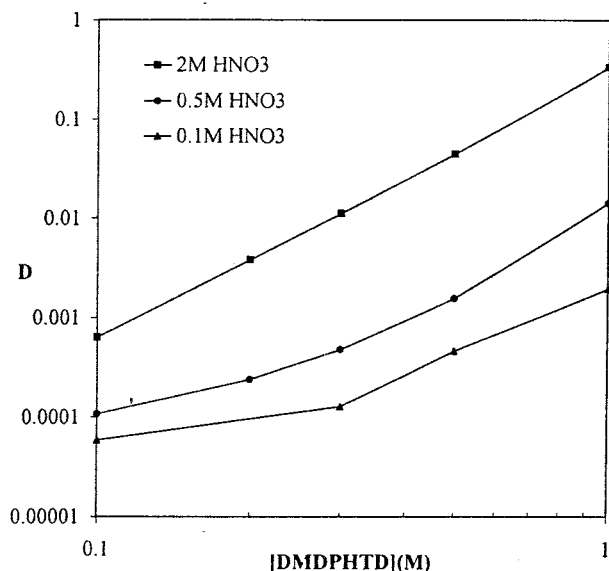


Fig. 8. Extraction of Am(III) by DMDPHTD in *tert*-butylbenzene at three different nitric acid concentrations.

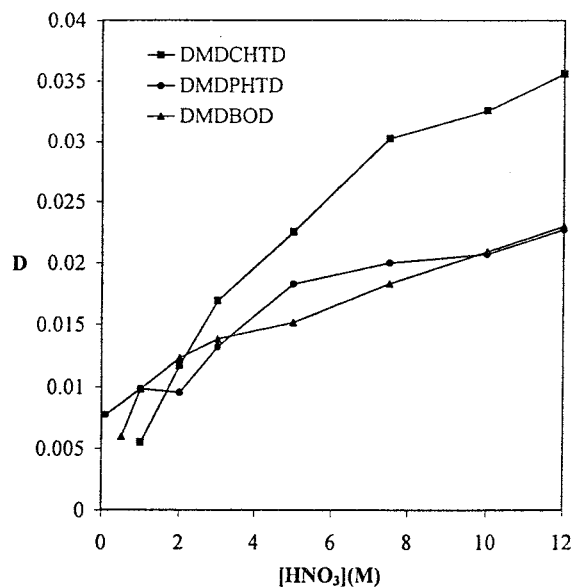


Fig. 10. Extraction of HNO_3 by 0.1 M malonamide in *tert*-butylbenzene.

(this is reflected in our extraction results). However, molecular modelling shows that the substitution of a tetradecyl group can lead to a substantial change in the conformation so even in the cyclohexyl malonamide, the $\text{O}=\text{C}\dots\text{C}=\text{O}$ torsion angle is significantly decreased making complexation more readily achieved.

In non-acidic media the malonamides are unprotonated and thus no ion-pair extraction can occur. When the nitrate concentration is increased, in the form of LiNO_3 , the metal extraction increases for both DMDCHTD and DMDPHTD (Fig. 9). These data show that extraction occurs even though no protonated malonamide molecules are present, suggesting a coordination mechanism.

Nitric acid extraction

Nitric acid extraction by DMDCHTD is slightly higher than for the other two malonamides (Fig. 10). This could be due to a higher basicity of DMDCHTD. DMDPHTD is expected to have lower basicity because of the electron withdrawing properties of the phenyl group. The average number of extracted HNO_3 molecules per malonamide molecule is shown in Fig. 11. For DMDCHTD, at 10 M HNO_3 , three HNO_3 molecules are bound to one malonamide. However, for DMDPHTD and DMDBOD two HNO_3 molecules are bound to one malonamide at the same nitric acid concentration. The nitric acid extracted by the diluent has

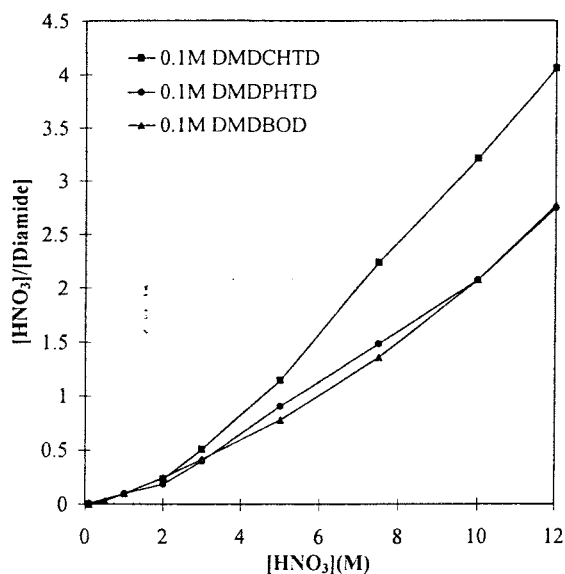


Fig. 11. The average number of HNO_3 molecules extracted per malonamide molecule for the three different malonamides dissolved in *tert*-butylbenzene.

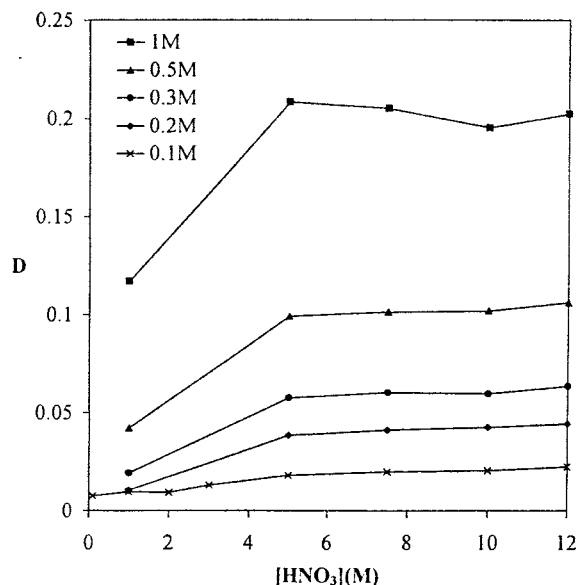


Fig. 13. Extraction of HNO_3 by DMDPHTD in *tert*-butylbenzene.

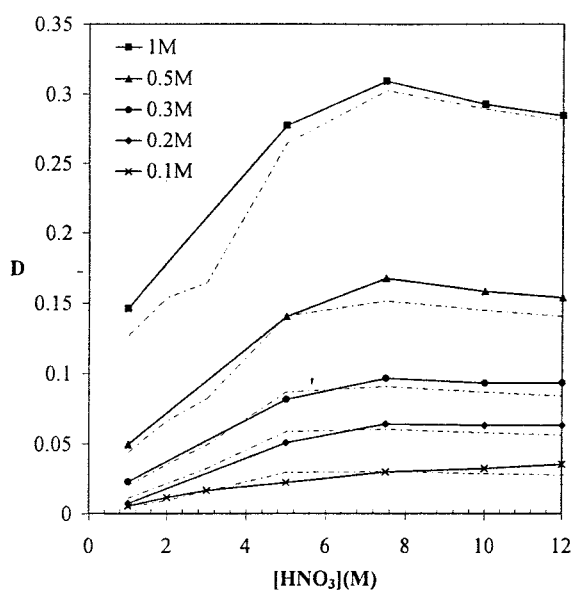


Fig. 12. Extraction of HNO_3 by DMDCHTD in *tert*-butylbenzene. The dotted lines are the calculated D-values using the proposed mechanism from Eq. (9) ($M = 2$, $Y = 1$ and $M = 1$, $Y = 4$).

been shown to be negligible. Nitric acid can interact with malonamides, which are weak bases, either by hydrogen bonding or by proton transfer. Proton transfer has a greater effect on the vibrational spectra than hydrogen bonding and it has earlier been shown by IR measurements that in the adducts with more than one HNO_3 molecule, a proton is transferred to one of the oxygen atoms in the malonamide forming an intramolecular hydrogen bond to the other carbonyl oxygen atom. The increase in dielectric constant of the organic phase as more HNO_3 is extracted is assumed to favour

Table 1. Results from plot of $\log D_{\text{HNO}_3}$ vs. malonamide concentration at various DMDCHTD concentrations

$[\text{HNO}_3]$	Gradient	r
1 M ^a	1.8	0.9804
5 M	1.1	0.9982
7.5 M	1.0	0.9982
10 M	0.96	0.9995
12 M	0.91	0.9992

^a Slope analysis from concentration of 0.2–1 M malonamide only.

the proton transfer from HNO_3 to the malonamide [4]. Nitric acid extraction data indicate that most of the diamide molecules in the organic phase are connected to HNO_3 in some way. The formation of different HNO_3 -malonamide adducts, with up to three HNO_3 bound to the malonamide, has been shown previously [4, 8]. The protonated malonamide has been characterized by single crystal X-ray structure determination of the complex $[\text{H}^+\text{DMDCHMA}]_2[\text{CoCl}_4]^{2-}$, where DMDCHMA is *N,N'*-dimethyl-*N,N'*-dicyclohexylmalonamide [14]. An ion-pair extraction mechanism is supported by these data.

Nitric acid extraction is increased when the malonamide concentration is increased, Figs. 12–13, but the average number of extracted HNO_3 molecules per malonamide molecule only changes slightly with malonamide concentration. If $\log(D_{\text{HNO}_3})$ is plotted versus $\log[\text{Malonamide}]$ the gradient is less than 1. Values given in Tables 1–2, for both DMDCHTD and DMDPHTD at 10–12 M HNO_3 , indicating the formation of $(\text{L})(\text{HNO}_3)_y$ adducts. At 1 M HNO_3 the gradient is larger than 1 for the two malonamides which indicates that $(\text{L})_m(\text{HNO}_3)$ adducts are formed.

Table 2. Results from plot of $\log D_{\text{HNO}_3}$ vs. malonamide concentration at various DMDPHTD concentrations

[HNO ₃]	Gradient	<i>r</i>
1 M ^a	1.5	1.0
5 M	1.1	0.9999
7.5 M	1.1	0.9998
10 M	0.97	0.9993
12 M	0.95	0.9998

^a Slope analysis from concentration of 0.2–1 M malonamide only.

Table 3. Results from plot of $\log D$ vs. malonamide concentration (0.1 M–1 M) in *tert*-butylbenzene for the extraction of Th(IV) at various HNO₃ concentrations

Malonamide	[HNO ₃]	Gradient	<i>r</i>
DMDCHTD ^a	0.5 M	3.4	0.9949
DMDCHTD ^a	1 M	3.6	0.9961
DMDCHTD	10 M	2.3	0.9884
DMDPHTD ^a	0.5 M	2.2	0.9991
DMDPHTD ^a	1 M	2.6	0.9999

^a Slope analysis from concentration of 0.2–1 M malonamide only.

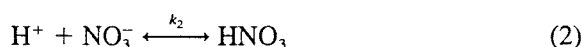
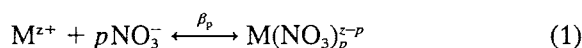
Table 4. Results from plot of $\log D$ vs. malonamide concentration (0.1 M–1 M) in *tert*-butylbenzene for the extraction of Am(III) at various HNO₃ concentrations

Malonamide	[HNO ₃]	Gradient	<i>r</i>
DMDCHTD ^a	0.3 M	3.0	0.9761
DMDCHTD	1 M	3.6	0.9916
DMDCHTD	7.5 M	2.2	0.9979
DMDPHTD ^a	0.5 M	2.6	0.9835
DMDPHTD	2 M	2.7	0.9992
DMDBOD ^a	0.3 M	2.5	0.9940
DMDBOD	3 M	2.3	0.9937

^a Slope analysis from concentration of 0.2–1 M malonamide only.

Extraction mechanism

The extraction mechanisms that have been considered for the malonamides are an ion-pair mechanism and a coordination mechanism. The metal ions are complexed with nitrate ions from the nitric acid.



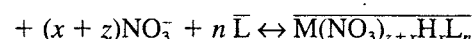
$$D_{\text{H}} = \frac{\sum_{m=1}^M \sum_{y=1}^Y y [\overline{(\text{HNO}_3)_y \text{L}_m}]}{[\text{H}^+] + [\text{HNO}_3]} = \frac{\sum_{m=1}^M \sum_{y=1}^Y P_{y,m} [\text{H}^+]^y \cdot [\text{NO}_3^-]^y \cdot [\text{L}]^m \cdot \frac{Y_{\text{H}^+}^y \cdot Y_{\text{NO}_3^-}^y \cdot \overline{Y}_{\text{L}}^m}{Y_{\overline{(\text{HNO}_3)_y \text{L}_m}}}}{[\text{H}^+] + k_a \cdot [\text{H}^+]^2} \quad (9)$$

Table 5. Results from plot of $\log D$ vs. malonamide concentration (0.1–1 M) in *tert*-butylbenzene for the extraction of Tb(III) at various HNO₃ concentrations

Malonamide	[HNO ₃]	Gradient	<i>r</i>
DMDCHTD ^a	1 M	3.9	0.9971
DMDCHTD	3 M	3.2	0.9987
DMDCHTD	7.5 M	2.1	0.9981
DMDBOD ^a	1 M	2.9	0.9981
DMDBOD	5 M	2.4	0.9988

^a Slope analysis from concentration of 0.2–1 M malonamide only.

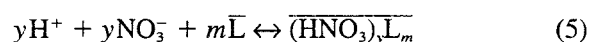
The metal nitrate species are extracted by the malonamide (L). Overlined species denotes species in the organic phase and Y denotes activity coefficients.



$$K_{xn} = \frac{[\overline{M(\text{NO}_3)_{z+x}\text{H}_x\text{L}_n}]}{[M^{z+}] \cdot [\text{NO}_3^-]^{x+z} \cdot [\text{H}^+]^x \cdot [\text{L}]^n} \quad (4)$$

$$\frac{\overline{Y}_{M(\text{NO}_3)_{z+x}\text{H}_x\text{L}_n}}{Y_{M^{z+}} \cdot Y_{\text{NO}_3^-}^{x+z} \cdot Y_{\text{H}^+}^x \cdot \overline{Y}_{\text{L}}^n}$$

If a coordination mechanism is considered ($x = 0$), a neutral metal-nitrate complex is coordinated to the carbonyl oxygens in the malonamide. In an ion-pair mechanism ($x > 0$), the malonamide is considered to be protonated and extracts an anionic metal-nitrate species. The metal extraction is effected by the extraction of HNO₃ to the organic phase. Several HNO₃-malonamide adducts may be formed;



$$P_{ym} = \frac{[\overline{(\text{HNO}_3)_y \text{L}_m}]}{[\text{H}^+]^y \cdot [\text{NO}_3^-]^y \cdot [\overline{\text{L}}]^m} \cdot \frac{\overline{Y}_{(\text{HNO}_3)_y \text{L}_m}}{Y_{\text{H}^+}^y \cdot Y_{\text{NO}_3^-}^y \cdot \overline{Y}_{\text{L}}^m} \quad (6)$$

When tracer amounts of metal is used, $[\text{H}^+] \approx [\text{NO}_3^-]$ and the total concentrations of malonamide and nitric acid can be written as;

$$C_{\text{HNO}_3} = [\text{H}^+] + [\text{HNO}_3] + \sum_{m=1}^M \sum_{y=1}^Y y [\overline{(\text{HNO}_3)_y \text{L}_m}] \quad (7)$$

$$= [\text{H}^+] + k_a \cdot [\text{H}^+]^2 + \overline{c}_{\text{HNO}_3}$$

$$\overline{C}_{\text{L}} = [\overline{\text{L}}] + \sum_{y=1}^Y \sum_{m=1}^M m [\overline{(\text{HNO}_3)_y \text{L}_m}] \quad (8)$$

The distribution ratio for nitric acid and metal can than be described as;

$$D_M = \frac{\sum_{x=0}^x \sum_{n=1}^N \overline{[M(NO_3)_{z+x}H_xL_n]}}{\sum_{p=0}^p [M(NO_3)_p]} = \frac{\sum_{x=0}^x \sum_{n=1}^N K_{xn} [M^{z+}] \cdot [NO_3^-]^{x+z} \cdot [H^+]^x \cdot [L]_n \cdot \frac{Y_{M^{z+}} \cdot Y_{NO_3^-}^{x+z} \cdot Y_{H^+}^x \cdot \overline{Y}_L^n}{Y_{M(NO_3)_{z+x}H_xL_n}}}{\sum_{p=0}^p \beta_p [M^{z+}] [NO_3^-]^p} \quad (10)$$

A minimization program was used to fit experimental D_H to the calculated D_H , using Eqs. (7)–(9) and experimental data for DMDCHTD (Fig. 12). Activity coefficients for H^+ and NO_3^- presented in [18] were used and the ratio of activity coefficients in the organic phase were assumed to be constant. The best mechanism that fitted the model was when five different HNO_3 -malonamide adducts were considered; $(HNO_3)L_2$, $(HNO_3)L$, $(HNO_3)_2L$, $(HNO_3)_3L$ and $(HNO_3)_4L$ (see Fig. 12). The formation constants from Eq. (6) were calculated to;

$$P_{12} = 0.32, P_{11} = 0.057, P_{21} = 0.0013, P_{31} = 1.7 \cdot 10^{-6} \text{ and } P_{41} = 4.5 \cdot 10^{-10}.$$

Slope analysis

If $\log [D]$ is plotted as a function of $\log [L]$ and all the other parameters are held constant, then the gradient would correspond to n in Eq. (10), which is the number of malonamide molecules in the dominating extracted complex. Thus, slope analysis of the experimental data from Figs. 4–8 indicate that 2–4 malonamide molecules are present in the extracted complexes. The results of slope analysis is presented in Tables 3–5. Previous saturation studies and crystallographic X-ray measurements indicate 1–2 malonamides in the inner coordination sphere and the larger value of the gradient can be explained by extra amide molecules in the outer coordination sphere [5, 19]. These interactions might be due to the formation of an induced dipole when the electrons are transferred from the nitrogen to the carbonyl oxygen and generates a higher positive charge on the nitrogen. This induced dipole might interact with non-complexed malonamides. At higher acidities, the competition from HNO_3 reduces the number of amide molecules available for outer sphere coordination because of the formation of HNO_3 -malonamide adducts [5, 8]. The gradients at higher nitric acid concentrations, shown in Tables 3–5, might confirm this. Malonamides have been shown to form micelles in non-acidic solutions and, at high malonamide concentrations, with C_6D_6 as diluent, about 6 molecules are associated in each aggregate [4, 5, 8]. This micelle formation complicates the evaluation of the extracted complex and simple slope analysis might not be valid for a larger concentration range of malonamide. Non-ideality of the organic phase could also be one of the reasons for the non-integral gradient [4–5].

Conclusions

It may be concluded that at a sufficiently high malonamide concentration all of the studied molecules

are able to extract actinides and lanthanides from strong nitric acid solutions. DMDPHTD was able to extract metal species even at 14 M nitric acid concentration.

The points of inflection observed for the distribution ratio as a function of nitric acid in Figs. 1–3, indicates that there are different extraction mechanisms dominating at different nitric acid concentrations.

The experimental data are somewhat contradictory as they are consistent with both a coordination mechanism and an ion-pair mechanism. The large amount of extracted nitric acid in the organic phase, crystallographic data and IR measurements indicates that the malonamide might be protonated and thus extracts by an ion-pair mechanism. However, the metal extraction from $LiNO_3$ solution suggests a coordination mechanism since there are no protonated malonamide molecules present. Thus the question about what mechanism is responsible for metal extraction is still unclear. A curve fit for the extraction of nitric acid by DMDCHTD indicated that several HNO_3 -malonamide adducts, with up to four HNO_3 molecules bound to the malonamide, were formed.

Acknowledgements

We wish to thank the Swedish Nuclear and Waste Management Co., SKB and the European Union (NEWPART CT F14I-CT96-0010) for financial support.

References

- Musikas, C., Hubert, H.: *Solvent Extr. Ion Exch.* **5**, 151 (1987).
- Musikas, C., Hubert, H.: *Solvent Extr. Ion Exch.* **5**, 877 (1987).
- Musikas, C.: *Inorg. Chim. Acta* **140**, 197 (1987).
- Nigond, L., Musikas, C., Cuillerdier, C.: *Solvent Extr. Ion Exch.* **12**, 261 (1994).
- Nigond, L., Musikas, C., Cuillerdier, C.: *Solvent Extr. Ion Exch.* **12**, 297 (1994).
- Siddall, III, T. H.: *J. Phys. Chem.* **64**, 1863 (1960).
- Fritz, J. S., Orf, G. M.: *Anal. Chem.* **47**, 2043 (1975).
- Nigond, L., Condamines, N., Cordier, P. Y., Livet, J., Madic, C., Cuillerdier, C., Musikas, C., Hudson, M. J.: *Sep. Sci. Techn.* **30**, 2075 (1995).
- Qinzhi, T., Hughes, M. A.: *Hydrometallurgy* **36**, 79 (1994).
- Nakamura, T., Miyake, C.: *Solvent Extr. Ion Exch.* **13**, 253 (1995).
- Nigond, L.: Thèse, de Doctorat de l'Université Blaise Pascal, CEA-R-5610 (1992).
- Musikas, C., Condamines, N., Cuillerdier, C.: *Advances in Separations by Solvent Extraction. Research and Applications*. In: *Solvent Extraction* (T. Sekine, ed.), Elsevier Science Publishers B.V. 1992.

13. Cuillerdier, C., Musikas, C., Nigond, L.: *Sep. Sci. Techn.* **28**, 155 (1993).
14. Chiarizia, R., Horwitz, E. P.: *Solvent Extr. Ion Exch.* **10**, 101 (1992).
15. Thiollet, G., Musikas, C.: *Solvent Extr. Ion Exch.* **7**, 813 (1989).
16. Cuillerdier, C., Musikas, C., Hoel, P., Nigond, L., Vitart, X.: *Sep. Sci. Techn.* **26**, 1229 (1991).
17. Chan, G. Y. S., Drew, M. G. B., Hudson, M. J., Iveson, P. B., Liljenzin, J. O., Skålberg, M., Spjuth, L., Madic, C.: *J. Chem. Soc. Dalton Trans.*, accepted (1996).
18. Davis, W., de Bruin, H. J.: *J. Inorg. Nucl. Chem.* **26**, 1069 (1964).
19. Byers, P., Drew, M. G. B., Hudson, M. J., Isaacs, N. S., Madic, C.: *Polyhedron* **13**, 349 (1994).

:
:
:

Appendix

II

**SYNTHESIS AND EXTRACTION STUDIES
OF A DIPYRIDYLTRIAZINE**

**Jonas Halvarsson
1998**

MASTER OF SCIENCE THESIS, 20P

**DEPARTMENT OF NUCLEAR CHEMISTRY
CHALMERS UNIVERSITY OF TECHNOLOGY
GÖTEBORG
SWEDEN
98 05 11**

**Examiner: Prof. Jan-Olov Liljenzin
Supervisors (Chalmers): M.Sc. Åsa Enarsson,
M.Sc. Anders Landgren and M.Sc. Lena Spjuth
(University of Reading): Dr Peter B Iveson**

ABSTRACT

In this work a new solvent extraction reagent, 4-octanoyl amino-2,6 di(2-pyridyl)-1,3,5 triazine (OADPTZ), was prepared. OADPTZ was then evaluated in solvent extraction studies for the difficult actinide(III)-lanthanide(III) separation. The radionuclides used in the experiments were ^{241}Am , ^{152}Eu and ^{147}Pm . Experiments were also performed with ^{234}Th as an example of the tetravalent actinides. It was found that OADPTZ has a good actinide(III)-lanthanide(III) separating potential at 0.01-0.1 M nitric acid concentrations. The results from the actinide(IV) extraction were difficult to interpret, possibly due to kinetic problems.

An attempt to synthesise the solvent extraction reagent 4-octanoyl amino-2,6 di(4-methyl 2-pyridyl)-1,3,5 triazine was also made but failed due to solubility problems.

A main requirement for the new reagent has been that it should be an organic extractant composed of only the elements C, H, O and N, i.e. it should obey the CHON-principle, in order to make the secondary waste produced completely incinerable.

Complexation studies of 4-Amino-2,6 di(pyridyl)-1,3,5-triazine - Pb^{2+} and of 4-Amino-2,6,di(4-methyl pyridyl)-1,3,5-triazine with Ni^{2+} and Nd^{3+} were also performed.

Contents

1. Introduction	1
2. Theory	4
2.1. Distribution ratio	4
2.2. Metal extraction	5
2.2.1. Extraction with 2-bromodecanoic acid	5
2.2.2. Extraction with 2-bromodecanoic acid and TPTZ derivatives	6
2.3. Measurement of $[H^+]$	6
2.3.1. Gran titrations	6
3. Experimental	8
3.1. Synthesis	8
3.1.1. Preparation of 4-amino-2,6-di(pyridyl)-1,3,5 triazine (ADPTZ)	8
3.1.2. Acylation of ADPTZ with octanoyl chloride	9
3.1.3. Preparation of 4-amino-2,6-di(4-methyl pyridyl)-1,3,5 triazine (ADMPTZ)	10
3.1.4. Acylation of ADMPTZ with octanoyl chloride	11
3.2. Complexation studies	12
3.2.1. ADPTZ and $Pb(NO_3)_2$	12
3.2.2. ADMPTZ and $Ni(NO_3)_2 \cdot 6H_2O$	12
3.2.3. ADMPTZ and $Nd(NO_3)_3 \cdot 6H_2O$	12
3.3. Extraction studies	13
3.3.1. Radionuclides	13
3.3.2. Procedures	14
3.3.3. Solubility test	14
3.3.4. Gran-titrations	14
3.3.5. Test tube experiments	15
4. Results and Discussion	16
4.1. pH- $[H^+]$ correlation	16
4.2. Metal extraction	17
4.2.1. Trivalent actinides versus trivalent lanthanides	17
4.2.2. Trivalent actinides versus tetravalent actinides	18
4.3. Complexation studies	19
4.3.1. Crystallisation of $ADPTZ_2 \cdot Pb(NO_3)_2$	19
4.3.2. Crystallisation of $ADMPTZ_2 \cdot Ni(NO_3)_2 \cdot 6H_2O$	20
4.3.3. Crystallisation of $ADMPTZ \cdot Nd(NO_3)_3 \cdot 6H_2O$	21
5. Conclusions	22
6. Further investigations	22
7. Acknowledgements	23
8. References	24

Appendices

1. ^1H -NMR spectra of 4-octanoyl amino-2,6 di(2-pyridyl)-1,3,5 triazine (OADPTZ)
2. ^{13}C -NMR spectra of 4-octanoyl amino-2,6 di(2-pyridyl)-1,3,5 triazine (OADPTZ)
3. Extraction data for ^{241}Am - ^{152}Eu
4. Extraction data for ^{241}Am - ^{147}Pm
5. Extraction data for ^{241}Am - ^{234}Th
6. X-ray crystallography data for $\text{ADPTZ}_2\text{-Pb}(\text{NO}_3)_2$
7. X-ray crystallography data for $\text{ADMPTZ}_2\text{-Ni}(\text{NO}_3)_2\cdot 6\text{H}_2\text{O}$
8. X-ray crystallography data for $\text{ADMPTZ-NdNO}_3\cdot 6\text{H}_2\text{O}$

1. INTRODUCTION

Separation of the trivalent actinides, An(III), from the lanthanides, Ln(III), has become a topic of great importance to reduce the radiotoxicity of the waste from the reprocessing industries [CEC]. This is due to the need for safe and economical disposal of the nuclear waste. The final deposit of this waste often involves deep geological repositories which are very expensive compared to near surface sites where the low level waste can be stored.

The spent nuclear fuel from nuclear power plants contains, among others, trivalent actinides as well as trivalent lanthanides. The aim is to separate the actinides, primarily ^{237}Np , $^{241,242,243}\text{Am}$ and $^{243,244,245}\text{Cm}$ and if possible, some of the long-lived fission products (FP) from the spent nuclear fuel and to convert them into short-lived or stable nuclides by neutron irradiation, so called transmutation. The problem is that the lanthanides have neutron absorbing properties and therefore must be separated before irradiation. Since the actinides are the primary targets for the neutron irradiation, a separation process must be developed in order to enhance the efficiency of the transmutation process. In fact, the transmutation process is unrealistic without this separation. This separation of the trivalent actinides from the lanthanides is difficult due to their similar chemical properties charge and radii. However, there are some differences. Due to the fact that the electrons of the 5f orbitals of the actinides are more shielded than the electrons of the 4f orbitals of the lanthanides, the actinides are more likely to form covalent bonds with donor molecules [NAS 95]. Hence it follows that ligands containing soft donors such as nitrogen or sulphur, form more stable complexes with the actinides than with the lanthanides.

The PUREX process is using tributyl phosphate for the separation of uranium and plutonium from the spent nuclear fuel. However, it is unsatisfactory for the actinide(III) lanthanide(III) separation [KOL 91]. With a small modification of the PUREX process, it is possible to separate neptunium [CEC] but new reagents are required in order to separate americium and curium from the spent nuclear fuel. To minimise the volume of secondary waste the new extractant should be composed of the elements C, H, O and N alone, i.e. it must be completely incinerable. The separation process should also be operational at nitric acid concentrations of at least 0.1 M [CEC]. A relatively high nitric acid concentration prevents the hydrolysis of metal ions (actinides, lanthanides and other FP) in the solution. The hydrolysis is, otherwise, liable to cause the formation of precipitates which are likely to ruin the solvent extraction process.

The An(III)-Ln(III) separation is only one part in the process of separating the long-lived radionuclides from the spent nuclear fuel. The proposed separation strategy [CEC] contains multiple steps (Fig. 1.1.). The PUREX process is a process originally designed for U and Pu recycling but it also permits separation of some other elements for example: Np as well as Tc, I and Zr. The DIAMEX process, based on the use of a diamide, is being developed to separate An(III) and Ln(III) from the other FP [CEC]. The actinides are then separated from the lanthanides in a second step.

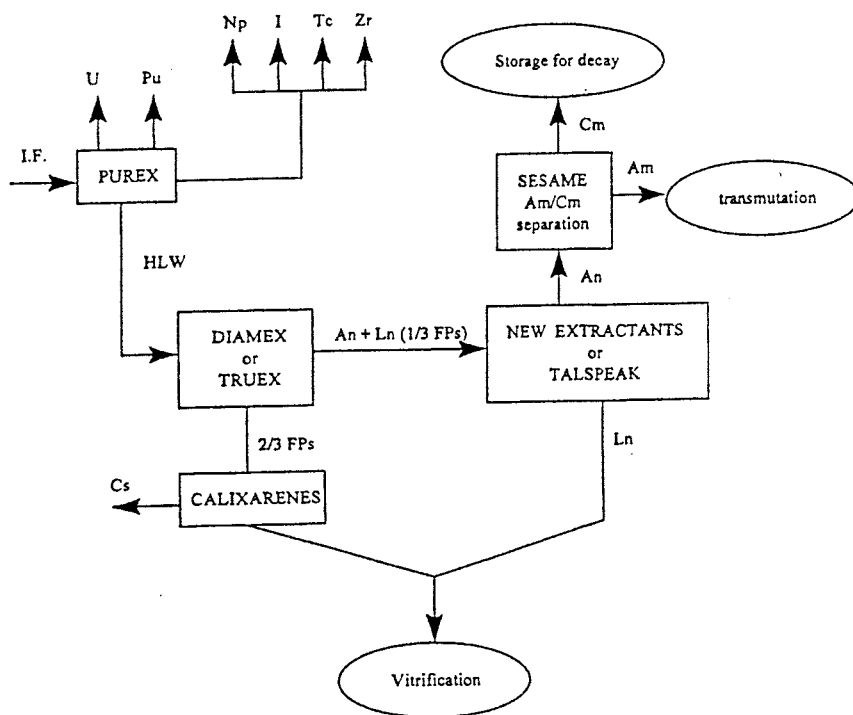


Figure 1.1. General flow chart of operations required for the separation of long-lived radionuclides[CEC]

The TRUEX process and the TALSPEAK process are two methods designed to separate the An(III) from the Ln(III) in the spent nuclear fuel but, unfortunately, both processes are based on phosphorus containing extractants [CHO 95] which is incompatible with the demand that all extractants used should be completely incinerable.

There is a great deal of interest in the reagent, 2,4,6-tri-(2-pyridyl)-1,3,5-triazine, TPTZ, and its derivatives [CEC] which in synergy with an organic acid is able to separate An(III) from Ln(III).

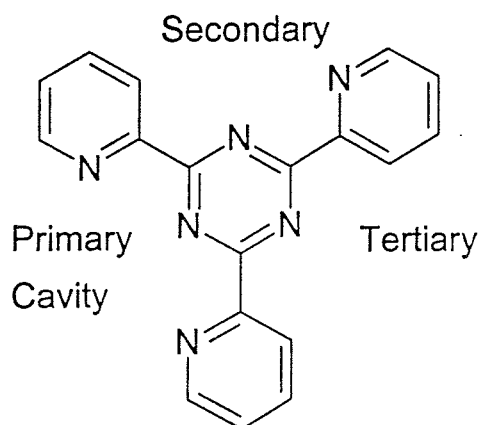


Figure 1.2. Structure of TPTZ

Due to poor hydrophobic properties, especially in the protonated form, TPTZ has a high solubility in the aqueous phase. However, it has been shown that the

An(III)-Ln(III) separation is possible with synergistic extraction from nitric acid with TPTZ and 2-bromo decanoic acid in decanol [VIT 84].

Co-ordination is believed to occur between the metal ion and the three nitrogen atoms of the "Primary Cavity" (Fig. 1.3.). Nitrate ions are also needed to achieve an uncharged complex.

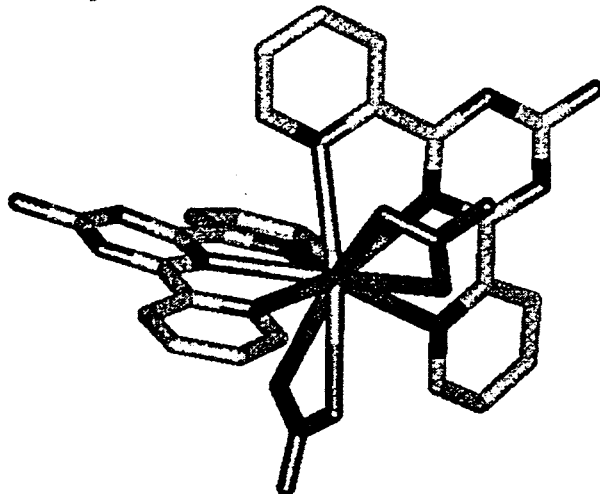


Figure 1.3. Molecular structure in the solid phase of 4-Amino-2,6-di(pyridyl)-1,3,5-triazine and $Pb(NO_3)_2$, prepared in this work, as an example of the complexation between a metal ion and the "Primary Cavity"

To improve the extraction behaviour and simplify the synthesis new extractants have been considered. The general idea is to substitute one of the pyridyl rings on the triazine-ring of TPTZ with an alkyl chain to make the reagent more lipophilic but still keep the "Primary Cavity" intact.

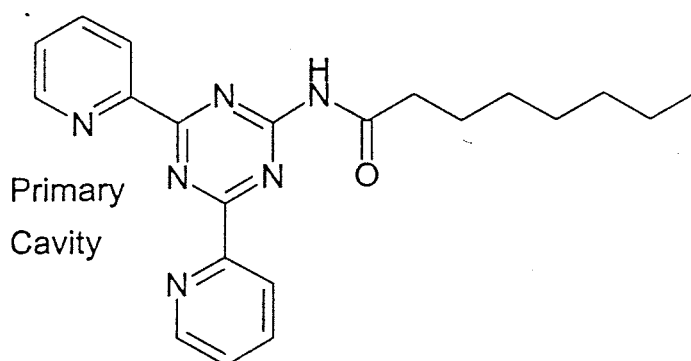


Figure 1.4. Structure of 4-octanoyl amino-2,6 di(2-pyridyl)-1,3,5 triazine (OADPTZ)

The aim of this report has been to synthesise 4-octanoyl amino-2,6 di(2-pyridyl)-1,3,5 triazine (OADPTZ), and to evaluate its extraction ability.

2. Theory

2.1. Distribution ratio

The distribution of a solute, M, between two immiscible liquid phases is the key feature in solvent extraction. The distribution ratio or the D -value, D_M , is defined as:

$$D_M = \frac{[M]_{\text{tot,org}}}{[M]_{\text{tot,aq}}} = \frac{\text{Total concentration of M in the organic phase}}{\text{Total concentration of M in the aqueous phase}} \quad (2.1.1)$$

If the D -values of two solutes differ then it is possible to separate them by solvent extraction. The more they differ, the more efficient separation. When dealing with radionuclides the determination of D -values usually becomes trivial. If R_{org} , R_{aq} , $R_{0,\text{org}}$ and $R_{0,\text{aq}}$ are the count rates of the organic phase, aqueous phase and the background sample respectively and ψ is the detection efficiency then we have:

$$D_M = \frac{(\psi_{\text{org}} \cdot R_{\text{org}} - \psi_{0,\text{org}} \cdot R_{0,\text{org}}) / V_{\text{org}}}{(\psi_{\text{aq}} \cdot R_{\text{aq}} - \psi_{0,\text{aq}} \cdot R_{0,\text{aq}}) / V_{\text{aq}}} \quad (2.1.2)$$

where V represent the sample volumes. If we use the same detector and the same geometry for each phase, i.e. $\psi_{\text{org}} = \psi_{\text{aq}} = \psi_0$ then equation (2.1.2) reduces to:

$$D_M = \frac{(R_{\text{org}} - R_{0,\text{org}}) / V_{\text{org}}}{(R_{\text{aq}} - R_{0,\text{aq}}) / V_{\text{aq}}} \quad (2.1.3)$$

The separation factor, F , between two extracted species, 1 and 2, is defined as:

$$F = \frac{D_{M1}}{D_{M2}} \quad (2.1.4)$$

There is a statistical uncertainty, σ_D , attached to the D -values that comes from the activity measurements. σ_D can be calculated according to:

$$\sigma_D = D_M \cdot \sqrt{\frac{(R_{\text{aq}} / t_{\text{aq}} + R_{0,\text{aq}} / t_{0,\text{aq}})}{(R_{\text{aq}} - R_{0,\text{aq}})^2} + \frac{(R_{\text{org}} / t_{\text{org}} + R_{0,\text{org}} / t_{0,\text{org}})}{(R_{\text{org}} - R_{0,\text{org}})^2}} \quad (2.1.5)$$

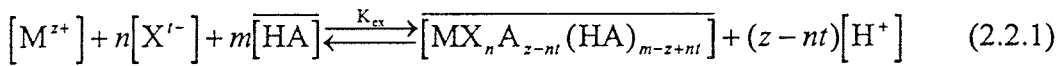
Important to note is that σ_D does not consider the pipetting error and the case of incomplete phase separation.

2.2. Metal extraction

General conditions for the extraction of metal ions from an aqueous phase to an organic phase are that the metal complex to be extracted must be uncharged in the organic phase and that it must be lipophilic enough to remain in the organic phase once it has been extracted. The extraction mechanisms for the two extractants, 2-bromodecanoic acid and OADPTZ, are different but they reinforce each other in what is called a synergistic effect. This means that the extraction effect of the two extractants together is better than each extractant alone.

2.2.1. Extraction with 2-bromodecanoic acid

2-bromodecanoic acid extracts by a cation exchange mechanism. If M^{z+} is the cation extracted, X^{t-} the anion in the aqueous solution (NO_3^- in the case of a HNO_3 -solution) and HA the extractant, then, if the formed complex is insoluble in the aqueous phase, the cation exchange mechanism can be written as:



where $nt \leq z$. K_{ex} is the extraction constant defined as follows:

$$K_{ex} = \frac{[\overline{MX_n A_{z-nt} (HA)_{m-z+nt}}] [H^+]^{z-nt}}{[M^{z+}] [X^{t-}]^n [\overline{HA}]^m} \quad (2.2.2)$$

If only one extracted species is considered then the distribution ratio can be expressed as:

$$\log D_M = \log K_{ex} - (z-nt) \log [H^+] + n \log [X^{t-}] + m \log [\overline{HA}] \quad (2.2.3)$$

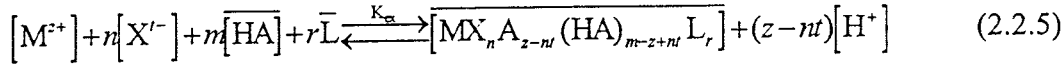
When a HNO_3 -solution is used as the aqueous phase, $[H^+] = [NO_3^-]$ and $t=1$, then equation (2.2.3) reduces to:

$$\log D_M = \log K_{ex} - z \log [H^+] + m \log [\overline{HA}] \quad (2.2.4)$$

It has been shown [VIT 84] that extraction with 2-bromodecanoic acid alone does not give a significant separation between the trivalent actinides and the trivalent lanthanides.

2.2.2. Extraction with 2-bromodecanoic acid and TPTZ derivatives

TPTZ extracts with a solvation mechanism [VIT 84]. The synergistic extraction mechanism with cation exchange and solvation extraction mechanism can, if L is the extracting ligand, be written as ($nt \leq z$):



K_{ex} is expressed, analogous to equation (2.2.2), as:

$$K_{ex} = \frac{[MX_n A_{z-nt} (HA)_{m-z+nt}][H^+]^{z-nt}}{[M^{z+}][X^{t-}]^n [\overline{HA}]^m [\overline{L}]^r} \quad (2.2.6)$$

Analogous to equation (2.2.4) the distribution ratio, D_M , can, if a HNO_3 -solution is used as the aqueous phase, be written as:

$$\log D_M = \log K_{ex} - z \log [H^+] + m \log [\overline{HA}] + r \log [\overline{L}] \quad (2.2.7)$$

By investigating the D -value at different $[H^+]$ and then plotting $\log D_M$ versus $\log [H^+]$ the slope should correspond to the ionic charge of the metal ion extracted.

2.3. Measurement of $[H^+]$

The acidic solutions needed for reprocessing are far from ideal which makes accurate measurements of the H^+ -concentration, $[H^+]$, very difficult. Measuring pH is not good enough since pH is defined as:

$$pH = -\log([H^+] \gamma_{H^+}) \quad (2.3.1)$$

where γ_{H^+} = activity factor and γ_{H^+} is difficult to estimate correctly at low pH. Since the D -value is a function of $[H^+]$ a correlation of measured pH to $[H^+]$ is necessary in order to plot D_M versus $[H^+]$. This correlation is achieved by measuring pH in nitric acid solutions with different H^+ -concentrations and the same ionic strengths as in the solvent extraction studies, covering the pH-range studied. The H^+ -concentration can then be determined by Gran titration.

2.3.1 Gran titrations

The methodology behind a Gran titration of a strong acid with a strong base is quite simple. If a volume V of acid of initial concentration $[H^+]$ is titrated with a volume v of strong base of concentration B and pH is measured, then we may use the Gran functions defined as [ROS 65]:

$$\phi = (V + v) \cdot [H^+] \gamma_{H^+} = (V + v) \cdot 10^{-pH} \quad v \leq v_e \quad (2.3.2)$$

$$\phi' = (V + v) / [H^+] \gamma_{H^+} = (V + v) \cdot 10^{pH} \quad v \geq v_e \quad (2.3.3)$$

By plotting ϕ and ϕ' against v and extrapolating them to zero, the equivalence volume v_e can be obtained. The equivalence volume, v_e , is obtained as the volume v where the extrapolated ϕ and ϕ' functions cross the abscissa. Once v_e has been determined the initial $[H^+]$ of the acid may be calculated using the formula:

$$[H^+] = \frac{B \cdot v_e}{V} \quad (2.3.4)$$

However, sometimes, especially at high ionic strengths, the linearity of the Gran functions are far from perfect. This is due to the fact that γ_{H^+} is not constant during the titration. Then, if the plots are linear nearer the equivalence point, the value of v_e must be obtained from this region alone.

3. EXPERIMENTAL

3.1. Synthesis

All starting materials were used as supplied, except for pyridine (GPR-grade), which was dried twice over 4 Å molecular sieves. The octanoyl chloride, guanidine hydrochloride and 2-cyano-4-methylpyridine were supplied by Lancaster Synthesis. Microanalyses were carried out by Medac Ltd., Brunel University. ^1H and ^{13}C (400 MHz) NMR spectra were obtained on a JEOL JNM-EX 400 spectrometer using either CDCl_3 or DCl (20 wt %) in D_2O .

3.1.1. Preparation of 4-amino-2,6-di(pyridyl)-1,3,5 triazine (ADPTZ)

The synthesis was carried out as described previously [CAS 58].

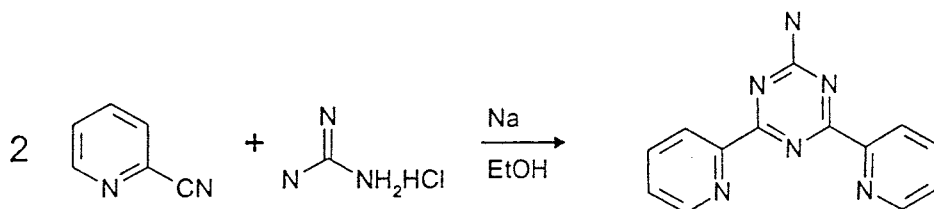
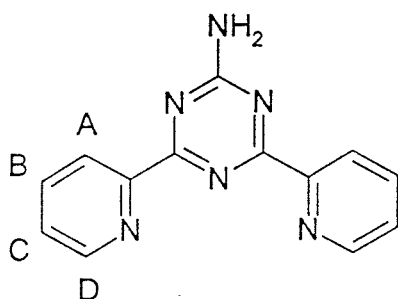


Figure 3.1. ADPTZ synthesis-route

Guanidine hydrochloride (25.06 g, 0.262 mol) was dissolved in 200 ml of absolute ethanol. After the clear solution had been cooled in an ice-bath, freshly cut sodium metal (6.53 g, 0.284 mol) was added in small pieces over 30 minutes and left to react for 45 minutes. The precipitated sodium chloride was removed by filtration and washed with 70 ml of absolute ethanol. Then 2-cyano pyridine (62.04 g, 0.596 mol) was added to the solution and the mixture was left to reflux for 18 h.

The off-white precipitate (42.1 g), which was collected by filtration, was washed with absolute ethanol. The precipitate was then dried under vacuum in a desiccator (Yield: 36.7 g, 56%). The compound (4-Amino-2,6 di(pyridyl)-1,3,5-triazine) was analysed by ^1H -NMR.



Since the solvent used was DCl it was difficult to get accurate shifts but the integrals were correct :
A (2H, d), B (2H, tr), C (2H, tr), D (2H, d)

Figure 3.2. Structure of 4-Amino-2,6-di(pyridyl)-1,3,5-triazine, labelled for NMR assignment

3.1.2. Acylation of ADPTZ with octanoyl chloride

The synthesis was carried out according to the method published previously [BEI 96] using dry glassware under a nitrogen atmosphere.

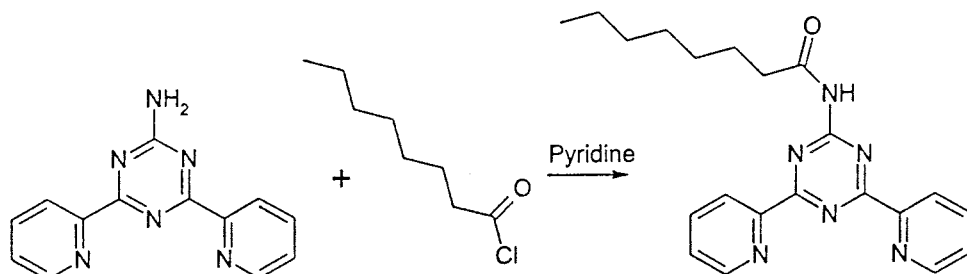


Figure 3.3. Preparation of 4-octanoyl amino-2,6 di(2-pyridyl)-1,3,5 triazine (OADPTZ)

ADPTZ (5 g, 0.02 mol) in 250 ml pyridine was heated to 90°C. Octanoyl chloride (3.25 g, 0.02 mol) was then added over a period of 15 seconds. The solution was then refluxed for 45 minutes leaving a brown, clear solution. Most of the pyridine was removed at 60°C under vacuum and 200ml of CH₂Cl₂ was added to the resulting brown liquid. After a small amount of undissolved solid had been filtered off, the solution was washed twice with NaHCO₃, twice with deionised water and dried with Na₂SO₄. A brown oil was formed after the CH₂Cl₂ had been removed under vacuum. The oil was dissolved in ethyl acetate and left overnight. The following day a white solid had formed which was filtered off and discarded. Hexane was added to the remaining solution and left for 36 h. A whitish solid had precipitated. This was collected by filtration and washed with ethyl acetate (Yield: 1.92 g, 25%). Melting point was 144°C. The compound was analysed by ¹H-NMR, ¹³C-NMR and CHN analysis. (Analysis: Calculated for C₂₁H₂₄N₆O, C: 67.0%, H: 6.4%, N: 22.3%, Found, C: 66.7%, H: 6.4%, N: 22.4 %)

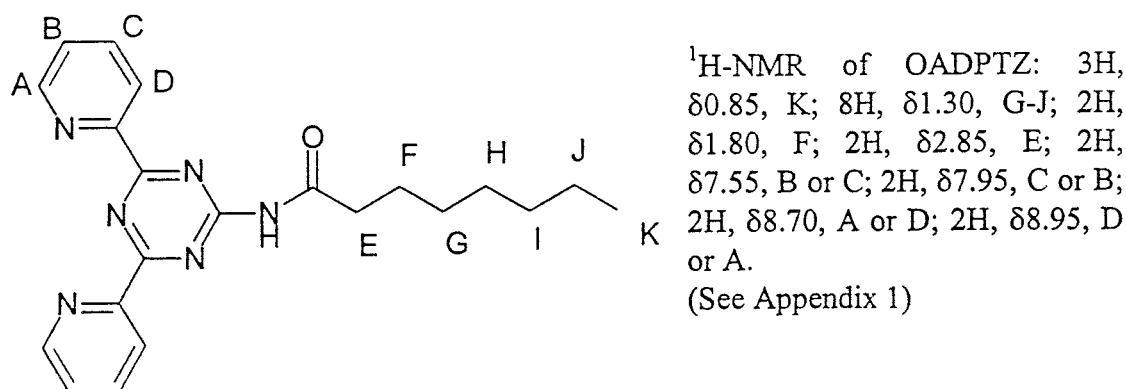


Figure 3.4. Structure of 4-octanoyl amino-2,6 di(2-pyridyl)-1,3,5 triazine, OADPTZ, labelled for ¹H-NMR assignment.

The ¹³C-NMR spectra clearly shows 7 aromatic carbons with δ14-38 and 8 aliphatic carbons with δ125-173. (See appendix 2)

3.1.3. Preparation of 4-amino-2,6,di(4-methyl pyridyl)-1,3,5 triazine (ADMPTZ)

The synthesis was carried out according to the method previously published [CAS 58].

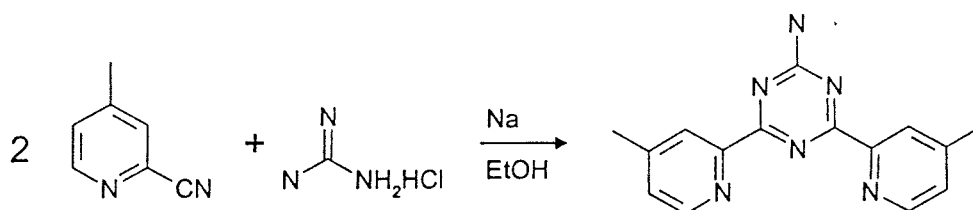
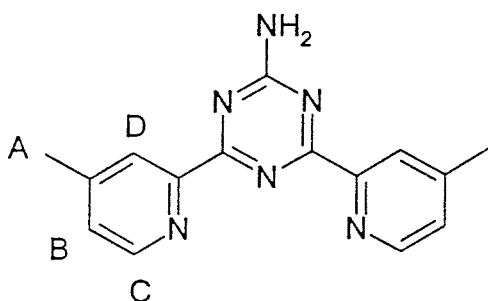


Figure 3.5. ADMPTZ synthesis-route

Guanidine hydrochloride (7.27 g, 0.076 mol) was dissolved in 64 ml of absolute ethanol. After the clear solution had been cooled in an ice-bath, freshly cut sodium metal (1.75 g, 0.076 mol) was added in small pieces over 20 minutes and left to react for 45 minutes. The precipitated sodium chloride was removed by filtration and washed with 23 ml of absolute ethanol. Then 2-cyano-4-methyl pyridine (15.0 g, 0.127 mol) was added to the solution and the mixture was left to reflux for 16.5h.

The brownish-white precipitate (16.1 g) collected after filtration, was washed with absolute ethanol and refluxed with 2-methoxyethanol for 1 h. The precipitate was collected by filtration and dried under vacuum (Yield: 13.8 g, 65%). The compound was analysed by NMR and CHN analysis. (Analysis: Calculated for C₁₅H₁₄N₆, C: 64.4, H: 5.1, N: 30.2, Found, C: 64.3, H: 5.1, N: 30.2 %)



¹H NMR of 4-Amino-2,6,di(4-methyl pyridyl)-1,3,5-triazine. Since the solvent used was DCl it was difficult to get accurate shifts but the integrals were correct :

A (6H, s), B (2H, d), C (2H, d), D (2H, s)

Figure 3.6. Structure of 4-Amino-2,6,di(4-methyl pyridyl)-1,3,5-triazine, labelled for NMR assignment.

3.1.4. Acylation of ADMPTZ with octanoyl chloride

The synthesis was carried out according to the method published previously [BEI 96] using dry glassware under a nitrogen atmosphere.

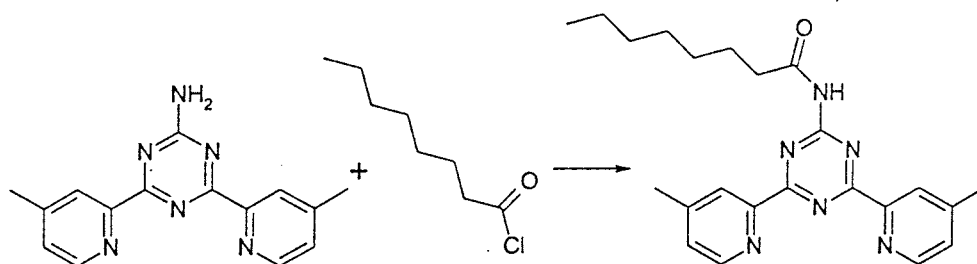


Figure 3.7. Preparation of 4-octanoyl amino-2,6 di(4-methyl 2-pyridyl)-1,3,5 triazine

4-Amino-2,6,di(4-methyl pyridyl)-1,3,5-triazine (1 g, 3.6 mmol) in 200 ml pyridine was heated to 90°C. Octanoyl chloride (0.58 g, 3.6 mmol) was then added over a period of 30 seconds. Although the solution was refluxed for 40 minutes, no dissolution of the ADMPTZ appeared to take place. The triazine starting material did not have the required solubility in pyridine for the reaction to take place. The preparation was terminated at this stage.

3.2. Complexation studies

Data for the crystals were collected at 293(2) K with Mo-K α radiation (λ 0.71073 Å) using the MARresearch image-plate system. Each crystal was placed at 100 mm from the plate. Ninety-nine frames were measured at 2° intervals with a counting time of 10 minutes. Data analysis was carried out with the XDS program. The structures were solved using heavy-atom methods with the SHELXS 86 program. Refinement of the structures was then done using the SHELXL program. All calculations were carried out on Silicon Graphics R4000 Workstations at the University of Reading.

3.2.1. ADPTZ and Pb(NO₃)₂

Pb(NO₃)₂-crystals (6.3 mg, 0.019 mmol) were ground to a fine powder and mixed with ADPTZ (4.7 mg, 0.019 mmol). After 15 ml of methanol had been added, the mixture was refluxed for a short time until a clear solution had been formed. The solution was allowed to cool down slowly and then left to evaporate slowly. Crystals suitable for single X-ray crystallography were formed after three weeks.

3.2.2. ADMPTZ and Ni(NO₃)₂·6H₂O

Ni(NO₃)₂·6H₂O (6.8 mg, 0.023 mmol) was mixed with ADMPTZ (6.1 mg, 0.022 mmol). After 7 ml of methanol had been added, the mixture was refluxed for a short time until a clear solution had been formed. The solution was allowed to cool down slowly. The solution was left to evaporate slowly. Crystals suitable for single X-ray crystallography were formed after two weeks.

3.2.3. ADMPTZ and Nd(NO₃)₃·6H₂O

Nd(NO₃)₃·6H₂O (12.2 mg, 0.028 mmol) was mixed with ADMPTZ (7.5 mg, 0.027 mmol) and a small amount of acetonitrile was added. The mixture was refluxed and acetonitrile was added until a clear solution had been formed. The solution was allowed to cool down slowly. The solution was left to evaporate slowly. Crystals suitable for single X-ray crystallography were formed after two weeks.

3.3. Extraction studies

The aqueous phase was prepared by diluting concentrated nitric acid (65%, Riedel-de Haën) with milli-Q grade water. The organic phase was composed of 0.02 M OADPTZ and 1 M 2-bromodecanoic acid (~98% (AT), Fluka) in tert-Butylbenzene (TBB) (99%, Acros). ^{147}Pm was provided by Nycomed Amersham and ^{234}Th was prepared according to the method [ALB] which is a modified version of the previously published method [RYD 53]. The sodium hydroxide (NaOH, 1/10 val = 4.001g \pm 0.1%, provided by P-H TAMM Laboratorier AB) used for the Gran-titrations, was prepared in accordance with the instructions given in the package and used within 3 days after preparation. A PHM 64 RESEARCH pH METER from Radiometer Copenhagen was used for the pH-measurements. (Calibrations of the pH-detector were done with Radiometer's 1.09 and 4.01 buffers.) γ -spectroscopy measurements were performed with an HPGe-detector (EG&G ORTEC). A liquid scintillation counter (WALLAC LKB 1219 RACKBETA) was used for β -measurements. The scintillation cocktail used was Emulsifier SafeTM, provided by Packard.

3.3.1. Radionuclides

The radionuclides used in these experiments were the lanthanides $^{152,154}\text{Eu}$ and ^{147}Pm , and the actinides ^{234}Th and ^{241}Am .

- ^{147}Pm : β -emitting nuclide with a half-life of 2.62 years, measured with a liquid scintillation counter.
- $^{152,154}\text{Eu}$: The stock solution used contained $^{152,154}\text{Eu}$. ^{152}Eu was measured with an HPGe-detector at the γ energy 344.29 keV. ^{152}Eu is a β - and γ -emitting nuclide with a half-life of 13.33 years.
- ^{234}Th : β - and γ -emitting nuclide with a half-life of 24.10 days. The β -decay of the nuclide was measured with a liquid scintillation counter.
- ^{241}Am : α - and γ -emitting nuclide with a half-life of 432.6 years. γ was measured at 59.54 keV.

3.3.2. Procedure

Three types of experiments have been conducted. First, a solubility test to investigate the solubility of OADPTZ in TBB. Second, Gran-titrations to correlate the pH to the actual H^+ -concentration and, third, test tube experiments at room temperature to determine the distribution ratio for some metals as a function of the H^+ -concentration.

3.3.3. Solubility test

OADPTZ (0.015 g, $4.0 \cdot 10^{-5}$ mol) was diluted to 2 ml with TBB in a flask, vigorously shaken for several minutes and left overnight without showing any signs of dissolving. The same test was repeated once again using heat with the same result. OADPTZ (0.0757 g, $2.0 \cdot 10^{-4}$ mol) and 2-bromodecanoic acid (2.5630 g, 0.01 mol) were diluted to 10 ml with TBB in a flask. The OADPTZ dissolved after it had been shaken for several minutes and left to stand for 1 hour. A clear, yellowish solution was formed.

3.3.4. Gran-titrations

HNO_3 -solutions were prepared in 0.004, 0.01, 0.02, 0.05, 0.125 and 0.25 M concentrations. The acid solutions were then titrated with 0.100 M NaOH, except for the case of 0.004 M HNO_3 where 0.010 M NaOH-solution was used. The equivalence volume, v_e [ROS 65], was then obtained by extrapolation of the Gran functions to zero. The v_e was then used to calculate the $[H^+]$ of the nitric acid solutions (c.f. equation 2.3.4.) and a correlation between pH and $[H^+]$ was obtained by second order polynomial regression.

All titrations were carried out in the same way. The pH-meter was calibrated with pH 1.09 and pH 4.01 buffers, immediately before the titration. The acid and the base were stored at room temperature and no heating was used during the titration. The solution was left to equilibrate for 1 minute after each addition of base.

3.3.5. Test tube experiments

General procedure:

The aqueous phase (1 ml), containing the radionuclides, were prepared and mixed with 1 ml of the organic phase (0.02 M OADPTZ and 1 M 2-bromodecanoic acid in TBB) in a 3.5 ml test tube. The mixture was shaken vigorously for 5 minutes and left 10 minutes for phase separation. The sample was then centrifuged at 4500 rpm for 5 minutes. When separating the two phases, care was taken not to contaminate the aqueous phase with organic phase. The pH was measured on the remaining aqueous phase immediately after samples from both phases were withdrawn. After the activity on the separated phases had been measured, D -values, statistical uncertainties- σ_D and the total addition of radioactivity to each sample were calculated.

$^{152,154}\text{Eu}$ and ^{241}Am :

Samples containing $^{152,154}\text{Eu}$ and ^{241}Am were prepared according to the general procedure. The samples was measured on an HPGe-detector.

^{147}Pm :

Samples containing ^{147}Pm were prepared according to the general procedure. After the samples were withdrawn, 15 ml of scintillation liquid was added to each sample and the count rate was measured on a liquid scintillation counter.

^{234}Th :

Samples containing ^{234}Th were prepared according to the general procedure. The withdrawal of samples were done immediately after the phase separation. The samples were then left to stand for 70 h in order to let ^{234}Th and its decay product ^{234}Pa reach a transient equilibrium [CHO 95]. Then, 15 ml of scintillation liquid was added to each sample and the count rate was measured on a liquid scintillation counter.

4. Results and Discussion

4.1. pH - [H⁺] correlation

By measuring pH on acid solutions used in the experiments and evaluating [H⁺] by using Gran titrations, a log[H⁺]-pH plot could be obtained. A log[H⁺]-pH correlation, valid for the pH-range studied, was then obtained by fitting data to a second order polynomial. The correlation was found to be:

$$\log[H^+] = 0.1024 \cdot (\text{pH})^2 - 1.3031 \cdot \text{pH} + 0.232$$

with an R^2 -value of:

$$R^2 = 0.9993$$

R is defined as:

$$R = \frac{n(\sum XY) - (\sum X)(\sum Y)}{\sqrt{[n\sum X^2 - (\sum X)^2][n\sum Y^2 - (\sum Y)^2]}}$$

where X and Y are the x- and y-values and n is the number of data points. This correlation was used throughout the experiments.

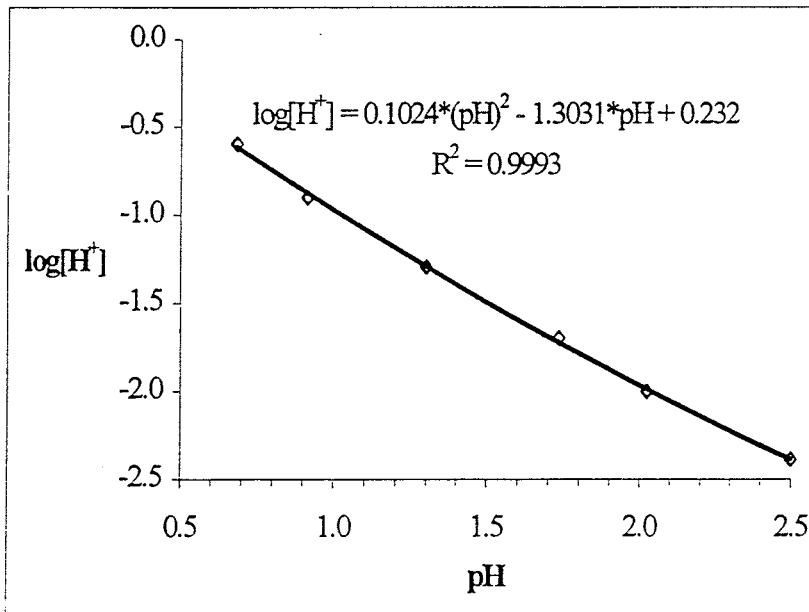


Figure 4.1.1. log[H⁺] - pH plot with data fitted to a second order polynomial

4.2. Metal extraction

4.2.1. Trivalent actinides versus trivalent lanthanides

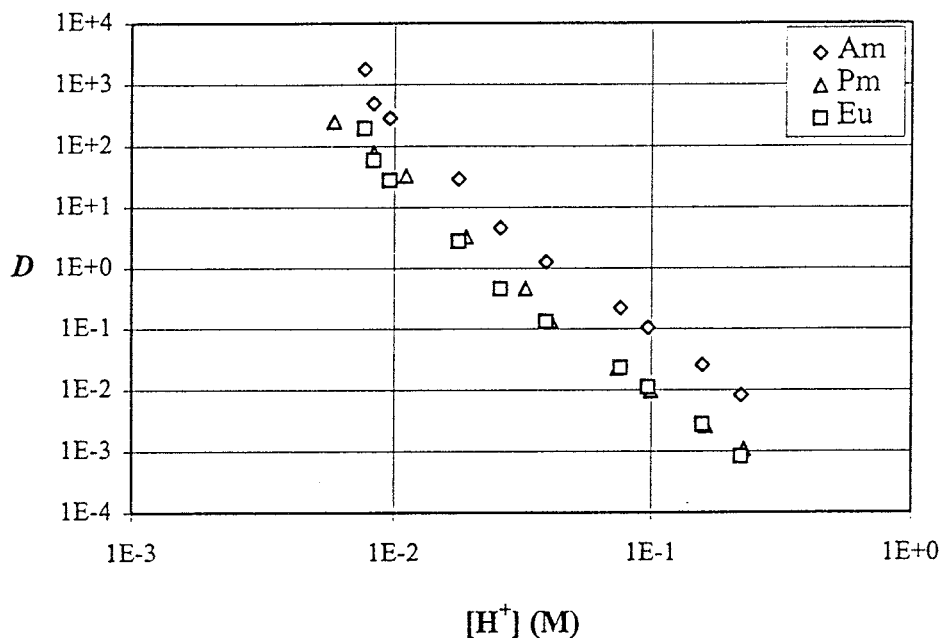


Figure 4.2. D - $[H^+]$ plot for Am-, Eu- and Pm-extraction from nitric acid with 0.02 M OADPTZ and 1 M 2-bromodecanoic acid in TBB.

The test tube experiments show that OADPTZ is a good extractant for both An(III) and Ln(III) at low $[H^+]$ but poorer when $[H^+]$ is higher than ~ 0.1 M. OADPTZ separates An(III) from Ln(III) well, $F \approx 7-10$, over the whole nitric acid concentration range. No significant difference in extraction between Eu and Pm was observed. This means that the ionic radii does not seem to be very important for the extraction. (For extraction data, see Appendix 3-4)

The D - $[H^+]$ lines are quite straight which implies that the ligand does not go over to the aqueous phase once protonated, at least not as much as in the case of TPTZ [OLS 95].

The slope when D is plotted versus $[H^+]$ using a logarithmic scale, is between -3.3 and -3.5 which, according to equation (2.2.7), should correspond to the ionic charge of the metal ion extracted if the ligand and HA concentrations are assumed to be constant. Deviations in ligand and HA concentrations because of protonation of ligand and adduct formation between ligand and HA at different HNO_3 concentrations could be one of the reasons for the higher slope.

4.2.2. Trivalent actinides versus tetravalent actinides

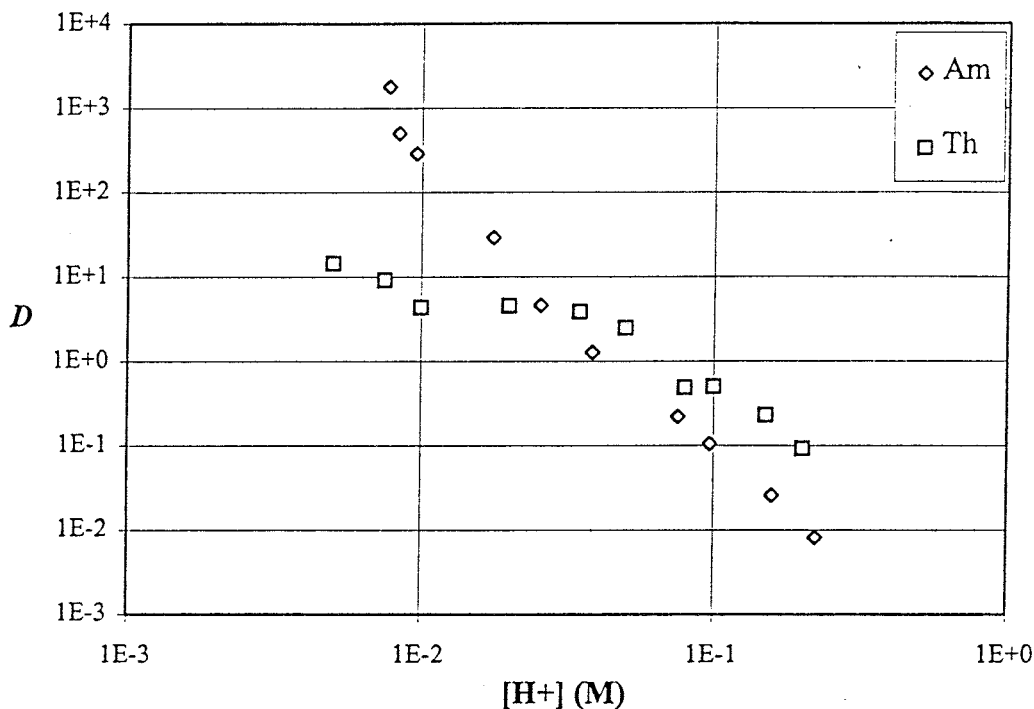


Figure 4.2. D - $[H^+]$ plot for Am- and Th-extraction from nitric acid with 0.02 M OADPTZ and 1 M 2-bromodecanoic acid in TBB.

There is a clear difference in the extraction of Th(IV) and Am(III). A possible reason for this difference could be slow kinetics when the extracted Th-complex polymerise in the organic phase which has been shown previously when carboxylate ions are present [MAD 75]. Furthermore, Th(IV), like all the other An(IV) ions, can form colloidal hydroxo complexes in aqueous solutions, even at very low metal concentrations. Moreover, at trace level Th(IV) can be engaged in pseudo-colloidal hydroxo complexes when Th(IV) traces are in the presence of an inactive metal ion present at slightly higher concentrations in the same solution. In that case, the behavior of Th(IV), trapped on the colloid of the foreign ion, is identical with that of this colloid [MAD 98].

4.3. Complexation studies

Crystallography can be used to study the co-ordination between a metal ion and different ligands. The crystal structure shows how the complex looks like in solid phase and might differ from the extracted complex in solution. To be able to discuss the different crystal structures it is necessary to know the relative size of the different metals involved in the crystals.

Ion	Ionic radii (pm) [GRE 84]
Pb ²⁺	119
Ni ²⁺	69
Nd ³⁺	129

4.3.1. Crystallisation of ADPTZ₂-Pb(NO₃)₂

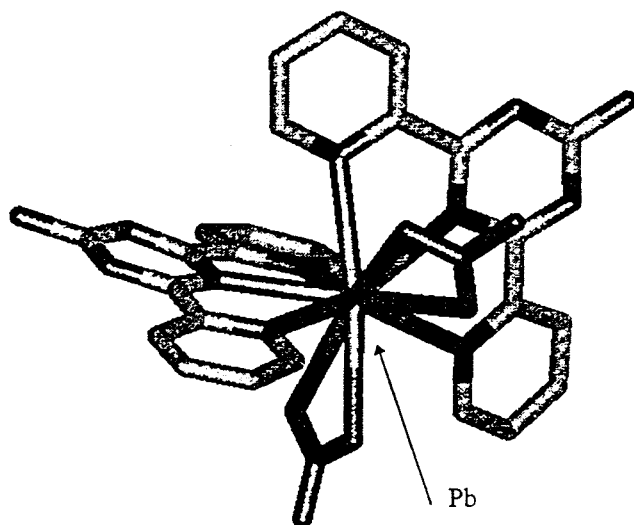


Figure 4.4. Molecular structure in the solid phase of ADPTZ₂-Pb(NO₃)₂

The lead ion is co-ordinated to three nitrogen atoms in the “Primary Cavity” in two ADPTZ molecules. The two ligands are almost perpendicular to each other. The relatively large Pb²⁺-ion also co-ordinates to two bidentate nitrates in order to neutralise the complex which makes the lead 10 co-ordinate.

4.3.2. Crystallisation of ADMPTZ₂-Ni(NO₃)₂·6H₂O

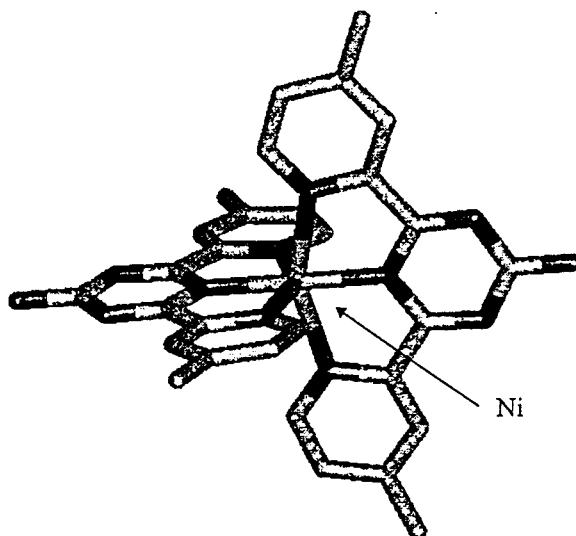


Figure 4.3.2. Molecular structure in the solid phase of ADMPTZ₂-Ni(NO₃)₂

The nickel ion is co-ordinated to the three nitrogen atoms in the "Primary Cavity" in two ADMPTZ molecules. The two ligands are almost perpendicular to each other. No nitrates were co-ordinated to the metal. Lack of space around the relatively small Ni²⁺ ion may be the reason for this.

4.3.3. Crystallisation of ADMPTZ-Nd(NO₃)₃·6H₂O

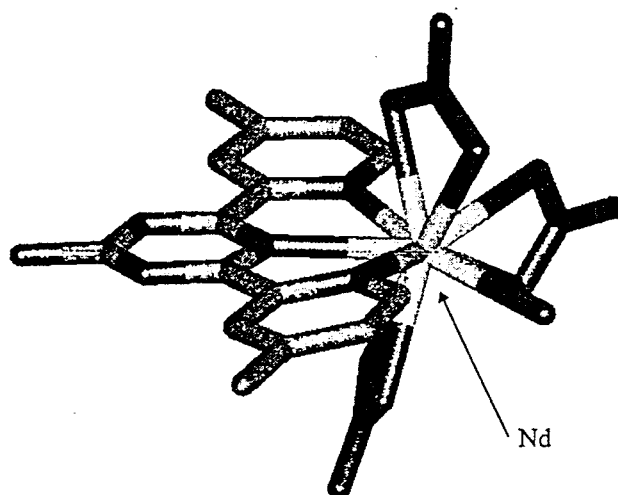


Figure 4.3.3. Molecular structure in the solid phase of ADMPTZ-Nd(NO₃)₃·H₂O

The trivalent neodymium ion is co-ordinated to three bidentate nitrates to make an uncharged complex. Only one ADMPTZ molecule was observed in the unit cell and since Nd is 10 co-ordinate the co-ordination sphere is filled by a water molecule.

5. Conclusions

Synergistic extraction from nitric acid with and 2-bromodecanoic acid in TBB has a separation factor of approximately 7-10 between the investigated trivalent actinides and trivalent lanthanides. This fact leads to the conclusion that the An(III)-Ln(III) separation is possible in this system.

The synthesis of OADPTZ was performed in two quite simple steps using relatively cheap starting materials with a final yield of approximately 15% with a satisfying purity, at least 98 %. This must be considered as acceptable considering that the synthesis was performed on a small scale and that no measures of optimising the synthesis had been taken. The conclusion must be that the method of synthesis probably is suitable for the development of new extractants.

6. Further investigations

The experiments performed in this work has shown that OADPTZ has a potential for the An(III)-Ln(III) separation. However, there are some further investigations to be done and some problems to be solved before the goal of finding a suitable ligand for the An(III)-Ln(III) separation is achieved:

- The organic acid, 2-bromodecanoic acid, used in the experiments must be replaced with an acid that obeys the CHON-principle.
- The radiolysis of OADPTZ at high dose rates must be investigated. What happens to the ligand when it is subjected to high dose rates? What decomposition products are formed and how do they affect the separation process?
- A modification of the ligand to improve the extraction at higher HNO₃-concentrations would be desirable.
- Precise experiments where the concentrations of 2-bromodecanoic acid, OADPTZ and HNO₃ are varied in order to determine the extraction mechanism.
- Experiments where the metal concentration is varied should be performed in order to investigate the loading capacity of the organic phase.

7. Acknowledgements

I have had the privilege to do one part of this work, the synthesis part, in England at the Department of Chemistry at the University of Reading and one part of the work, the extraction part, at the Department of Nuclear Chemistry at Chalmers University of Technology in Göteborg, Sweden.

There are quite a few persons that I would like to mention and express my gratitude to. First of all I want to mention my supervisors, Dr Peter B. Iveson in Reading, M.Sc. Anders Landgren, M.Sc. Åsa Enarsson and M.Sc. Lena Spjuth at Chalmers.

I would also like to mention the people at the Department of Chemistry in Reading, Mark, James "Want to go for a quick one?", Philippe and even John, for contributing in making my stay in England so pleasant. Dr. Michael J. Hudson is gratefully acknowledged for making it possible for me to come to England and for his kindness in letting me stay at his home for two weeks.

The people at Chalmers are all appreciated for the help they have given me and for the kindness that they have shown. I would especially want to mention Dr. Gunnar Skarnemark for always taking the time to answer questions concerning solvent extraction, chemistry and English. I would also like to thank Professor Jan-Olov Liljenzin for valuable discussions at those times when the progress of my work had come to a stand still.

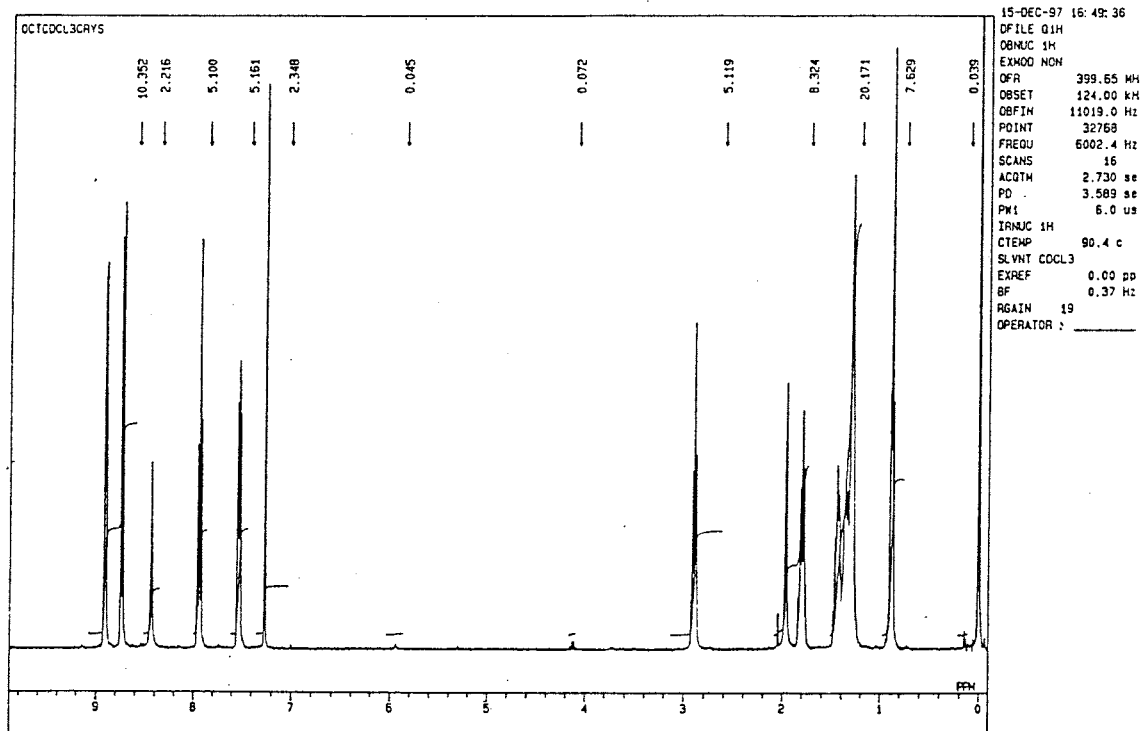
Finally and, perhaps, most of all I would like to thank my parents, Bo and Barbro, for their unconditional support through my many years of studying.

8. References

- [ALB] Y. Albinsson, C. Ekberg, *A method for preparing of ^{234}Th* , In Prep.
- [BEI 96] F.H. Beijer, R.P. Sijbesma, J.A.J.M. Vekemans, E.W. Meijer, H. Kooijman and A.L. Speek, *J. Org. Chem.* **1996**, 61, 6371
- [CAS 58] F.H. Case and E. Croft, *J. Org. Chem.* **1958**, 81, 905
- [CEC] Commission of the European Communities, Nuclear science and technology, *High-Level Liquid Waste Partitioning by Means of Completely Incinerable Extractants, Final report*, Contract N° F12W-CT91-0112
- [CHO 95] G. Choppin, J. Rydberg, J.O. Liljenzin, *Radiochemistry and nuclear chemistry*, Butterworth-Heinemann Ltd, **1995**
- [GRE 84] N.N. Greenwood and A. Earnshaw, *Chemistry of the elements*, Pergamon Press Ltd., **1984**
- [KOL 91] Z. Kolarik, *Separation of Actinides and Long-Lived Fission Products from High-Level Radioactive Wastes (A Review)*, Institut für Heiße Chemie, **1991**
- [MAD 75] Charles Madic, *Thèse de doctorat*, Université de Paris, **1975**
- [MAD 98] Charles Madic, *Personal communication*, **1998**
- [NAS 95] In "Separations of f-elements", Edited by K. L. Nash and G. R. Choppin, Plenum Press/New York, **1995**, pp 44
- [OLS 95] Å. Olsson, *Separation of Trivalent Actinides and Lanthanides by TPTZ*, Department of Nuclear Chemistry, Chalmers University of Technology, Göteborg, Sweden, **1995**
- [ROS 65] F.J.C. Rossotti and Hazel Rossoti, *Potentiometric Titrations Using Gran Plots*, *J. Chem. Edu.* **1965**, 42(7), 375
- [RYD 53] J. Rydberg, *Ark. Kemi*, **1953**, 62(39), 413
- [VIT 84] P. Vitorge, *Complexation de lanthanides et d'actinides trivalents par la tripyridyltriazine applications en extraction liquide-liquide*, Report **CEA-R-5270**, CEA Centre d'Etudes Nucleaires de Fontenoy-aux-Roses, 92(France), **1984**

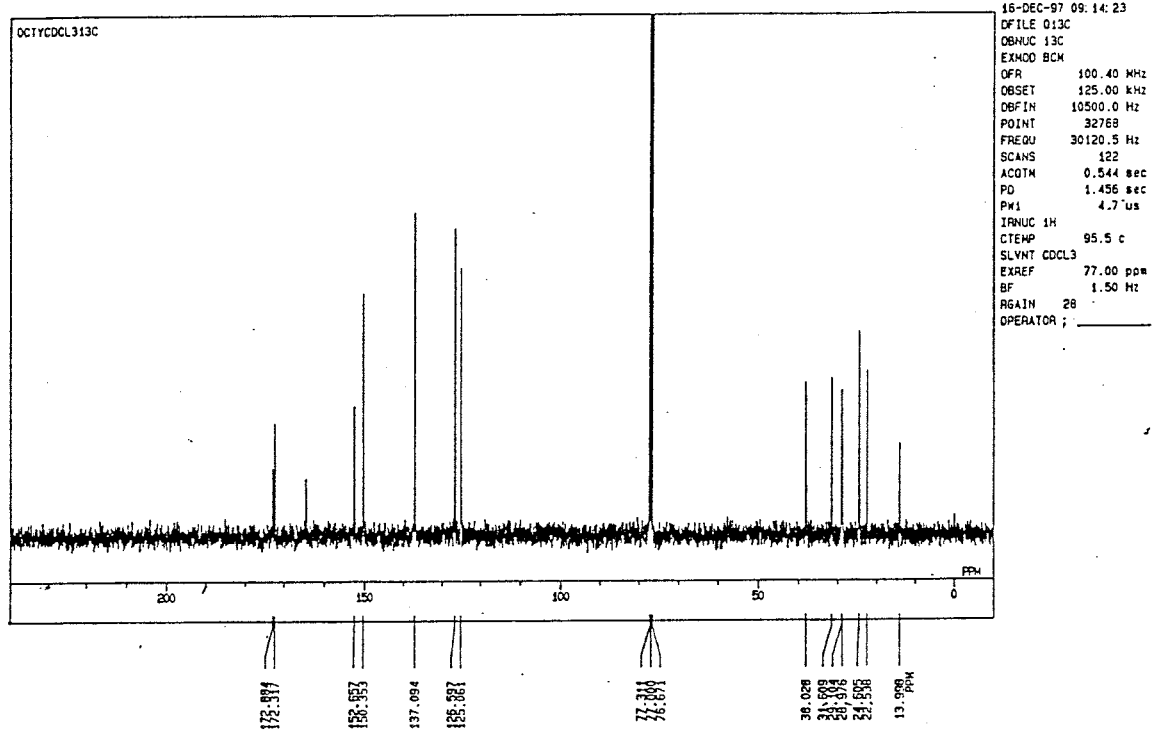
Appendix 1

¹H-NMR of 4-octanoyl amino-2,6 di(2-pyridyl)-1,3,5 triazine (OADPTZ)



Appendix 2

^{13}C -NMR of 4-octanoyl amino-2,6 di(2-pyridyl)-1,3,5 triazine (OADPTZ)



Appendix 3

Metal extraction ^{241}Am - ^{152}Eu

[HNO ₃]	pH	[H ⁺] (M)	$D(^{241}\text{Am})$	$\sigma_d(^{241}\text{Am})$	$D(^{152}\text{Eu})$	$\sigma_d(^{152}\text{Eu})$	Sep. factor =D(Am)/D(Eu)	Total counting rate (10 ³ cpm)	
								^{241}Am	^{152}Eu
0.005	2.17	7.70E-03	1.8E+3	5.8E-1	1.9E+2	4.1E-2	9.2	158.15	362.81
0.008	2.13	8.34E-03	5.0E+2	2.2E-1	5.9E+1	1.7E-2	8.4	156.58	349.70
0.010	2.06	9.60E-03	2.9E+2	9.6E-3	2.8E+1	3.7E-4	10.3	156.37	350.87
0.020	1.77	1.76E-02	2.9E+1	1.1E-2	2.8E+0	2.7E-4	10.5	155.47	352.45
0.035	1.60	2.57E-02	4.6E+0	5.7E-3	4.6E-1	1.9E-4	10.1	157.87	356.72
0.050	1.42	3.87E-02	1.3E+0	8.3E-4	1.3E-1	1.2E-4	9.7	154.69	361.45
0.080	1.14	7.58E-02	2.2E-1	6.1E-6	2.3E-2	1.1E-6	9.6	160.31	357.25
0.100	1.04	9.72E-02	1.1E-1	9.0E-5	1.1E-2	8.6E-6	9.55	159.31	341.22
0.150	0.85	1.58E-01	2.6E-2	1.1E-5	2.7E-3	8.1E-7	9.4	146.49	310.22
0.200	0.72	2.22E-01	8.2E-3	4.2E-6	8.3E-4	2.9E-7	9.9	167.66	369.10

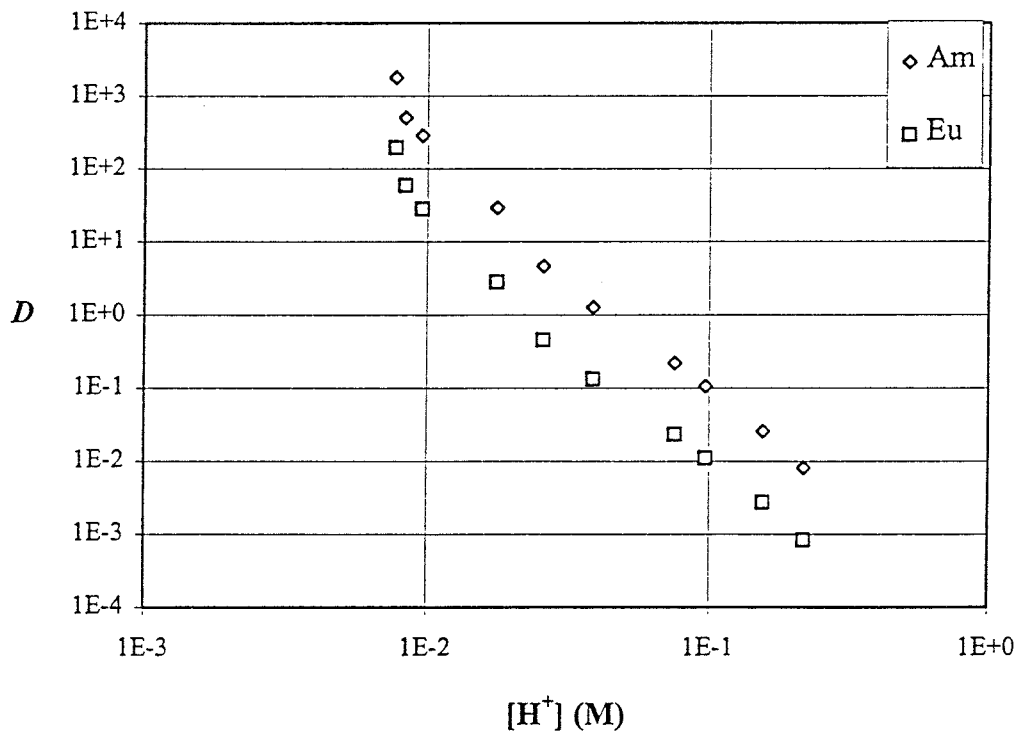


Figure A3.1 D - $[\text{H}^+]$ plot for Am and Eu extraction from nitric acid solutions with 0.02 M OADPTZ and 1 M 2-bromodecanoic acid in TBB

Slope analysis when all points except for the one with the lowest $[\text{H}^+]$, are taken into account gives:

	^{152}Eu	^{241}Am
slope	-3.313	-3.312
R^2	0.991	0.993

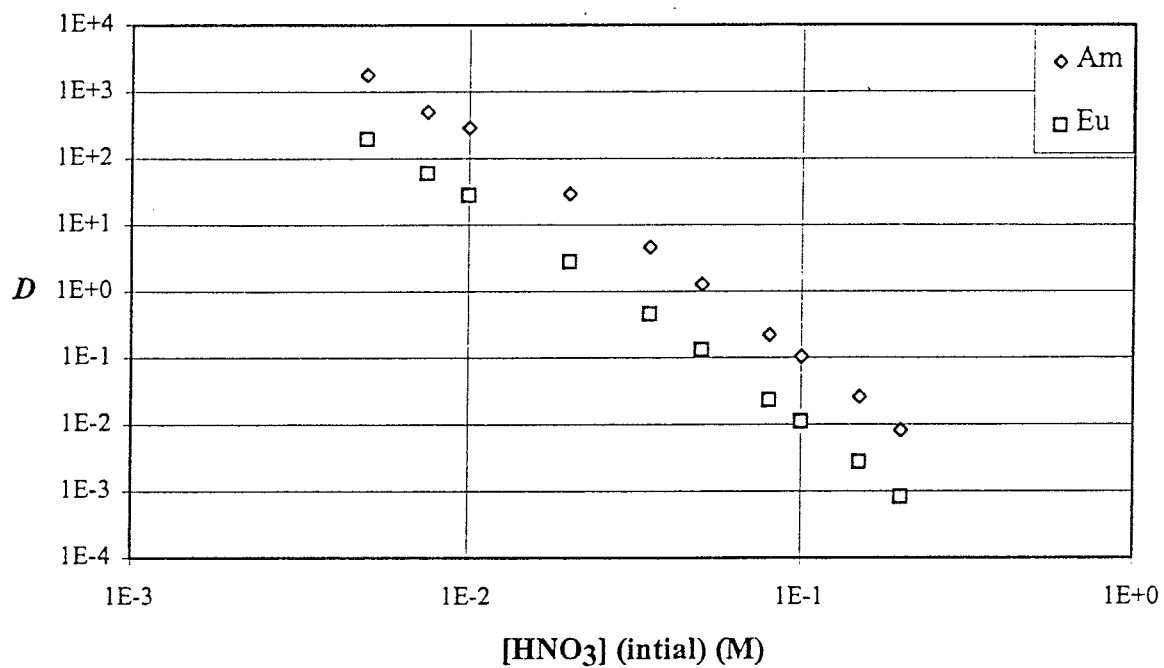


Figure A3.2 D - $[\text{HNO}_3]$ (initial)-plot for Am and Eu extraction from nitric acid with 0.02 M OADPTZ and 1 M 2-bromodecanoic acid in TBB

Appendix 4

Metal extraction ^{241}Am - ^{147}Pm

[HNO ₃]	pH	[H ⁺] (M)	D (^{147}Pm)	σ_D	Total counting rate (cpm)
0.005	2.31	5.86E-03	2.5E+2	4.4E+0	1.578E+5
0.0075	2.13	8.34E-03	7.9E+1	1.0E+0	1.567E+5
0.01	1.99	1.11E-02	3.3E+1	3.9E-1	1.567E+5
0.02	1.74	1.88E-02	3.3E+0	3.6E-2	1.556E+5
0.035	1.50	3.22E-02	4.6E-1	6.2E-3	1.548E+5
0.05	1.40	4.058E-02	1.3E-1	2.5E-3	1.485E+5
0.08	1.15	7.39E-02	2.3E-2	9.7E-4	1.543E+5
0.1	1.03	9.96E-02	9.6E-3	6.3E-4	1.574E+5
0.15	0.84	1.62E-01	2.6E-3	3.5E-4	1.574E+5
0.2	0.71	2.28E-01	1.1E-3	2.6E-4	1.592E+5

Since the Am- and Pm-experiments were performed in different test-tubes it was difficult to compare the test results directly. In order to get a rough estimate of the separation factor (F) between Am and Pm, a linear fit of respective experimental data were done.

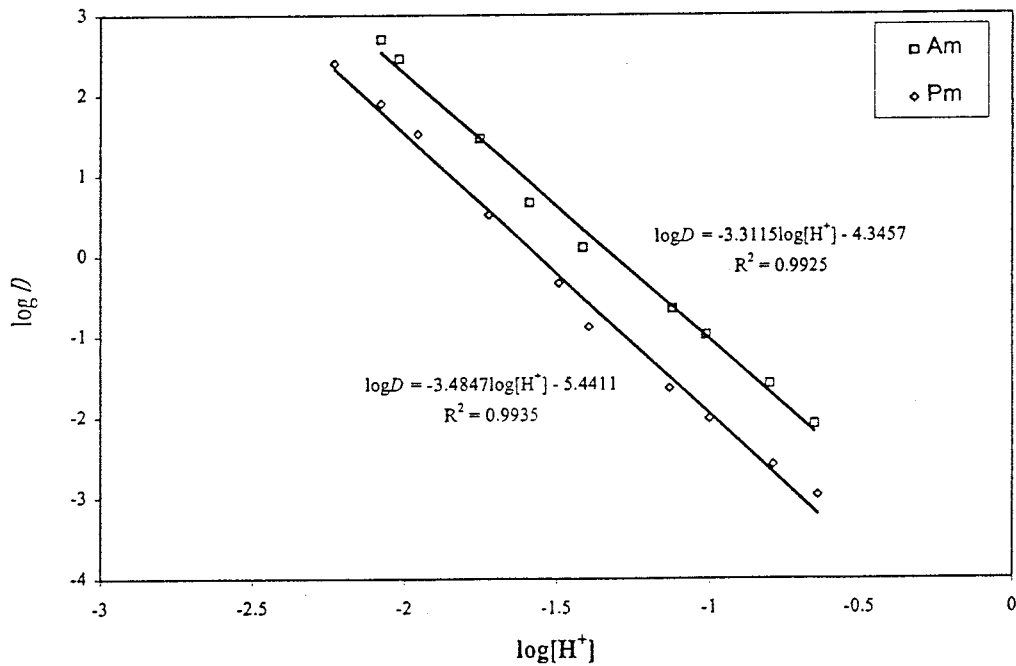


Figure A4.1 Linear fit of $\log D$ - $\log [H^+]$ data for Am and Pm extraction from nitric acid solutions with 0.02 M OADPTZ and 1 M 2-bromodecanoic acid in TBB

Slope analysis when all points, except for the Am-point with the lowest $[H^+]$, are taken into consideration gives:

	^{147}Pm
slope	-3.485
R^2	0.994

The F calculated from the linear regression was found to be between 5 and 10.

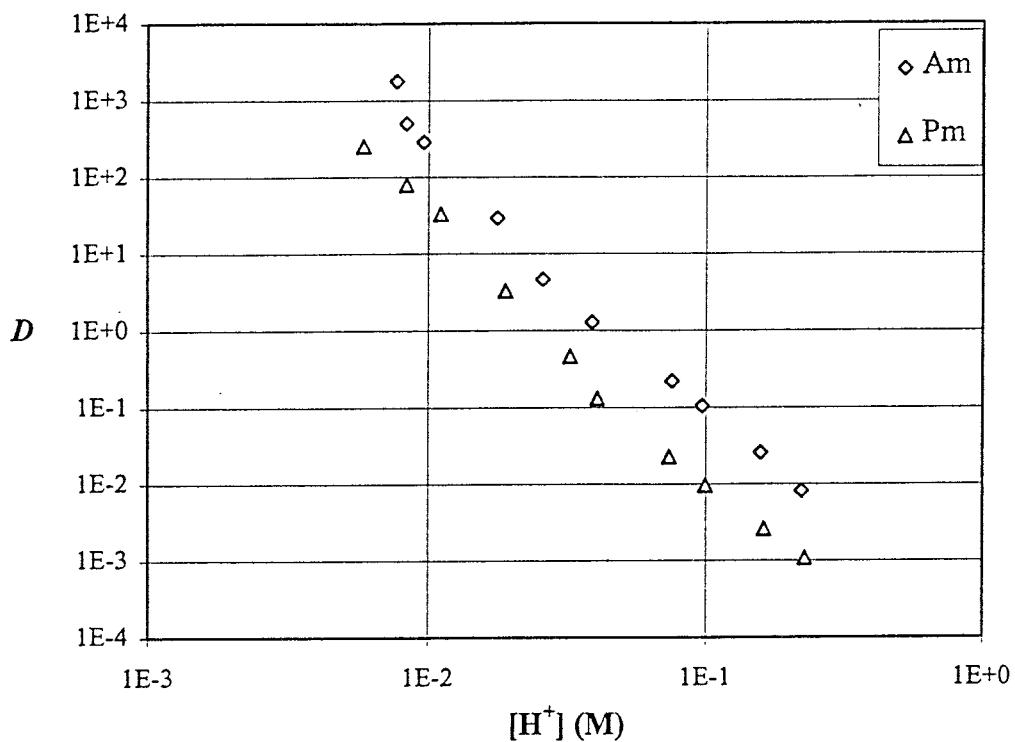


Figure A4.2 D - $[H^+]$ plot for Am and Pm extraction from nitric acid solutions with 0.02 M OADPTZ and 1 M 2-bromodecanoic acid in TBB

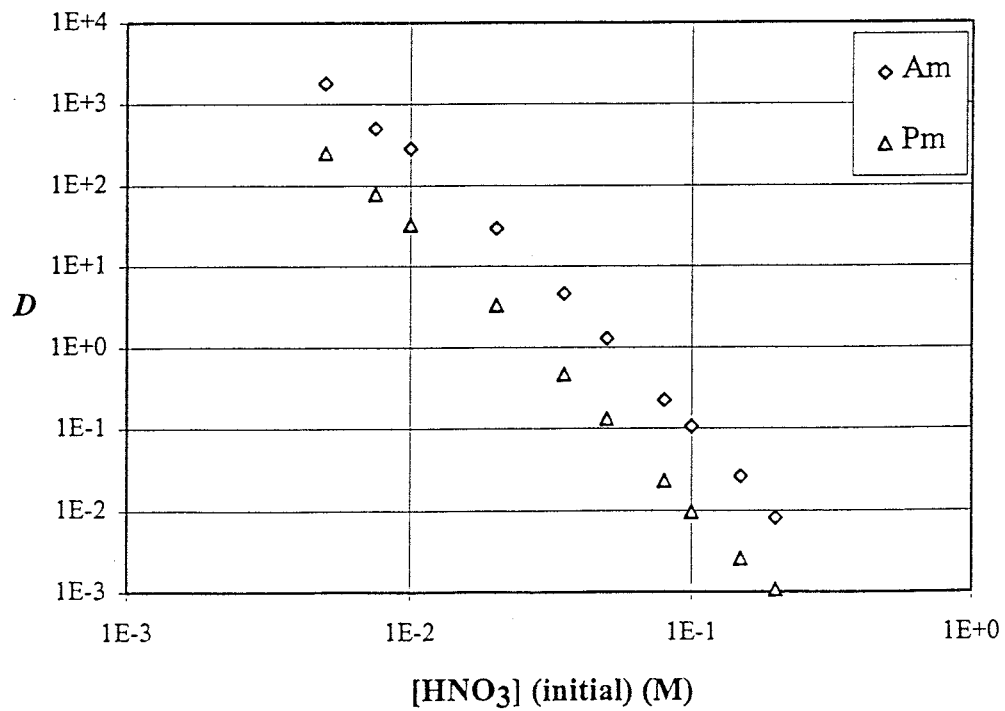


Figure A4.3 D - $[HNO_3]$ (initial) plot for Am and Pm extraction from nitric acid solutions with 0.02 M OADPTZ and 1 M 2-bromodecanoic acid in TBB

Appendix 5

Metal extraction ^{241}Am - ^{234}Th

[HNO ₃]	pH	[H ⁺] (M)	D (^{234}Th)	σ_D	Total counting rate (cpm)	Sample series
0.005	2.12	8.50E-3	1.4E+1	1.6E-1	6.174E+4	1
0.0075	2.00	1.08E-2	9.1E+0	1.1E-1	5.373E+4	2
0.01	1.82	1.58E-2	4.4E+0	5.3E-2	5.416E+4	2
0.02	1.71	2.01E-2	4.5E+0	5.5E-2	5.430E+4	2
0.035	1.52	3.07E-2	3.9E+0	4.6E-2	5.613E+4	2
0.05	1.40	4.06E-2	2.5E+0	3.2E-2	5.524E+4	2
0.08	1.17	7.04E-2	4.9E-1	9.6E-3	4.866E+4	2
0.1	1.07	9.01E-2	5.0E-1	9.2E-3	5.435E+4	1
0.15	0.89	1.43E-1	2.3E-1	5.4E-3	5.921E+4	1
0.2	0.74	2.11E-1	9.3E-2	3.3E-3	5.680E+4	1

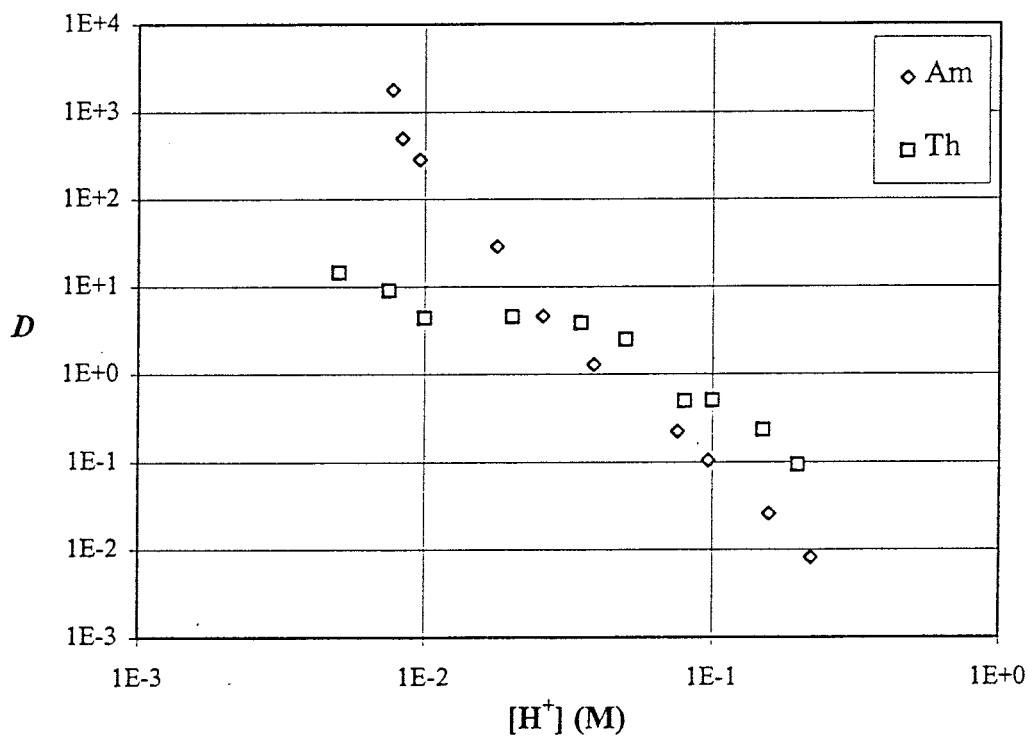


Figure A5.1 D - $[\text{H}^+]$ plot for Am and Th extraction from nitric acid solutions with 0.02 M OADPTZ and 1 M 2-bromodecanoic acid in TBB

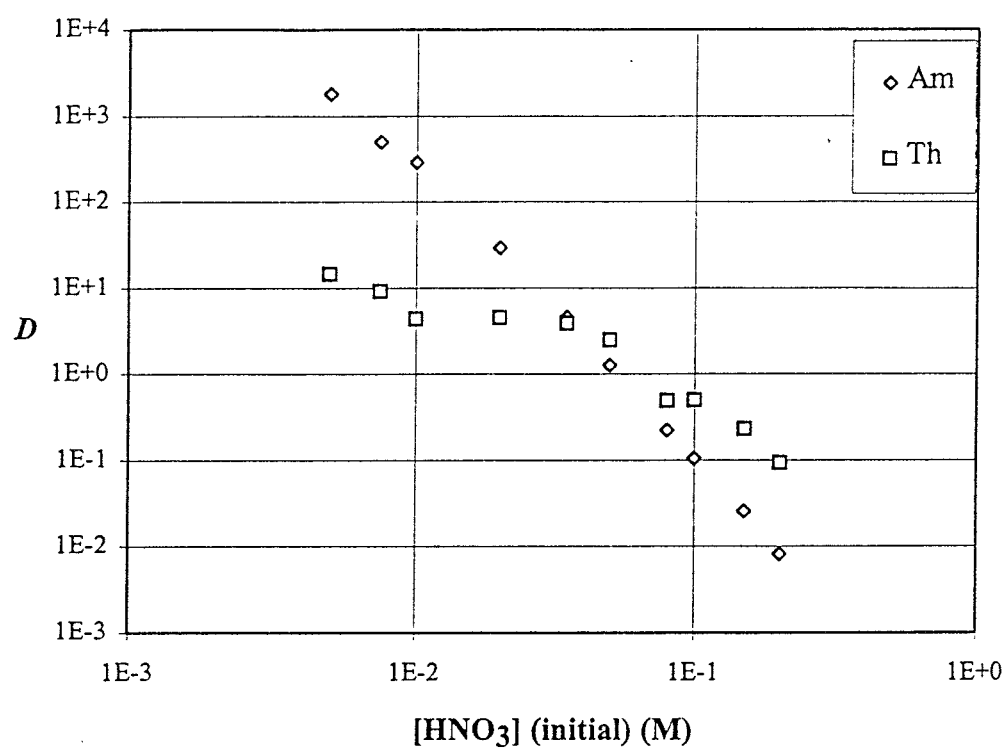


Figure A5.2 D - $[HNO_3]$ (initial)-plot for Am and Th extraction from nitric acid solutions with 0.02 M OADPTZ and 1 M 2-bromodecanoic acid in TBB

Appendix 6 – 8

Appendices 6, 7 and 8 contain X-ray crystallography data for:

- | | |
|---|--|
| 6 | $\text{ADPTZ}_2\text{-Pb}(\text{NO}_3)_2$ |
| 7 | $\text{ADMPTZ}_2\text{-Ni}(\text{NO}_3)_2 \cdot 6\text{H}_2\text{O}$ |
| 8 | $\text{ADMPTZ-NdNO}_3 \cdot 6\text{H}_2\text{O}$ |

These tables are not reproduced here but are available at the Nuclear Chemistry Department at Chalmers University of Technology.

Appendix

III

Contract FI41-CT-96-0010, Participant No. 3, Chalmers University of Technology, Progress Report from 1st November to 31st April 1998

Å. Enarsson, Anders Landgren, J.O. Liljenzin, M. Skålberg and L. Spjuth

Introduction

During the last semester synthesis, co-ordination studies and extraction studies have been performed with a new, substituted dipyridyltriazine. The synthesis and co-ordination studies were performed at Reading University by a swedish undergraduate student, J. Halvarsson, who thereafter continued with the extraction studies at Chalmers. A second visit in Reading by L. Spjuth, resulted in a new malonamide and basicity calculations were carried out using computational chemistry. Process calculations with 2,2':6',2''-terpyridine in synergy with 2-bromodecanoic acid in *tert*-butylbenzene has also been performed and the influence of different parameters on the extraction and stripping ability together with disturbances around the operating point has been investigated.

Results

Dipyridyltriazines

Extraction of americium, europium, promethium and thorium was investigated using 0.02M 4-octanoyl amino-2,6 di(2-pyridyl) 1,3,5 triazine (OADPTZ) and 1M 2-bromodecanoic acid in *tert*-butylbenzene. The extraction was high at low nitric acid concentration for both the trivalent actinides and lanthanides. There was no significant extraction above 0.1 M nitric acid concentration. The separation factor between Am(III) and Eu(III) was around 8-10 over the whole nitric acid concentration studied. The extraction at measured equilibrium H^+ concentration doesn't differ considerably from the extraction at initial nitric acid concentration, see figure 2-3, but the errors in measured H^+ concentration is greater than in the initial nitric concentration.

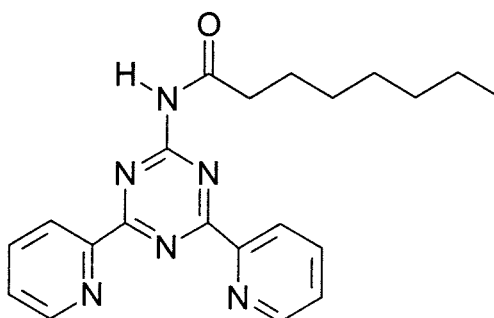


Figure 1. 4-octanoyl amino-2,6 di(2-pyridyl) 1,3,5 triazine (OADPTZ)

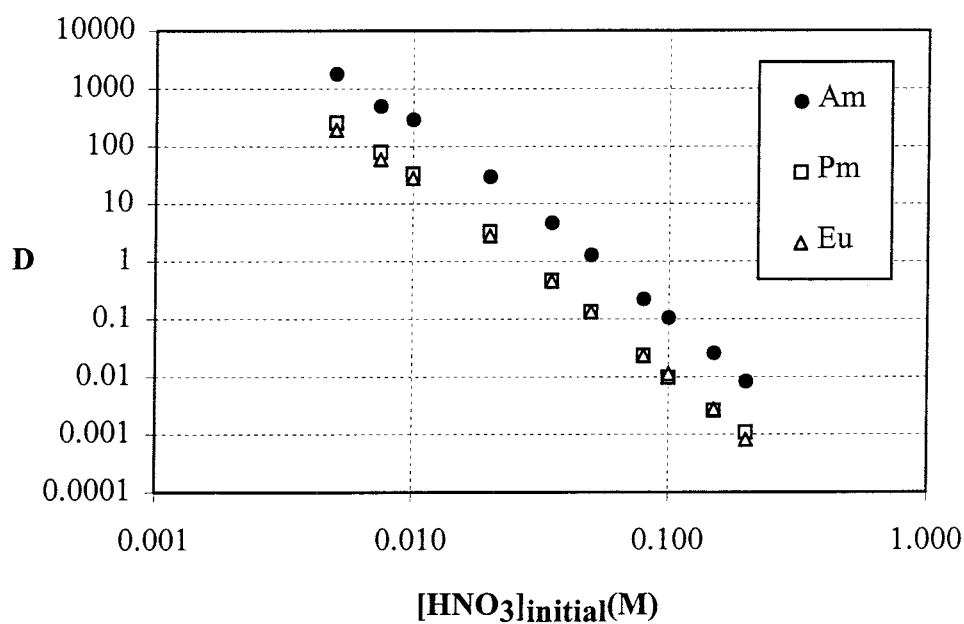


Figure 2. Extraction of americium, europium and promethium by 0.02M OADPTZ and 1M 2-bromodecanoic acid in *tert*-butylbenzene from different initial nitric acid concentrations.

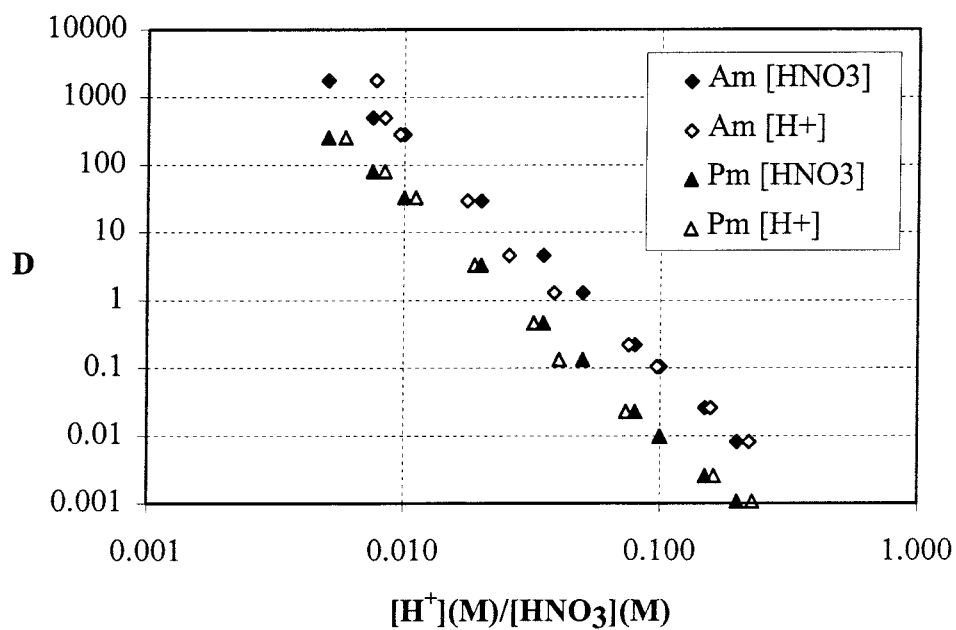


Figure 3. Extraction of americium and promethium by 0.02M OADPTZ and 1M 2-bromodecanoic acid in *tert*-butylbenzene from different initial nitric acid concentrations and at equilibrium H⁺ concentrations.

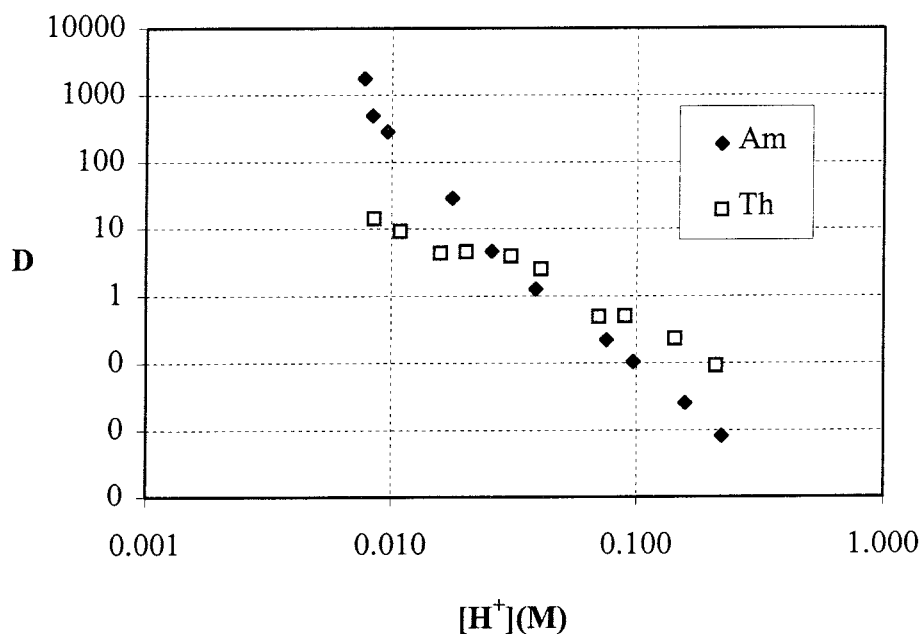


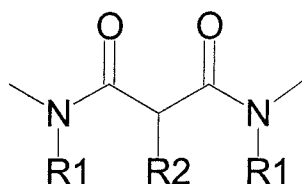
Figure 4. Extraction of americium(III) and thorium(IV) by 0.02M OADPTZ and 1M 2-bromodecanoic acid in *tert*-butylbenzene at different equilibrium H^+ concentrations.

The extraction of a tetravalent actinide, thorium(IV), was also investigated, see figure 4. The extraction curve differs significantly from the extraction of americium. Slow kinetics caused by polymerisation of the extracted complexes in the organic phase could be one of the reasons to this effect [1]. Complementary studies of other multivalent actinides has to be performed to verify the extraction mechanism.

Malonamides

The structure of the malonamides has previously been shown to have a big influence on the metal extraction. Both electroinductive and steric effects are expected to influence the extraction ability. A large number of substituted malonamides has previously been experimentally investigated and oxyalkylated malonamides have shown lower basicity and higher metal extraction than alkylated malonamides[2]. In this work, some different electronic parameters like charge densities and different energy terms have been calculated for a wide range of substituted malonamides using computational chemistry. The parameters will be compared with new experimental extraction and basicity data to be able to find a relation between basicity and metal extraction.

Both semiempirical and *ab initio* calculations were carried out for some different substituted malonamides. The general structure of a malonamide is:



Different electron withdrawing groups were substituted on the nitrogen (R_1) and on the central carbon (R_2) to achieve a change in calculated charge density on the carbonyl oxygens or in the basicity. The nitrogen substituent (R_1) was either a cyclohexyl group, a phenyl group or a chlorinated phenyl group and the different substituents on the central carbon (R_2) were;

H | butyl | 2-butoxy | 3-butoxy | phenyl | CN | NO₂ | Cl | Br

After scanning a lot of different parameters, ESPD charges (electrostatical potential derived charges) on the carbonyl oxygens calculated by Gaussian 94 using the basis set 6-31G* was shown to give the best relation between charge and experimental basicity and was therefore used for comparison between the different malonamides. The lower the electron density the lower the basicity and presumably better metal extraction. The Gaussian 94 computations were carried out on Silicon Graphics Origin 2000 Supercomputer at Reading University. Semiempirical methods didn't seem to be accurate enough to be able to compare the small differences in charge between the different structures.

Table 1. Average ESPD charges on the carbonyl oxygens for some different malonamides calculated by Gaussian 94 HF/6-31G* (# middle hydrogen substituted by a butyl group)

R_1	R_2	ESPD
2,6-dichlorophenyl	H	-0.5666
phenyl	CN	-0.5802
cyclohexyl	2-butoxy	-0.5877
phenyl	2-butoxy	-0.5982
cyclohexyl	NO ₂	-0.6026
phenyl	Cl #	-0.6061
3,5-dichlorophenyl	H	-0.6072
phenyl	butyl	-0.6095
cyclohexyl	butyl	-0.6150
4-chlorophenyl	H	-0.6158
Cl	H	-0.6159
phenyl	phenyl	-0.6173
phenyl	3-butoxy	-0.6201
phenyl	Br	-0.6309
cyclohexyl	Br	-0.6316
phenyl	Cl	-0.6344
phenyl	H	-0.6623
cyclohexyl	H	-0.6697

The basicity order for the phenyl N-substituted malonamides is;

CN < 2-butoxy < butyl < phenyl < 3-butoxy < Br < Cl < H

A disubstituted malonamide with both a butyl and a chlorine is less basic than the monosubstituted malonamide with only one chlorine. The basicity is also lower if the phenyl groups on the nitrogens are chlorinated.

2,6-dichlorophenyl < 3,5- dichlorophenyl < 4-chlorophenyl < phenyl

For the cyclohexyl N-substituted malonamide the basicity order is;

2-butoxy < NO₂ < butyl < Br < H.

An 2-alkoxy group on the central carbon has previously been shown to have lower basicity than a simple alkyl group, which is in agreement with these basicity orders [2]. Since the bromine and chlorine are strongly electronwithdrawing groups they were expected to give a lower basicity than the calculated charges shown above. The phenyl and cyclohexyl substituted malonamide show similar charges when the same functional group is substituted on the central carbon. The metal extraction has earlier been shown to differ drastically between a cyclohexyl substituent or a phenyl substituent on the nitrogen. The difference in extraction for these two molecules, as suggested earlier [3], is therefore probably due to steric hindrance rather than to electroinductive effects.

Instead of considering the electron density as a measure of the basicity the ΔG of the protonation reaction, $L + H^+ \leftrightarrow LH^+$, can be considered.

$$\Delta G_R = \Delta H_R - T\Delta S_R$$

$$\Delta H_R = E(LH^+) - E(L) - E(H^+) + \Delta(PV)$$

$$- T\Delta S_R = -298.15[S(LH^+) - S(L) - S(H^+)]$$

The electronic energy, thermal energy and entropy at 298K and the zero point energy at 0K for the protonated and unprotonated species can be obtained from frequency calculations preceded by a full geometry optimisation. The smaller the ΔG the more basic the molecule. These calculations are still running with some of the malonamides from table 1.

Computations to determine the most stable protonation conformation has previously been reported [4]. These calculations were continued to verify that the protonation takes place on the oxygens instead of the nitrogens. It is seen from table 2 that protonation favourable takes place on the carbonyl oxygens and not on the nitrogens.

Table 2. Calculated total energies for different protonation conformations with Gaussian 94 HF/6-31G* (# is previously reported values [3]).

Structure	C=O-H ⁺O=C	C=O-H ⁺	N-H ⁺O=C
DMDPHMA H ⁺	-913.296#	-913.287#	-913.262
DMDPHMA 2H ⁺	-913.519#	-913.526#	-913.476
DMDCHMA H ⁺	-920.293#	-920.280#	-920.270

Extraction studies have, so far, only been performed for oxyalkylated and alkylated malonamides and since the least basic of them, the oxyalkylated malonamide, showed the best metal extraction a new malonamide with even lower calculated basicity was synthesised. The 4-chlorophenyl derivative was chosen for basic investigations even though the molecule is not a CHON-reagent. The starting materials were commercially available. The dimethylmalonate is reacted with the secondary arylamine according to the standard procedure presented in [3].

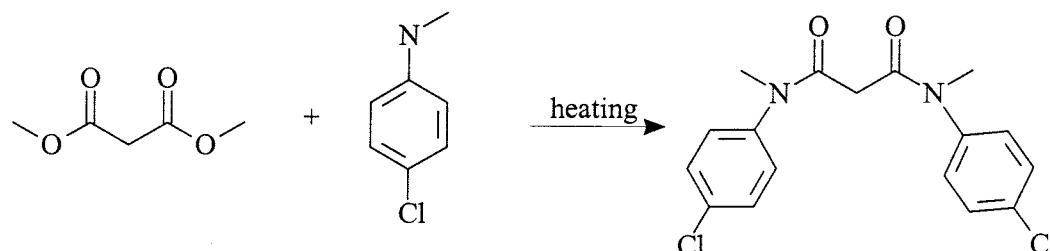


Figure 5. Synthesis route for preparation of N,N'-dimethyl-N,N'-di(4-chlorophenyl) malonamide

The malonamide is thereafter alkylated on the central carbon with NaH and 1-bromotetradecane to achieve the wanted malonamide. Extraction studies with this new malonamide has been initiated.

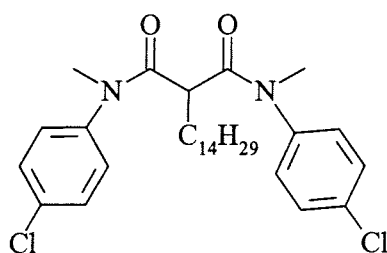


Figure 6. The newly synthesised N,N'-dimethyl-N,N'-di(4-chlorophenyl) tetradecylmalonamide

Process calculations

Process calculations for separation of actinides from the lanthanides with 2,2':6',2''-terpyridine (terpy) in synergy with 2-bromodecanoic acid (HA) has been performed. Terpy was chosen because of the considerably large amount of extraction data that is available even though terpy is relatively hydrophilic when it is protonated and is easily transferred to the aqueous phase. To be able to simulate the liquid-liquid extraction process with terpy in synergy with HA the ratios between different terpy and HA complexes in the aqueous and organic phase were determined. From the two-phase titration of terpy and HA, presented in the last report, a model has been adapted, which express the ratios between different terpy and HA complexes as a function of the concentrations of free protons at equilibrium. A model for the determined distribution ratios for the actinides (Am and Cm) and lanthanides (La, Nd, Pm and Tb) has also been adapted with the model for the ratios of different species of terpy and HA as a basis. These two models have been inserted into a FORTRAN77 program which simulates the process dynamically from the start of the process and stops when equilibrium is reached. Input files contain the flow rate of the aqueous feed, ratios between flows in the process, the number of stages in the different batteries and the

metal concentrations. The extraction batteries are all operated with the aqueous and organic phase flow countercurrent to each other.

The values for the different variables at the suggested operating point is presented in table 4. The concentrations of terpyridine and 2-bromodecanic acid in the organic feed to the extraction battery were 0.02 M and 1.0 M respectively. For these values the criterions of 99.9% extraction of the actinides and 0.1% extraction of the lanthanides are achieved.

Table 3. Specification of values of the variables in the operating point.

Specification of variables	Values in the operating point
number of stages in extraction battery	10
number of stages in wash battery	5
number of stages in strip battery	2
[HNO ₃] _{tot} in aqueous feed (M)	0.01
[HNO ₃] _{tot} in wash feed (M)	0.01
[HNO ₃] _{tot} in strip feed (M)	0.2
flow ratio organic feed/aqueous feed	0.44
flow ratio wash feed/aqueous feed	1.0
flow ratio strip feed/organic feed	0.2

For the proposed operating point the strip battery is insensitive to changes in flow ratio, with 20 % variation, and concentration of nitric acid in the aqueous feed to the strip battery, above 0.1 M nitric acid concentration.

However, the process is sensitive to changes in flow ratios and concentrations of nitric acid in the aqueous feeds to the extraction and wash batteries, table 4. The operating points that fulfill the condition 99.9 % extraction of the wanted species and 0.1 % extraction of the not wanted species is marked with OK.

Table 4. Values of the percentage extraction for the extraction and wash batteries for different nitric acid concentrations in the aqueous feed and strip feed at different flow ratios.

[HNO ₃] _{tot} (M)	Flow ratio between organic and aqueous feed						
	0.4	0.42	0.44	0.45	0.47	0.48	0.5
0.009	Ln >0.17	Ln >0.43	Ln >0.94	Ln >1.34	Ln >2.57	Ln >3.46	Ln >5.93
0.010	An <99.8	OK	OK	OK	Ln >0.2	Ln >0.3	Ln >0.5
0.011	An <94.0	An <98.8	An <99.6	An <99.7	An <99.8	OK	OK

When one of the variables in the process simulation is varied the effect on the percentage extraction, %E, has been evaluated for curium and terbium. Curium and terbium was chosen because these elements are most difficult to separate between the actinides and lanthanides. The value in the middle row in the tables are used as the reference case during the other variations.

When the number of extraction stages are increased, the percentage extraction of both terbium and curium are increased, but the percentage extraction of terbium is

increased in a larger extent than for curium, table 5. This indicates that a lot of terbium is extracted if almost all curium is extracted which means that other variables also needs to be varied if the process is going to work.

Table 5. Calculated percentage extraction for wash and extraction batteries when number of extraction stages are varied.

number of extraction stages	%E(Tb³⁺)	%E(Cm³⁺)
1	31.134	79.2
3	61.935	99.296
5	78.221	99.978

When the number of wash stages are increased the percentage extraction for terbium is decreased and is almost constant for curium, table 6. This implies that the product becomes cleaner when more wash stages are used and that some wash stages has to be present in the process.

Table 6 Calculated percentage extraction for wash and extraction batteries when number of wash stages are varied.

number of wash stages	%E(Tb³⁺)	%E(Cm³⁺)
1	64.109	99.269
2	61.935	99.296
3	60.775	99.3

When the nitric acid concentration in the aqueous feed is increased the percentage extraction of both terbium and curium is decreased, table 7, due to the lower D-values at higher nitric acid concentrations. At higher nitric acid concentrations the extraction of terbium is decreased in larger extent than for curium indicating an optimum in the choice of nitric acid concentration causing curium to be extracted to a larger extent than Tb.

Table 7. Calculated percentage extraction for wash and extraction batteries when [HNO₃]_{tot} in the aqueous feed is varied.

[HNO₃]_{tot} in aqueous feed (M)	%E(Tb³⁺)	%E(Cm³⁺)
0.005	89.506	99.879
0.01	61.935	99.296
0.02	10.724	91.129

When the nitric acid concentration in the wash feed is increased the percentage extraction for terbium is decreased in larger extent than for curium implying a cleaner

product, table 8. An optimum for nitric acid concentration in the wash feed can be chosen in the same way as for the aqueous feed.

Table 8. Calculated percentage extraction for wash and extraction batteries when $[\text{HNO}_3]_{\text{tot}}$ in the wash feed is varied.

$[\text{HNO}_3]_{\text{tot}}$ in wash feed (M)	%E(Tb^{3+})	%E(Cm^{3+})
0.005	91.166	99.866
0.01	61.935	99.296
0.02	4.609	91.74

When the nitric acid concentration is increased almost all terbium and curium are transferred to the aqueous phase, table 9, which is the purpose of the strip battery. This indicates that high nitric acid concentrations should be used in the strip feed. Stripping with 0.03 M nitric acid shows that if a too low nitric acid concentration is chosen the stripping is not sufficient.

Table 9. Calculated percentage extraction for strip battery when $[\text{HNO}_3]_{\text{tot}}$ in the strip feed is varied.

$[\text{HNO}_3]_{\text{tot}}$ in strip feed (M)	%E(Tb^{3+})	%E(Cm^{3+})
0.03	0.111	4.632
0.2	0	0
0.4	0	0

When two or more strip stages is used almost all terbium and curium is transferred to the aqueous phase, table 10. This implies that two strip stages are sufficient in the process for the reference conditions.

Table 10. Calculated percentage extraction for strip battery when number of strip stages are varied.

number of strip stages	%E(Tb^{3+})	%E(Cm^{3+})
1	0.001	0.006
2	0	0
3	0	0

When the flow ratio between the organic feed and the aqueous feed is decreased the percentage extraction for terbium is decreased in larger extent than for curium, table 11, and thus implying low flow ratio is desired in the process. The flow ratio has an

optimum in the separation between curium and terbium and the flow ratio is chosen to achieve enough extraction of curium but as little as possible for terbium.

Table 11. Calculated percentage extraction for wash and extraction batteries when the flow ratio organic feed/aqueous feed is varied.

flow ratio organic feed/aqueous feed	%E(Tb³⁺)	%E(Cm³⁺)
0.5	22.052	96.59
1.0	61.935	99.296
2.0	81.525	99.742

When the flow ratio between the organic feed and the aqueous feed to the wash battery is decreased a better separation between curium and terbium is achieved and the product becomes cleaner, table 12. This indicates that low flow ratios between the organic feed and the aqueous feed to the wash battery should be used in the process.

Table 12. Calculated percentage extraction for wash and extraction batteries when the flow ratio organic feed/wash feed is varied.

flow ratio organic feed/wash feed	%E(Tb³⁺)	%E(Cm³⁺)
0.5	19.546	97.328
1.0	61.935	99.296
2.0	82.58	99.713

When the flow ratio between the organic feed and the aqueous feed to the strip battery is decreased, almost all terbium and curium are transferred to the aqueous phase, table 13. The flow ratio can be as high as 5.0 and still almost all metal species in the organic phase is stripped and this indicates that flow ratios around 5.0 should be used to reach a high concentration of metal ions in the aqueous feed. The flow ratio of 20 is used in table 13 to show that when the flow ratio is too high the metal ions are not stripped.

Table 13. Calculated percentage extraction for strip battery when the flow ratio organic feed/strip feed is varied.

flow ratio organic feed/strip feed	%E(Tb³⁺)	%E(Cm³⁺)
0.5	0	0
1.0	0	0
20	0.755	15.546

Since the unsubstituted terpyridine is transferred to the aqueous phase when protonated the reagent a method for recovering the terpy from the aqueous has to be considered.

Future Work

- Extraction studies and experimental basicity measurements with the new malonamide
- Systematic study concerning extraction and basicity with OADPTZ derivatives.
- Since the solubility and third phase formation are influenced by the adduct formation between oligopyridine and 2-bromodecanoic acid in the organic phase, spectrophotometric studies will be performed to evaluate the adduct formation.
- Process calculations for the separation of trivalent actinides and lanthanides with the synergistic mixture of a more hydrophobic triazine-derivative and 2-bromodecanoic acid in *tert*-butylbenzene are planned.

References

- [1]. Madic, C., Thèse de Doctorat d'Université de Paris, 1975
- [2]. Nigond, L., Thèse de Doctorat d'Université de Clermont-Ferrand II, CEA-R-5610, 1992
- [3] Chan, G.Y.S., Drew, M.G.B., Hudson, M.J., Iveson, P.B., Liljenzin, J.O., Skålberg, M., Spjuth, L. and Madic, C., *J. Chem. Soc., Dalton Trans.*, 1997, 649-660.
- [4] Contract NEWPART (FI41-CT-96-0010), *Third Semestrial Report, 1st May 1997-31st October 1997*

Appendix

IV

Theoretical and experimental studies of the protonated terpyridine cation. *Ab initio* quantum mechanics calculations, and crystal structures of two different ion pairs formed between protonated terpyridine cations and nitratolanthanate(III) anions†

Michael G. B. Drew,^{*a} Michael J. Hudson,^a Peter B. Iveson,^a Mark L. Russell,^a Jan-Olov Liljenzin,^b Mats Skållberg,^b Lena Spjuth^b and Charles Madic^c

^a Department of Chemistry, University of Reading, PO Box 224, Whiteknights, Reading, UK RG6 6AD. E-Mail: m.g.b.drew@reading.ac.uk

^b Department of Nuclear Chemistry, Chalmers University of Technology, S-412 96 Goteborg, Sweden

^c Commissariat à l'Energie Atomique, Direction du Cycle du Combustible, B.P. 171, 30207 Bagnols-sur-Cèze, Cedex, France

Ab initio quantum mechanics calculations have been carried out on all possible conformations of the terpyridine ligand and its mono- and di-protonated forms. Results show that the lowest energy form of the ligand is when the N–C–C–N torsion angles are *trans* but that in the protonated forms, the *cis* arrangement is prevalent being stabilised by intramolecular N–H···N hydrogen bonds. Results are consistent with the experimental crystal structure data found in the literature and also with two crystal structures reported here in which two different ion pairs formed between protonated terpyridine cations and lanthanate(III) nitrate anions have been prepared and analysed structurally. Compound **1** consists of discrete diprotonated terpyridine cations and hexanitratolanthanate anions, namely $3[\text{H}_2\text{terpy}]^{2+}2[\text{La}(\text{NO}_3)_6]^{3-}\cdot 3\text{H}_2\text{O}$. Water molecules are present as hydrogen bond acceptors in the diprotonated terpyridyl cavities. Each lanthanum atom is 12-co-ordinate and the La–O bond lengths vary between 2.609(11) and 2.765(10) Å. Compound **2** consists of a diprotonated $[\text{H}_2\text{terpy}]^{2+}$ cation together with a $[\text{Sm}(\text{terpy})(\text{NO}_3)_4]^-$ anion, and a NO_3^- anion which is present as a hydrogen bond acceptor in the diprotonated terpyridyl cavity. The samarium atom is 11-co-ordinate, the Sm–O bond lengths vary between 2.494(5) and 2.742(5) Å while the Sm–N bond lengths vary between 2.626(4) and 2.650(5) Å.

Introduction

There is much current interest in the separation of lanthanide(III) and actinide(III) complexes by solvent extraction routes.¹ Various oligoamines have been shown to co-extract lanthanides and actinides from nitric acid solutions into an organic phase. Among these are the oligoamine ligands 2,4,6-tris(4-*tert*-butyl-2-pyridyl)-1,3,5-triazine² ligand L^1 and 2,2':6',2''-terpyridine L^2 . It is thought that the species extracted at low levels of acidity are simple metal co-ordination complexes, for which there is plenty of structural evidence.³ It is clear that the lanthanides (and by implication the similarly sized actinides) can fit into the tridentate cavity of the terpyridyl moiety. Thus we have previously reported the structure of $\text{Ce}(\text{NO}_3)_4\text{L}^1$ (ref. 2) and in addition complexes of L^2 with lanthanides are well known [e.g. $\text{LnCl}_3(\text{L}^2)\cdot x\text{H}_2\text{O}$ (Ln = La, Ce, Nd, Sm, Eu, Gd, Tb, Dy, Ho, Er, Tm, Yb, Lu or Y)].⁴ For Ln = La–Nd, $x = 5$, for Ln = Tb–Lu, $x = 4$ and for Ln = Sm or Gd there are between four and five water molecules in the co-ordination sphere. Also isolated was a dimeric species in which the Sm is co-ordinated to three N atoms from L^2 , two bridging and two terminal chloride anions and one water molecule.

Although direct co-ordination of the metal ions to the polyamine ligands is thought to be necessary for the selective extraction of actinides over the lanthanides, the need still remains to establish the nature of the species which may be formed at higher acid concentrations, especially those in which the lanthanide or actinide ion exists as an anion such as $[\text{Ln}(\text{NO}_3)_6]^{3-}$ or the $[\text{LnL}(\text{NO}_3)_4]^-$ ion-pair. It has been demonstrated that terpyridine-type ligands in synergistic combination

with 2-bromodecanoic acid show some selectivity for An(III) over Ln(III) ions.⁵ The species involved in these extractions are not known with any certainty.

We have adopted a theoretical and experimental approach to the identification of these species. We are using quantum mechanical methods to investigate the conformational preferences of the ligand and also the likely structures of the protonated forms. In addition we are trying to prepare solid complexes in order to provide evidence for the kind of species which is involved in this type of extraction.

In this paper we report the results from our quantum mechanical calculations and also the crystal structures of two different ion pairs of diprotonated terpyridine and anionic lanthanide nitrates (**1** and **2**) both of which contain free diprotonated terpyridine moieties unco-ordinated to a metal ion. The asymmetric unit of **1** contains three diprotonated terpyridyl cations, two hexanitratolanthanate(III) anions and three water molecules, $3[\text{H}_2\text{L}^2]^{2+}2[\text{La}(\text{NO}_3)_6]^{3-}\cdot 3\text{H}_2\text{O}$ while the asymmetric unit of **2** contains an $[(\text{H}_2\text{L}^2)(\text{NO}_3)]^+$ cation together with a $[\text{SmL}^2(\text{NO}_3)_4]^-$ anion.

Experimental

The compounds $\text{Ln}(\text{NO}_3)_3\cdot 6\text{H}_2\text{O}$ (99.99%), $\text{Sm}(\text{NO}_3)_3\cdot 6\text{H}_2\text{O}$ (99.99%) and 2,2':6',2''-terpyridine (L^2) (98%) were used as received from Aldrich. 2-Bromodecanoic acid (98%) was purchased from Fluka and used without further purification.

Preparation of complex **1**

This compound was prepared from $[\text{H}_2\text{L}^2][\text{NO}_3]_2$ which was initially prepared as a solid: L^2 (0.25 g, 0.001 mol) was dissolved

† Non-SI unit employed: cal = 4.184 J.

Table 1 Crystal data and structure refinement for compounds **1** and **2**

	1	2
Formula	$3[\text{H}_2\text{L}^2]^{2+} \cdot 2[\text{La}(\text{NO}_3)_6]^{3-} \cdot 3\text{H}_2\text{O}$	$[(\text{H}_2\text{L}^2)(\text{NO}_3)]^+ [\text{Sm}(\text{L}^2)(\text{NO}_3)_4]^-$
Empirical formula	$\text{C}_{45}\text{H}_{45}\text{La}_2\text{N}_{21}\text{O}_{39}$	$\text{C}_{30}\text{H}_{24}\text{SmN}_{11}\text{O}_{15}$
<i>M</i>	1781.84	928.95
<i>T</i> /K	293(2)	293(2)
<i>λ</i> /Å	0.710 73	0.710 73
Crystal system	Monoclinic	Monoclinic
Space group	$P2_1$	$P2_1/n$
<i>a</i> /Å	10.826(9)	17.29(2)
<i>b</i> /Å	30.00(2)	10.230(9)
<i>c</i> /Å	11.140(9)	20.31(2)
β /°	104.76(1)	106.53(1)
<i>U</i> /Å ³	3498(5)	3445(6)
<i>Z</i> , <i>D</i> _c /g cm ⁻³	2, 1.692	4, 1.791
μ /mm ⁻¹	1.316	1.796
<i>F</i> (000)	1776	1852
Size/mm	0.2 × 0.2 × 0.5	0.25 × 0.25 × 0.20
θ Range/°	2.82 to 25.07	1.83 to 25.94
<i>hkl</i> Range	$0 \leq h \leq 11, -35 \leq k \leq 35,$ $-13 \leq l \leq 12$	$0 \leq h \leq 21, -12 \leq k \leq 12,$ $-24 \leq l \leq 23$
Reflections observed, <i>R</i> _{int}	8750, 0.0508	9872, 0.0289
Unique reflections	8570	5838
Weighting scheme <i>a</i> , <i>b</i> *	0.144, 35.48	0.181, 25.94
Reflections, parameters	8570, 965	5838, 515
Final indices [<i>I</i> > 2σ(<i>I</i>)] <i>R</i> ₁ , <i>wR</i> ₂	0.0582, 0.1779	0.0352, 0.0971
All data <i>R</i> ₁ , <i>wR</i> ₂	0.0657, 0.1901	0.0514, 0.1080
Largest difference peak, hole/e Å ⁻³	0.928, -1.615	1.116, -0.984

* Weighting scheme $w = 1/[2(F_o^2) + (aP)^2 + bP]$, where $P = (F_o^2 + 2F_c^2)/3$.

in methanol (1 ml). The addition of 69% AnalaR nitric acid (0.14 ml, 0.0022 mol) to a stirred solution of the ligand resulted in the formation of a precipitate (yield 82%).⁶

After the addition of methanol (2 ml), the solid was filtered off and dried under vacuum over calcium chloride. Then $[\text{H}_2\text{L}^2][\text{NO}_3]_2$ (0.05 g) was stirred for 10 min in acetonitrile (20 ml), heated to reflux and another solution containing $\text{La}(\text{NO}_3)_3 \cdot 6\text{H}_2\text{O}$ (0.0498 g, 0.0001 mol) dissolved in acetonitrile (15 ml) at ca. 40 °C was added dropwise to the stirred ligand solution. After the addition, the solution was stirred for 10 min and then allowed to stand at ambient temperature. Crystals suitable for X-ray analysis were deposited overnight at room temperature, $3[\text{H}_2\text{L}^2]^{2+} \cdot 2[\text{La}(\text{NO}_3)_6]^{3-} \cdot 3\text{H}_2\text{O}$ (Found: C, 30.1; H, 2.7; N, 16.2. Calc. for $\text{C}_{45}\text{H}_{45}\text{La}_2\text{N}_{21}\text{O}_{39}$: C, 30.3; H, 2.5; N, 16.5%).

Preparation of complex **2**

A solution of $\text{Sm}(\text{NO}_3)_3 \cdot 6\text{H}_2\text{O}$ (0.077 g, 0.0002 mol) in acetonitrile (5 ml) was heated to around 40 °C and then added dropwise to a stirred solution of L^2 (0.051 g, 0.0002 mol) and 2-bromodecanoic acid (0.087 g, 0.00035 mol) in acetonitrile (5 ml), also at around 40 °C. A small amount of precipitate appeared on mixing and a further four quantities of acetonitrile (5 ml) were added to dissolve the solid. After a few minutes of heating the solution was allowed to cool down slowly in an oil bath and crystals were formed on standing overnight, $[(\text{H}_2\text{L}^2)(\text{NO}_3)]^+ [\text{Sm}(\text{L}^2)(\text{NO}_3)_4]^-$ (Found: C, 38.5; H, 2.55; N, 16.3. $\text{C}_{30}\text{H}_{24}\text{N}_{11}\text{O}_{15}\text{Sm}$ requires C, 38.8; H, 2.6; N, 16.6%).

Crystallography

Crystal data for complexes **1** and **2** are given in Table 1, together with refinement details. Data for both crystals were collected with Mo-K α radiation using the MARresearch Image Plate System. The crystals were positioned at 75 mm for **1** and 70 mm for **2** from the Image Plate. 95 Frames were measured at 2° intervals with a counting time of 2 min. Data analysis was carried out with the XDS program.⁷ The structures were solved using direct methods with the SHELXS program.⁸ In both structures the non-hydrogen atoms were refined with anisotropic thermal parameters. The locations of the nitrogen atoms

in the rings were selected *via* thermal parameters and confirmed from the structure refinement by comparison with other assignments which gave higher *R* values and unreasonable thermal parameters. The hydrogen atoms bonded to carbon were included in geometric positions and given thermal parameters equivalent to 1.2 times those of the atom to which they were attached. An empirical absorption correction was made for both structures using the DIFABS program.⁹ In **2**, the two extra protons in the cation were readily observed in a Fourier-difference map bonded to N(11) and N(31) and successfully included in the refinement with no constraints. By contrast in **1** these hydrogen atoms bonded to nitrogen (and also those bonded to the water oxygen atoms) could not be located definitively although positive areas of electron density were located in appropriate positions. In order to establish whether the data were of sufficient quality so that the hydrogen atoms bonded to nitrogen should be locatable (and that therefore we should draw the conclusion from their absence that they were not positioned on the nitrogen atom) we looked at the Fourier-difference map for the hydrogen atoms bonded to carbon in these cations. In the first 200 peaks, only 12 of the 33 hydrogen atoms could be located, *i.e.* peaks were within 0.5 Å of calculated positions. We conclude that the data are not of sufficient quality so that we would necessarily expect to find definitive positions for the hydrogen atoms bonded to nitrogen and we therefore conclude that their likely positions are equivalent to those in **2** [bonded to atoms N(11) and N(31)], which is consistent with the formation of hydrogen bonds to the water molecule. Therefore the hydrogens in the cations A, B and C were included in calculated positions bonded to these outer nitrogen atoms. The assignment of absolute structure in **1** was carried out by comparisons of two structures with opposite signs for *y* coordinates. The structure with the lowest *R* value was chosen. Both structures were refined on *F*² till convergence using SHELXL.¹⁰ All calculations were carried out on a Silicon Graphics R4000 Workstation at the University of Reading. Relevant bond lengths in each structure are shown in Table 2. The hydrogen bonds are shown in Table 3.

CCDC reference number 186/1074.

See <http://www.rsc.org/suppdata/dt/1998/2973/> for crystallographic files in .cif format.

Table 2 Bond lengths (Å) for compounds 1 and 2

Compound 1			
La(1)–O(13)	2.609(11)	La(2)–O(45)	2.635(11)
La(1)–O(32)	2.649(11)	La(2)–O(56)	2.653(12)
La(1)–O(22)	2.663(11)	La(2)–O(52)	2.666(10)
La(1)–O(14)	2.665(13)	La(2)–O(58)	2.669(11)
La(1)–O(37)	2.672(12)	La(2)–O(66)	2.692(11)
La(1)–O(33)	2.674(10)	La(2)–O(41)	2.702(10)
La(1)–O(26)	2.683(11)	La(2)–O(47)	2.706(11)
La(1)–O(27)	2.702(13)	La(2)–O(53)	2.702(9)
La(1)–O(18)	2.726(11)	La(2)–O(43)	2.733(12)
La(1)–O(24)	2.734(12)	La(2)–O(63)	2.725(11)
La(1)–O(36)	2.741(12)	La(2)–O(68)	2.762(12)
La(1)–O(16)	2.758(14)	La(2)–O(64)	2.765(10)
Compound 2			
Sm(1)–O(72)	2.494(5)	Sm(1)–O(82)	2.627(5)
Sm(1)–O(62)	2.537(5)	Sm(1)–N(11B)	2.635(5)
Sm(1)–O(51)	2.535(4)	Sm(1)–N(31B)	2.650(5)
Sm(1)–O(53)	2.554(4)	Sm(1)–O(74)	2.690(5)
Sm(1)–O(83)	2.559(4)	Sm(1)–O(63)	2.742(5)
Sm(1)–N(21B)	2.626(4)		

Table 3 Hydrogen bond distances (Å) in compounds 1 and 2

Compound 1			
O(1A)···O(63)	2.812(18)	O(1A)···O(16 ¹)	3.005(19)
O(1A)···N(31A ^{III})	2.814(19)	N(11A)···N(21A)	2.691(17)
O(1A)···N(11A ^{III})	2.823(20)	N(21A)···N(31A)	2.691(19)
O(1B)···O(66 ^{II})	2.800(18)	O(1B)···O(17 ¹)	2.965(22)
O(1B)···N(11B)	2.861(16)	O(1B)···O(67)	3.213(20)
O(1B)···N(31B)	2.800(16)	N(11B)···N(21B)	2.702(18)
O(1B)···O(16 ^{II})	3.018(19)	N(21B)···N(31B)	2.712(18)
O(1C)···O(38 ^{II})	2.799(18)	O(1C)···O(36 ^{II})	3.210(18)
O(1C)···N(31C ^{IV})	2.827(18)	O(1C)···O(41)	3.255(19)
O(1C)···N(11C ^{IV})	2.860(21)	N(11C)···N(21C)	2.660(21)
O(1C)···O(58)	3.035(19)	N(21C)···N(31C)	2.651(20)
O(1C)···O(47)	3.142(18)		

Compound 2			
N(11A)···O(303)	2.750(14)	N(31A)···O(303)	2.767(14)
N(11A)···O(302)	3.095(16)	N(21A)···N(11A)	2.677(13)
N(21A)···O(303)	3.101(14)	N(21A)···N(31A)	2.648(13)

Symmetry elements: I $1 + x, y, z$; II $1 - x, 0.5 + y, -z$; III $x, y, 1 + z$; IV $x - 1, y, z - 1$.

Results and Discussion

Structure of $3[\text{H}_2\text{L}^2]^{2+} \cdot 2[\text{La}(\text{NO}_3)_6]^{3-} \cdot 3\text{H}_2\text{O}$

The asymmetric unit of **1** contains three diprotonated terpyridyl cations $[\text{H}_2\text{L}^2]^{2+}$, two $[\text{La}(\text{NO}_3)_6]^{3-}$ anions and three water molecules. Thus the protonated terpyridine ligand is not co-ordinated to the lanthanate(III) nitrate anion. Instead the two terminal pyridine nitrogen atoms are protonated. Each protonated terpyridyl cation encapsulates a water molecule with which it forms two strong hydrogen bonds. Two parts of the structure are shown in Figs. 1 and 2. Fig. 1 shows the environment of one protonated terpyridyl cation and Fig. 2 of one lanthanate(III) anion. It is noteworthy that the environments of the other cations and anions are almost identical such that there are three cations in the asymmetric unit together with just three water molecules each of which is similarly encapsulated. There are no additional water molecules in the unit cell, indicating that the role of the water molecules in the structure is to stabilise the cations by forming hydrogen bonds and also to stabilise the packing by additional hydrogen bonds to the anions. While it is not impossible to imagine a structure in which the lanthanate nitrate anions are hydrogen bonded directly to the diprotonated cation, clearly the present arrangement in which the interaction between cation and anion is mediated by the water molecules is more favoured.

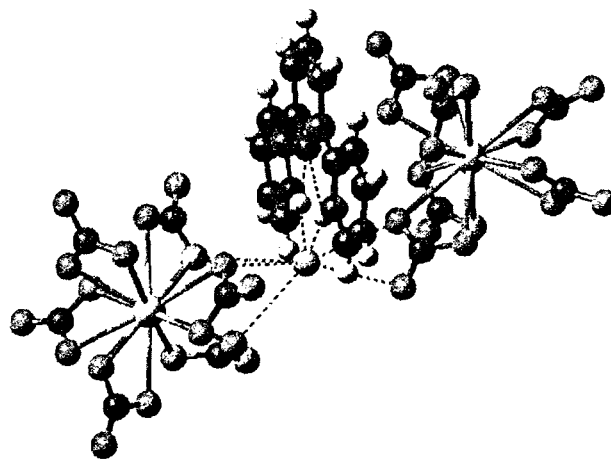


Fig. 1 The structure of compound **1** showing the environment of one $[\text{H}_2\text{L}^2]^{2+}$ cation with a water encapsulated within the cavity and forming N–H···O hydrogen bonds. In addition, the water molecule forms hydrogen bonds with oxygen atoms from the nitrates in the $[\text{La}(\text{NO}_3)_6]^{3-}$ anions. All hydrogen bonds are shown as dotted lines. The environments of the other two $[\text{H}_2\text{L}^2]^{2+}$ cations in the asymmetric unit are similar. Lanthanum yellow, oxygen red, carbon green, hydrogen yellow, nitrogen purple.

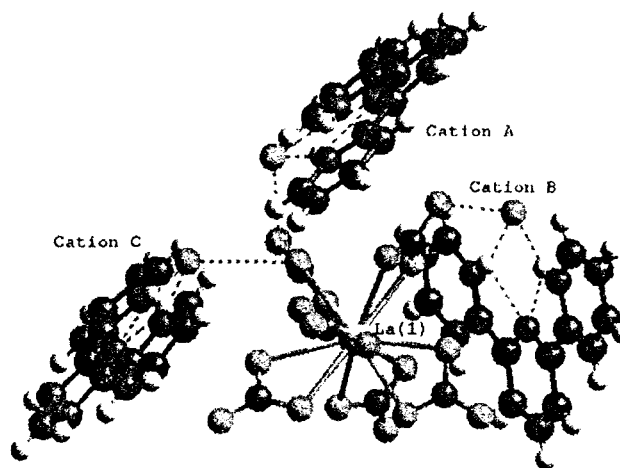


Fig. 2 The structure of compound **1** showing the environment of one $[\text{La}(\text{NO}_3)_6]^{3-}$ anion forming hydrogen bonds to the three water molecules which are each encapsulated within $[\text{H}_2\text{L}^2]^{2+}$ cations. All hydrogen bonds are shown as dotted lines. The environment of the second $[\text{La}(\text{NO}_3)_6]^{3-}$ anion in the unit cell is similar. Lanthanum yellow, oxygen red, carbon green, hydrogen yellow, nitrogen purple.

While there are literally hundreds of examples of L^2 complexed to metals recorded in the Cambridge Crystallographic Database (CCDS), there is only one previously reported example of the $[\text{H}_2\text{L}^2]^{2+}$ cation, namely in the salt $2[\text{H}_2\text{L}^2]^{2+} \cdot [\text{Tb}(\text{OH}_2)_6] \cdot 7\text{Cl}^-$.¹¹ The nitrogen atoms in the outer pyridine rings are protonated and a chloride anion was located in the diprotonated cavity. This structure containing $[\text{H}_2\text{L}^2]^{2+}$ together with those established in the four structures presented in our previous work² for $[\text{H}_n\text{L}^2]^{n+}$ suggest that the diprotonated terpyridyl species always attracts hydrogen bonding species into the tridentate cavity.

In **1** in addition to the above three $[\text{H}_2\text{L}^2]^{2+} \cdot \text{H}_2\text{O}$ moieties the asymmetric unit contains two $[\text{Ln}(\text{NO}_3)_6]^{3-}$ anions. The Ln–O distances in this structure vary between 2.609(11) and 2.765(10) Å. Although there are numerous structures in the CCDS with Ln–O (nitrate) bonds, there are only three previously reported structures with $[\text{Ln}(\text{NO}_3)_6]^{3-}$ anions. For these anions and the two in the present work, the average Ln–O distance is 2.67 Å [$n = 60$, $\sigma(n - 1) = 0.044$ Å]. It has been suggested previously that an analysis of the metal co-ordination sphere for this type

of structure can be simplified by considering a bidentate ligand of small 'bite' such as nitrate to occupy only one site of a coordination polyhedron rather than two. The new metal coordination sphere would have a lower co-ordination number which is easier to analyse.¹² Thus, for $[\text{Ln}(\text{NO}_3)_6]^{3-}$ the arrangement of nitrogen atoms around Ln should be close to an octahedral geometry. This is indeed the case for the environment around Ln(2) in which the N–Ln–N angles only vary between 82(1) and 97(1)° and indeed there are six O–Ln(2)–O angles within 8° of 180°. There are larger deviations, however, around Ln(1), the N–Ln–N angles varying between 71(1) and 117(1)° and while there are three O–Ln–O angles within 5° of 180°, the other potentially *trans* angles are *ca.* 160°. It is not clear why there should be such big geometrical differences between the two anions though it seems likely that the geometry could well be affected by the significant numbers of hydrogen bonds found in the unit cell. Non-bonded nitrate oxygen atoms and bonded nitrate oxygen atoms in both anions are involved to approximately the same extent in hydrogen bonding with the water molecules in the terpyridyl cavity. This has the effect of weakening the corresponding Ln–O bonds, for example, there are 10 bonds longer than 2.7 Å in the anions; however it is not clear why the geometry of one anion should be so different from that of the other.

The hydrogen bond dimensions are shown in Table 3. The distances between each water atom and the two protonated nitrogen atoms with which hydrogen bonds are formed are all between 2.80 and 2.87 Å. In addition, each water molecule forms several hydrogen bonds to the nitrate oxygen atoms, one strong at a distance of *ca.* 2.80 Å and several weaker (at distances of 3.0–3.3 Å). In Fig. 1 we show the arrangement of one water molecule which forms hydrogen bonds to two different anions. The cations are approximately planar with N–C–C–N torsion angles of –0.1(2), 3.4(2)° in ligand A, 1.7(1), –0.9(1)° in ligand B and –0.5(2), –6.4(2)° in ligand C, respectively. It is difficult to establish the exact hydrogen bond pattern around each oxygen as there are so many short contacts [four for O(1A), six for O(1B), seven for O(1C)] less than 3.26 Å. It seems likely that the positions of the hydrogen atoms are fluxional and that weak interactions can occur to any of the close nitrate oxygen atoms.

In Fig. 2 the environment around one anion which forms hydrogen bonds to all three $[\text{H}_2\text{L}^{2+}] \cdot \text{H}_2\text{O}$ moieties is shown. It is interesting that one of the nitrate oxygen atoms forms hydrogen bonds to two different water molecules. The distances between the protonated N(11) and N(31) atoms and the central unprotonated N(21) atom vary between 2.65(2) and 2.71(2) Å while the corresponding N–H···N angles are all between 106 and 108°. These angles are similar to those found in the structure of 2,2':6',2''-terpyridinium trifluoromethanesulfonate (Fig. 7) which contains a monoprotonated terpyridyl cation with an N–N distance of 2.65 Å and an N–H···N angle of 103°, dimensions which are considered to be indicative of weak intramolecular hydrogen bonds.¹³ The corresponding N–N distances in the salt $2[\text{H}_2\text{L}^{2+}][\text{Tb}(\text{OH}_2)_8]^{3+} \cdot 7\text{Cl}^-$ are also very similar, varying between 2.61 and 2.67 Å.¹¹

Structure of $[\text{H}_2\text{L}^{2+}][\text{SmL}^2(\text{NO}_3)_4][\text{NO}_3]^- \cdot 2$

The structure of **2** is shown in Fig. 3. The asymmetric unit contains a $[\text{Sm}(\text{L}^2)(\text{NO}_3)_4]^-$ anion and an $[\text{H}_2\text{L}^{2+}]$ cation with an encapsulated NO_3^- anion. The stoichiometry and indeed the structure of the $[\text{Sm}(\text{L}^2)(\text{NO}_3)_4]^-$ anion is similar to that recently observed in the structure of $[\text{La}(\text{L}^2)_2(\text{NO}_3)_2]^+[\text{La}(\text{L}^2)(\text{NO}_3)_4]^-$.¹⁴ In both structures the metal atoms in the anion are 11-co-ordinate. There are nine other structures in the Cambridge Database containing Sm–O (nitrate) bonds. However, the Sm(III) ion is co-ordinated only to oxygen atoms in the surveyed structures but to both oxygen and nitrogen atoms in our structure. Six of these previously reported structures

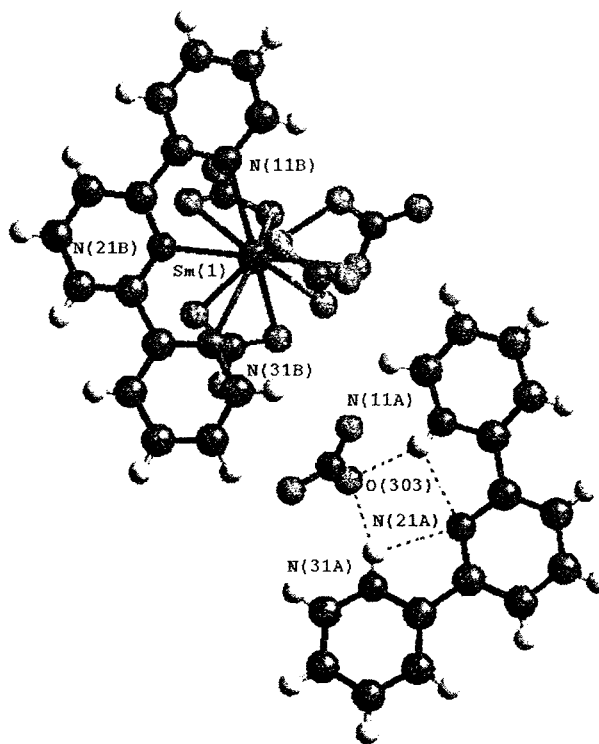


Fig. 3 The structure of compound **2** showing both the $[\text{H}_2\text{L}^{2+}]$ cation hydrogen bonded to a nitrate anion together with the $[\text{Sm}(\text{NO}_3)_4\text{L}^2]^-$ anion. Samarium brown, oxygen red, carbon green, hydrogen yellow, nitrogen purple.

contain a 10-co-ordinate Sm(III) ion. Only one of the reported structures contains Sm(III) in both the anion and the cation and in both ions the metal is 11-co-ordinate.¹⁵ The Sm–O bond lengths in our structure vary between 2.494(5) and 2.742(5) Å. The average Sm–O (nitrate) distance from all the surveyed structures is 2.56 Å [$n = 56$, $\sigma(n - 1) = 0.093$ Å]. It is difficult to explain why there is such a broad range in Sm–O distances in our structure. It is interesting to note that the oxygen atom involved in the longest Sm–O bond is *trans* to the shortest Sm–N bond which involves the nitrogen atom in the central pyridine ring. The three Sm–N bond lengths are all longer than those observed in the two previously published structures containing L^2 with Sm.⁴ In the first of these structures the Sm(III) is either eight- or nine-co-ordinate depending on the cation. Thus, the formula can be described as $\text{Sm}(\text{L}^2)(\text{Cl})(\text{H}_2\text{O})_{4,5}$. In the second structure the Sm(III) is eight-co-ordinate, the metal being co-ordinated to three L^2 N atoms, four Cl atoms and one water molecule. The Sm–N bond lengths vary between 2.56 and 2.59 Å in both of these structures, while in **2** the Sm(III) ion is 11-co-ordinate and the bond lengths vary between 2.62 and 2.65 Å. The increased Sm–N distances in **2** are clearly a consequence of the higher co-ordination number compared to the other structures.

The terpyridine co-ordinated to the Sm(III) ion is almost planar, the N–C–C–N dihedral angles are 5.6(1) and 3.7(1)°. The terpyridyl cation shows more distortion from planarity with corresponding dihedral angles of –3.6(1) and 11.0(1)°. The nitrate ion in the terpyridyl cavity is hydrogen bonded to the N–H protons through one oxygen only. As with the diprotonated terpyridine in **1**, it is also possible to describe the N–H···N interactions as weak intramolecular hydrogen bonds.

Theoretical structural analysis of L^2 , $[\text{HL}^{2+}]$ and $[\text{H}_2\text{L}^{2+}]$

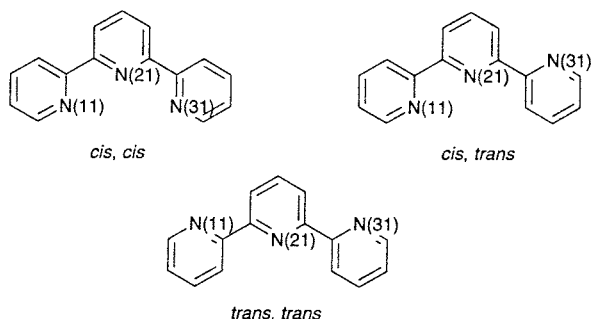
The terpyridyl ligand L^2 . There are three possible conformations for L^2 which can be characterised by the N–C–C–N torsion angles as *tt* (*trans,trans*), *ct* (*cis,trans*) and *cc* (*cis,cis*).

Table 4 Results from quantum mechanics calculations on terpy, [Hterpy]⁺ and [H₂terpy]²⁺. Geometry optimisation was carried out using the 6-31G** basis set. Energies in au (= 627.509 kcal mol⁻¹)

Compound	Protonated nitrogen	Conformation		
		<i>cis,cis</i>	<i>cis,trans</i>	<i>trans,trans</i>
L ²		-737.798 (<i>cc</i>)	-737.807 (<i>ct</i>)	-737.818 (<i>tt</i>)
[HL ²] ⁺	N(11)	-738.202 (H- <i>cc</i> 1)	-738.203 (H- <i>ct</i> 1)	-738.195 (H- <i>tt</i> 1)
	N(21)	-738.213 (H- <i>cc</i> 2)	-738.206 (H- <i>ct</i> 2)	-738.195 (H- <i>tt</i> 2)
	N(31)	<i>a</i>	-738.189 (H- <i>ct</i> 3)	<i>a</i>
[H ₂ L ²] ²⁺	N(11), N(21)	-738.457 (2H- <i>cc</i> 1)	-738.443 (2H- <i>ct</i> 1) ^b	-738.443 (2H- <i>tt</i> 1)
	N(11), N(31)	-738.486 (2H- <i>cc</i> 2)	-738.484 (2H- <i>ct</i> 2)	-738.479 (2H- <i>tt</i> 2)
	N(21), N(31)	<i>c</i>	-738.443 (2H- <i>ct</i> 3) ^b	<i>c</i>

^a Structures with N(31) protonated are equivalent to structures with N(11) protonated. ^b Structures unstable to geometry optimisation. The 2H-*tt*1 structure was obtained. ^c Structures with N(21) and N(31) protonated are equivalent to structures with N(21) and N(11) protonated.

We have analysed these conformations for L², [HL²]⁺ and [H₂L²]²⁺ using the GAUSSIAN 94 program.¹⁶ Starting models were built using the CERIU2 software¹⁷ and the three rings were made approximately coplanar but no symmetry was imposed. Structures were then optimised using the 6-31G* basis set.¹⁸ Results are summarised in Table 4.



For the neutral ligand L², it was found that the order of energies was *tt* < *ct* < *cc* and this is consistent with the fact that the *tt* conformation is observed in the crystal structure of L²¹⁹ and also the 4'-phenyl,²⁰ 4'-aniline²¹ and 4'-NMe₂²² derivatives. A structure with a boron cage in the 4' position *viz* 4'-(*closo-o*-carboranyl)terpyridine also has this *tt* conformation.²³ This *trans* conformation of pyridine rings is also found in quaterpyridine²⁴ and a *para* substituted sexipyridine.²⁵

The reasons for this order of conformational preference is clear from the geometry of the optimised structures (Fig. 4). In the *tt* form, the N-C-C-N torsion angles are both 180.0°. However in the *ct* form, while the *trans* torsion angle at -176.1° shows that the rings are close to being coplanar, the *cis* torsion angle at -43.0° shows that the rings are very much twisted away from planarity. This twist is caused by the repulsion between the two *ortho* hydrogen atoms and possibly also from electron-electron repulsion between the lone pairs on the nitrogen atoms. This pattern of conformational change is also observed in the *cc* form where the torsion angles are -47.9, 47.9°. Clearly, the *cis* arrangement reduces conjugation between the two rings and is particularly destabilised by repulsions between the *ortho* hydrogen atoms.

These calculations were carried out on the free ligands but it is possible that the conformational preferences may well change in the presence of hydrogen bond donors or acceptors. It is interesting that the *tt* form is the lowest energy conformation of neutral terpyridyl which is unsuitable for tridentate complexation with a metal atom. However it is possible that this conformation could be stabilised in polar solvents by the formation of intermolecular hydrogen bonds. Thus a water molecule could enter the cavity with the same arrangement as found for the [H₂L²]²⁺·H₂O cation found in **1** but with donor O-H...N instead of acceptor O...H-N hydrogen bonds [see Fig. 5(a)]. A precedence for this proposed structure is found for

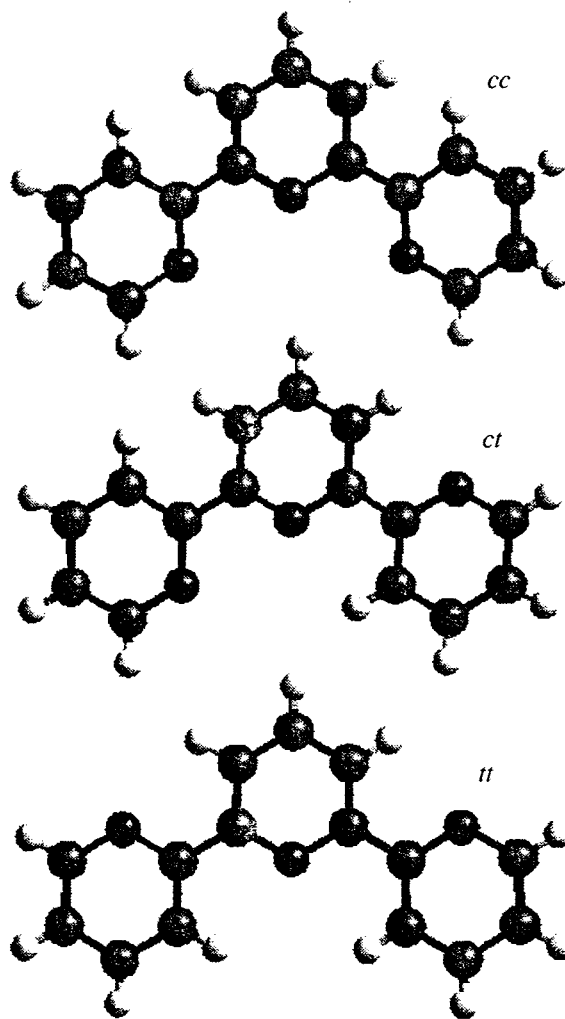


Fig. 4 The three conformations of L², *cis,cis* (*cc*), *cis,trans* (*ct*) and *trans,trans* (*tt*). Energies after geometry optimisation (au) and torsion angles (°) were for *cc* -737.798, -47.9, 47.9; for *ct* -737.807, -43.0, -176.1 and for *tt* -737.818, 180, 180.

a crystal structure of terpyridyl co-crystallised with [SnPh₃(NCS)(H₂O)].²⁶ This is the only crystal structure where an oligopyridine contains adjacent pyridine ligands in the *cis* conformation, but the conformation is stabilised by the formation of two hydrogen bonds to the water molecule which is situated in the terpyridine cavity as well as being bonded to the tin.

In order to calculate the effect of the formation of this L²·H₂O complex, a model structure was built using CERIU2 [Fig. 5(a)] and subjected to optimisation in GAUSSIAN 94. Results show that the energy of the complex was 11.29 kcal mol⁻¹, lower than that of the L² and H₂O separated at infinity.

Water adducts built with the *ct* and *tt* structures proved not to be stable to geometry optimisation, no doubt because of the repulsions from adjacent C-H groups. In the *cc* L·H₂O complex, the structure maintains C_s symmetry, though this was not imposed. The N-C-C-N torsion angles at 42.0, -42.0° are only slightly reduced (by 5.9°) from values in the unhydrated form.

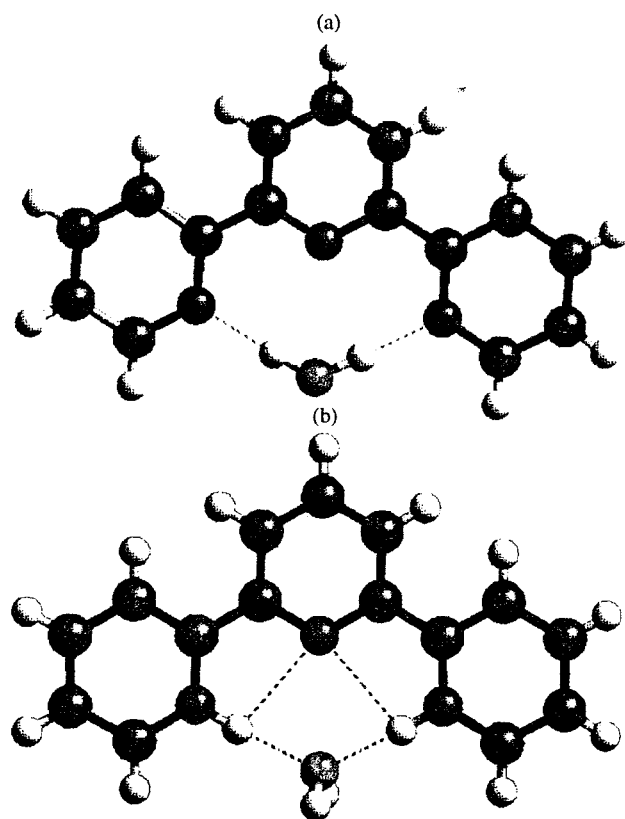


Fig. 5 The stabilisation of the *cis,cis* conformation by intramolecular hydrogen bonds with water molecules. Geometry optimisation via GAUSSIAN 94. (a) The *cc* form accepting hydrogen bonds from a water molecule; N-C-C-N torsion angles are -42.0, 41.9°. (b) The 2H-*cc2* form donating hydrogen bonds to a water molecule; N-C-C-N torsion angles are -18.7, 18.7°. Hydrogen bonds shown as dotted lines. Carbon green, hydrogen yellow, nitrogen purple, oxygen red.

The N...H and O...H distances are 2.2, 3.15 Å respectively with an O-H...N angle of 177.3°. This contrasts with torsion angles of 29.0, -18.0° and N...O distances of 2.80, 2.76 Å in ref. 26.

Monoprotonated [HL²]⁺. When L² is monoprotated, then there are seven possible structures (Fig. 6) depending on the conformation and which nitrogen atom is protonated. There are two *cis,cis* structures; H-*cc1*, H-*cc2* depending on whether N(11) or N(21) is protonated [N(11) is equivalent to N(31)]; three *cis,trans* structures H-*ct1*, H-*ct2*, H-*ct3* dependent upon whether N(11), N(21) or N(31) is protonated; and two *trans,trans* structures H-*tt1*, H-*tt2* dependent upon whether N(11) or N(21) is protonated. These seven structures were built with CERIUS2 and geometry optimised with GAUSSIAN 94 and the resulting structures are shown in Fig. 6. As with terpyridyl L², the energies of [HL²]⁺ can be correlated with two dominant structural features, one favourable and one unfavourable.

The lowest energy structures contain at least one pair of mutually *cis* nitrogen atoms of which one is protonated so that an energetically favourable intramolecular hydrogen bond interaction can be formed. Thus H-*cc2* has the lowest energy with two such interactions, next lowest are H-*cc1*, H-*ct1* and H-*ct2* with one such interaction and the three highest energies are H-*ct3*, H-*tt1* and H-*tt2* with no such interactions. The unfavourable interaction occurs when the N-H is *cis* to one or two C-H bonds leading to H...H repulsion. Two of these interactions are found in H-*tt2*, and one in H-*tt1*, H-*ct3* and H-*ct2*. It is interesting that this latter H-*ct2* structure also has a favourable hydrogen bond interaction which more than compensates for this repulsion as the energy is one of the lowest found. Unfavourable *ortho* C-H interactions are also found in several of the structures. The geometry in the structures (Fig. 6) follow a regular logical pattern. For the *cis* N-C-C-N torsions, the angle is close to zero when a hydrogen bond is formed (e.g. 5.1 in H-*cc1*, -0.1 in H-*cc2*, 6.8 in H-*ct1*, -0.3° in H-*ct2*) but otherwise is twisted significantly to relieve steric strain (e.g. -28.6 in H-*cc1*, -37.2° in H-*ct3*). For the *trans* N-C-C-N torsions, the angle is only close to 180° in H-*tt1* where there are no *ortho* repulsions but in all the other structures the absolute value of the angle ranges from 148.8 to 155.8°. There are other geometric changes concomitant with the formation of the intramolecular N-H...N hydrogen bonds. Thus in H-*ct2* the

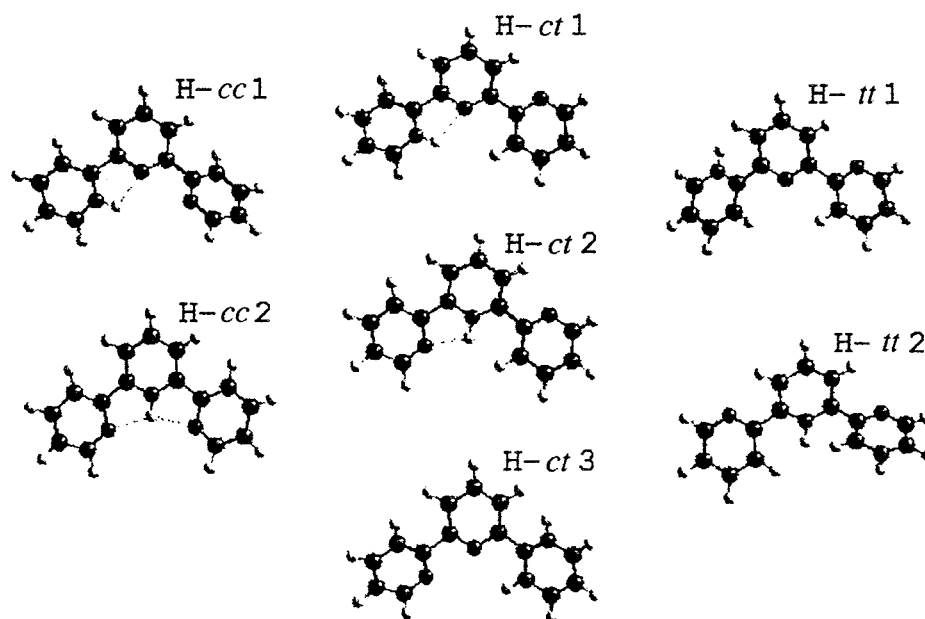


Fig. 6 The seven structures of [HL²]⁺ which are characterised by the conformation and the nitrogen that is protonated. Energies after geometry optimisation (au) and torsion angles (°) were for H-*cc1* -738.202, -28.6, 5.1; for H-*cc2* -738.215, -0.1, -0.1; for H-*ct1* -738.203, 6.8, -163.8; for H-*ct2* -738.206, -0.3, 155.8; for H-*ct3* -738.189, -37.2, -154.8; for H-*tt1* -738.195, -174.0, -148.8 and for H-*tt2* -738.195, -150.0, -150.0. Hydrogen bonds shown as dotted lines. Carbon green, hydrogen yellow, nitrogen purple.

two C-C-N angles to the central pyridine atom are 115.1° to ring 1 to facilitate the hydrogen bond and 119.1° to ring 3 where there is no such hydrogen bond. The H...N distances are 2.07 Å in H-cc1, but 2.16 Å in H-ct2 and 2.12 Å in H-ct1, 2.10 Å in H-ct2. The N-H...N angles range from 105 to 108° , rather small compared to the usual angle for a hydrogen bond, but the calculations presented here clearly indicate that the hydrogen bonds are significant. There is a significant change in the N-C bond lengths when the nitrogen is protonated and increases of ca. 0.01 Å are observed. Thus in H-cc2, the C-N distances are 1.338 Å compared to 1.326 and 1.315 Å where the N is unprotonated.

There is very little experimental evidence on $[\text{HL}^2]^+$ that can be correlated with these calculations. There is only one crystal structure containing $[\text{HL}^2]^+$, viz the salt with $[\text{CF}_3\text{SO}_3]^-$ ¹³ and this has the H-ct1 structure. However the structure of diproton-

ated quinquepyridinium which has the *cis,trans,trans,cis* conformations shows the outer two nitrogens to be protonated so that the structure contains two moieties equivalent to the H-ct1 structure.²⁷ As is apparent from the energy values in Table 4, this H-ct1 structure is not the lowest energy structure, but unlike the more favourable H-cc2 and H-ct2 structures, it retains the possibility of being able to form intermolecular hydrogen bonds. Indeed in the two crystal structures, this is precisely what is found, that the protonated nitrogen atom forms an intramolecular hydrogen bond but also an intermolecular hydrogen bond to the anion in the crystal. The anion is situated well away from the cavity (Fig. 7) and calculations show that this anion (or indeed any other) could not form stable hydrogen bonds to the protonated central nitrogen atom as occurs in H-cc2 and H-ct2. We conclude, therefore, that in the presence of solvents and/or anions which can accept hydrogen bonds that the H-ct1 structure is more likely to be found in preference to H-cc2 and H-ct2 despite these having lower energies in the gas phase.

Diprotonated $[\text{H}_2\text{L}^2]^{2+}$. For $[\text{H}_2\text{L}^2]^{2+}$ there are also seven different structures. There are two with the *cis,cis* conformation called 2H-cc1 [with N(11) and N(21) protonated], and 2H-cc2 [with N(11) and N(31) protonated]; three with the *cis,trans* conformation; 2H-ct1 [N(11), N(21) protonated], 2H-ct2 [N(11), N(31) protonated] and 2H-ct3 [N(21), N(31) protonated] and two with the *trans,trans* conformation; 2H-tt1 [N(11), N(21) protonated] and 2H-tt2 [N(11), N(31) protonated].

Models were built with CERIUS2 and then geometry optimised with GAUSSIAN 94 and the results are given in Table 4 and illustrated in Fig. 8. The same two structural features are crucial to determining the relative energy values, thus lower energy structures contain intramolecular hydrogen bonds and higher energy structures N-H...C-H repulsions. There are more of these latter types of repulsion in the diprotonated structures than in the monoprotated structures and there is also the possibility of N-H...N-H repulsions. The C-H...C-H repulsions are present in all structures but seem to be less important, possibly because the electrostatic repulsions between hydrogen atoms is less.

Because of these *ortho-ortho* repulsions only three structures contain intramolecular hydrogen bonds 2H-cc2, 2H-ct2 and 2H-cc1 and these together with 2H-tt2 have the lowest energies. The lowest energy conformation (2H-cc2) is also observed in the two crystal structures reported above. In this structure the

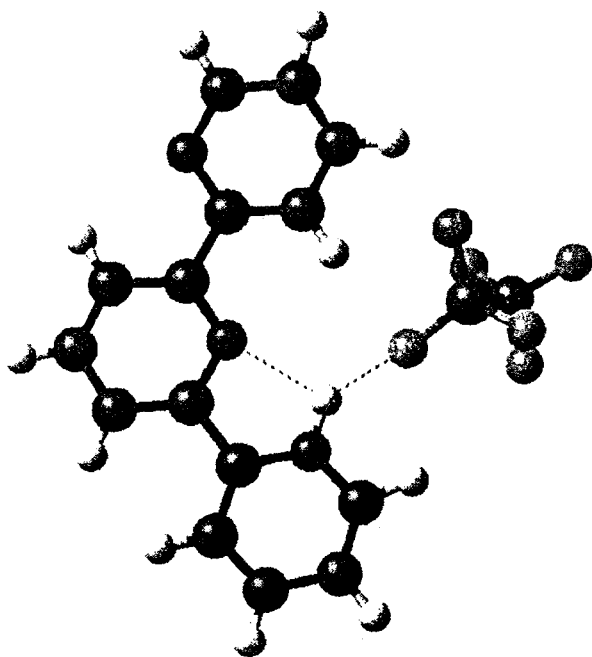


Fig. 7 The structure of $[\text{HL}^2]^+[\text{CF}_3\text{SO}_3]^-$ showing the intermolecular hydrogen bond between N-H and an oxygen atom in the anion.¹³ Sulfur brown, oxygen red, carbon green, fluorine light green, nitrogen purple, hydrogen yellow.

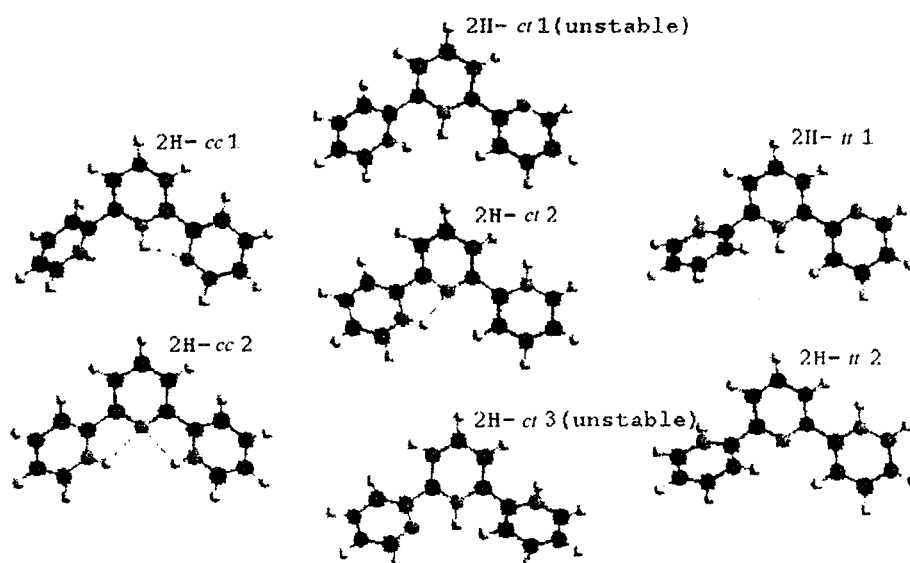


Fig. 8 The seven structures of $[\text{H}_2\text{L}^2]^{2+}$ which are characterised by the conformation and the nitrogen that is protonated. Energies after geometry optimisation (au) and torsion angles ($^\circ$) were for 2H-cc1 -738.456, 0.6, 58.7; for 2H-cc2 -738.486, -28.3, -28.3; for 2H-ct1 unstable; 2H-ct2 -738.484, 12.8, -139.1; for 2H-ct3 unstable; for 2H-tt1 -738.444, -130.5, -155.1 and for H-tt2 -738.479, -145.0, -145.0. Hydrogen bonds shown as dotted lines. Carbon green, hydrogen yellow, nitrogen purple.

N–C–N torsion angles are -28.3° and the N–H \cdots N distance is 2.43 Å. This compares with torsion angles of 0.4, 6.0; -3.3 , 0.5; -1.9 , 0.1° in **1** and 10.8, -3.7° in **2** and distances of 2.28–2.34 Å in the two structures (though it must be borne in mind that these are calculated hydrogen positions from the crystal structure determinations) and indeed to the 2.16 Å observed in the 1H-*cc1* structure. The distance in 2H-*cc2* is also large by comparison at 2.37 Å. It seems likely that the ligand in the crystal structures is more planar because of the intermolecular hydrogen bonds formed to the nitrate. In order to test this proposition, we carried out a GAUSSIAN 94 geometry optimisation of a water molecule contained within the cavity of the 2H-*cc2* structure [Fig. 5(b)]. On optimisation the two torsion angles had decreased to 18.7 and -18.7° and the two H \cdots N distances reduced to 2.13, 2.13 Å. Results show that the energy of the complex was 18.72 kcal mol $^{-1}$, lower than that of [H₂L²]²⁺ and H₂O separated at infinity. We conclude that in the case of the diprotonated [H₂L²]²⁺ the gas phase preference for the 2H-*cc2* structure is enhanced in solution and that this is likely to be the only diprotonated species present.

The conformation found in the 2H-*cc1* structure is particularly interesting as it contains a N–H \cdots N–H repulsion which is alleviated with a torsion angle of 58.7° while the second *cis* interaction contains a N–H \cdots N attraction and the torsion angle remains close to zero at 0.6° . Of the other structures 2H-*cc1* and 2H-*cc3* proved not to be stable to geometry optimisation and reverted to the 2H-*tt1* structure. The 2H-*tt2* structure contains no hydrogen bonds but has a relatively low energy because there are no significant *ortho* repulsions. The 2H-*tt1* structure has the highest energy of all because of significant repulsions between N–H and C–H in the cavity.

Conclusion

Theoretical calculations have shown that the lowest energy conformation of the terpyridyl ligand is the *trans,trans* form. However *cis* forms are stabilised on protonation by the formation of weak intramolecular N–H \cdots N hydrogen bonds. It is likely that the lowest energy forms in solution for the protonated and diprotonated forms are the H-*cc1* and 2H-*cc2*. These results are consistent with evidence from crystal structure determinations presented here and from the literature. It is suggested that any theory of extraction based on the ion-pair mechanism must be consistent with the presence of these cations both of which will be stabilised by the formation of intermolecular hydrogen bonds to solvent and/or accompanying anions.

Acknowledgements

We are grateful for the financial support by the EC Research Programme Contract NEWPART (FI41-CT-96-0010) and the Swedish Nuclear and Waste Management Co., SKB. We would also like to thank the EPSRC and the University of Reading for funding of the image-plate system. The use of the Origin 2000 at the High Performance Computer Centre at the University of Reading is gratefully acknowledged.

References

- 1 K. L. Nash, *Solvent Extraction and Ion Exchange*, 1993, **11**, 729.
- 2 G. Y. S. Chan, M. G. B. Drew, M. J. Hudson, N. S. Isaacs, P. Byers and C. Madic, *Polyhedron*, 1996, **15**, 3385.
- 3 E. C. Constable, *Adv. Inorg. Chem.*, 1986, **30**, 69.
- 4 C. J. Kepert, L. Weimin, B. W. Skelton and A. H. White, *Aust. J. Chem.*, 1994, **47**, 365.
- 5 I. Hagström, L. Spjuth, Å. Enarsson, J. O. Liljenzin, M. Skålberg, M. J. Hudson, P. B. Iveson, P. Y. Cordier, C. Hill and C. Madic, *Solvent Extraction and Ion Exchange*, in the press.
- 6 A referee has commented that adding concentrated nitric acid to a methanol solution is highly dangerous. For this reason, as stated, we used extremely small quantities.
- 7 W. Kabsch, *J. Appl. Crystallogr.*, 1988, **21**, 916.
- 8 G. M. Sheldrick, SHELXS, program for structure determination, University of Göttingen, 1997.
- 9 N. Walker and D. Stuart, DIFABS, *Acta Crystallogr., Sect. A*, 1983, **39**, 158.
- 10 G. M. Sheldrick, SHELXL, program for crystal structure refinement, University of Göttingen, 1997.
- 11 C. J. Kepert, B. W. Skelton and A. H. White, *Aust. J. Chem.*, 1994, **47**, 391.
- 12 J. G. Bergman and F. A. Cotton, *Inorg. Chem.*, 1966, **5**, 1208.
- 13 A. Hergold-Brundic, Z. Popovic and D. Matkovic-Calogovic, *Acta Crystallogr., Sect. C*, 1996, **52**, 3154.
- 14 M. Frechette and C. Bensimon, *Inorg. Chem.*, 1995, **34**, 3520.
- 15 J. H. Burns, *Inorg. Chem.*, 1979, **18**, 3044.
- 16 M. J. Frisch, G. W. Trucks, H. B. Schlegel, P. M. W. Gill, B. G. Johnson, M. A. Robb, J. R. Cheeseman, T. A. Keith, G. A. Petersson, J. A. Montgomery, K. Raghavachari, M. A. Al-Laham, V. G. Zakrzewski, J. V. Ortiz, J. B. Foresman, J. Cioslowski, B. B. Stefanov, A. Nanayakkara, M. Challalcombe, C. Y. Peng, P. Y. Ayala, W. Chen, M. W. Wong, J. L. Andrews, E. S. Replogle, R. Gomperts, R. L. Martin, D. L. Fox, J. S. Binkley, D. J. Defrees, J. Baker, J. P. Stewart, M. Head-Gordon, C. Gonzalez and J. A. Pople, GAUSSIAN 94, Revision A1, Gaussian, Inc., Pittsburgh, PA, 1995.
- 17 CERIOUS2 software, Molecular Simulations Inc., San Diego, CA, 1997.
- 18 For all the structures reported here, geometry optimisation was carried out with no constraints and no imposed symmetry. It is possible particularly in cases where intramolecular 'bonds' are present that basis-set superposition errors may not be negligible but a detailed investigation is beyond the scope of this paper.
- 19 C. A. Bessel, R. F. See, D. L. Jameson, M. R. Churchill and K. J. Takeuchi, *J. Chem. Soc., Dalton Trans.*, 1992, 3223.
- 20 E. C. Constable, J. Lewis, M. C. Liptrot and P. R. Raithby, *Inorg. Chim. Acta*, 1990, **178**, 47.
- 21 G. D. Storrier, S. B. Colbran and D. C. Craig, *J. Chem. Soc., Dalton Trans.*, 1997, 3011.
- 22 E. C. Constable, A. M. W. C. Thompson, D. A. Tocher and M. A. M. Daniels, *New J. Chem.*, 1992, **16**, 855.
- 23 D. Armspach, E. C. Constable, C. D. Housecroft, M. Neuburger and M. Zehnder, *New J. Chem.*, 1996, **20**, 331.
- 24 E. C. Constable, S. M. Elder, J. Healy and D. A. Tocher, *J. Chem. Soc., Dalton Trans.*, 1990, 1669.
- 25 K. T. Potts, K. A. G. Raiford and M. Keshavarz, *J. Am. Chem. Soc.*, 1993, **115**, 2793.
- 26 L. Prasad and F. E. Smith, *Acta Crystallogr., Sect. B*, 1982, **38**, 1815.
- 27 E. C. Constable, S. M. Elder, J. V. Walker, P. D. Wood and D. A. Tocher, *J. Chem. Soc., Chem. Commun.*, 1992, 229.

Received 31st March 1998; Paper 8/02458H

Appendix

V

Contract FI41-CT-96-0010, Participant No. 3, Chalmers University of
Technology, Progress Report from 1st May to 31st October 1998

G. Källvenius, J.O. Liljenzin and L. Spjuth

Introduction

The extraction ability of three new substituted triazines has been studied and basicity measurements of these ligands and previously studied triazines and oligopyridines has been performed. Basicity measurements of different malonamides has also been conducted and compared with the calculated gas-phase basicities that were calculated with Gaussian 94 at the University of Reading earlier this year. Complementary investigations on the terpyridine, 2-bromodecanoic acid system has been performed prior to the process calculations for separation of trivalent actinides and lanthanides that will take place next semester. A MSci student, Göran Källvenius, has been working in the project during the last semester since Åsa Enarsson is on maternity leave.

Results

Tripyridyltriazines

The extraction of americium and europium was investigated using 0.02M TADPTZ, TADQTZ or OADQTZ in synergy with 1M 2-bromodecanoic acid in *tert*-butylbenzene.

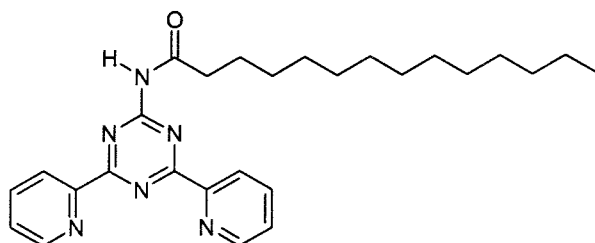


Figure 1. 4-tetradecanoyl amino-2,6 di(2-pyridyl) 1,3,5 triazine (TADPTZ)

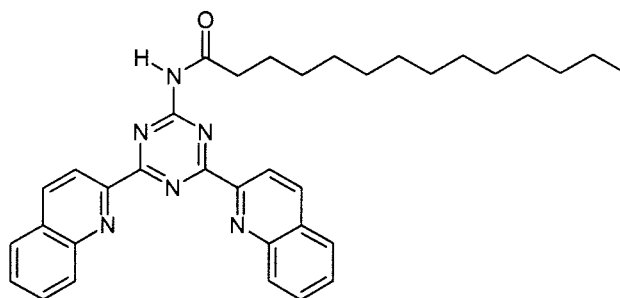


Figure 2. 4-tetradecanoyl amino-2,6 di(2-quinoliny) 1,3,5 triazine (TADQTZ)

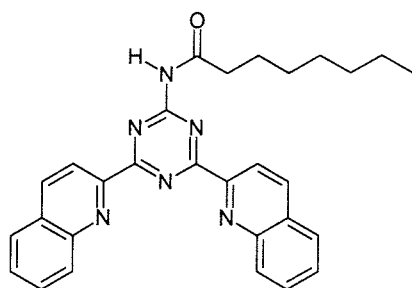


Figure 3. 4-octanoyl amino-2,6 di(2-pyridyl) 1,3,5 triazine (TADQ TZ)

All ligands showed similar extraction behaviour to that of the previous investigated triazines and oligopyridines; high extraction at low nitric acid concentration and a decrease in extraction with increase of nitric acid concentration. There was no significant extraction above 0.1 M nitric acid concentration, see Fig. 4. However, the triazines show better extraction compared to the substituted oligopyridines. The extraction of TADPTZ was slightly higher than the extraction with OADPTZ. The only difference between these two structures is the length of the carbon chain on the triazine ring. This indicates that the length of the carbon chain is of minor importance for the extraction, at least when the carbon chain is longer than 8 carbons. However, the separation factor seems to be slightly smaller, $SF_{Am/Eu}$ around 8, for the TADPTZ derivative compared to OADPTZ which has a $SF_{Am/Eu}$ around 10, see table 2.

The quinoline derivatives showed considerably lower extraction compared to the pyridyl derivatives, as seen in Fig. 4 and Table 2. Those ligands had D-values less than unity at all nitric acid concentrations studied and the separation factor was around 3. The low extraction might be due to that the quinolinyl groups sterically hinder the binding of a lanthanide or actinide ion at the binding site. Molecular modelling might be used to study this.

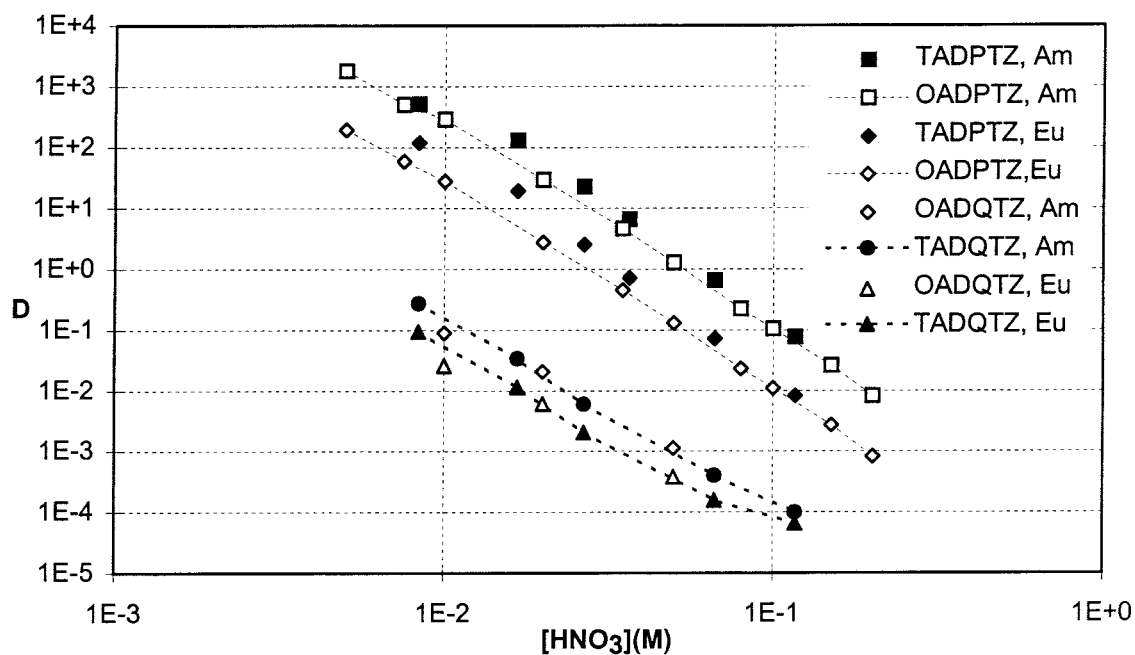


Figure 4. Extraction of americium and europium by 0.02M of different triazine ligands and 1M 2-bromodecanoic acid in *tert*-butylbenzene from different initial nitric acid concentrations.

Basicity measurements of the triazine derivatives and some oligopyridines were performed by non-aqueous titrations in both acetic anhydride and acetonitrile media. The potential at the half neutralisation point (HNP) was used as a measure for basicity of the different ligands. To avoid drift during the experiments, the HNP was adjusted by subtracting the HNP of a reference molecule. Pyridine was used as an external reference in the acetic anhydride system and imidazole was used as an internal reference in the acetonitrile system. To facilitate dissolution of the ligands in the titration media, the ligands were first dissolved in 0.25M 2-bromodecanoic acid in *tert*-butylbenzene and then added to the titration media. A constant addition of HA makes a comparison of the relative basicities possible but the presence of the 2-bromodecanoic acid has to be studied further.

The acetonitrile media is known to be more differentiating than acetic anhydride when titrating amines [1]. Aromatic amines have also shown a non-linear relation of $pK_A(\text{aq})$ to HNP (half neutralisation potential) in acetic anhydride media [2]. We therefore wanted to test both media in order to find which of them gave the larger and more linear response to differences in $pK_A(\text{aq})$.

Different amines with known $pK_A(\text{aq})$ was titrated in the two media to investigate the differentiating effect. The slope is 50 mV/pH in acetic anhydride and 61 mV/pH in acetonitrile when the $pK_A(\text{aq})$ for the different reference molecules are plotted versus the measured HNP, see Fig. 5. The potential range, for the triazines and oligopyridines investigated, was 106 mV in acetonitrile compared to only 61 mV in acetic anhydride. As a consequence of the better differentiating effect in acetonitrile, the second protonation is also easier to identify when using acetonitrile, see Fig. 7.

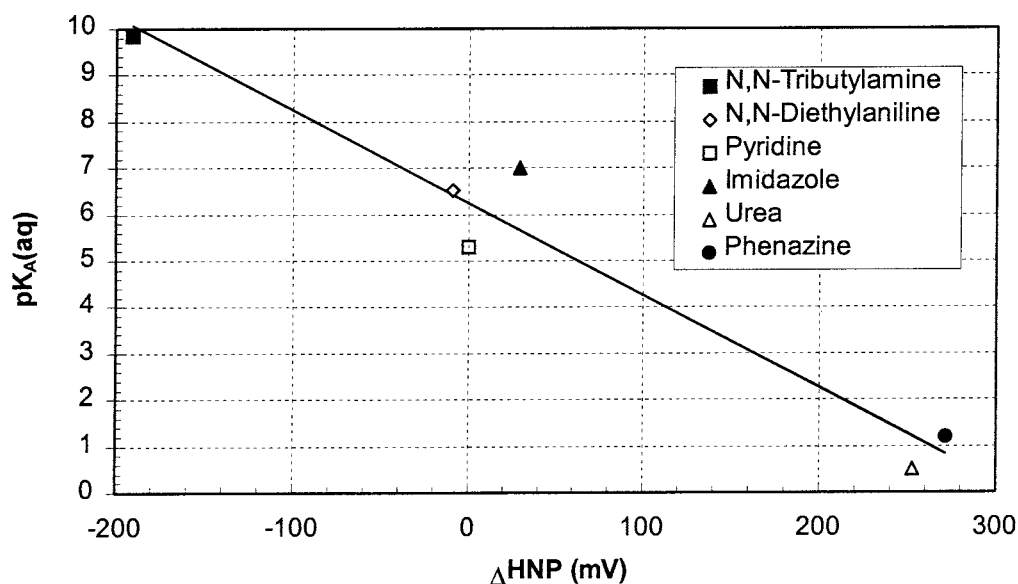


Figure 5. $pK_A(\text{aq})$ versus the ΔHNP in acetic anhydride for some substances with known $pK_A(\text{aq})$ [1]. ΔHNP is compared to HNP of pyridine

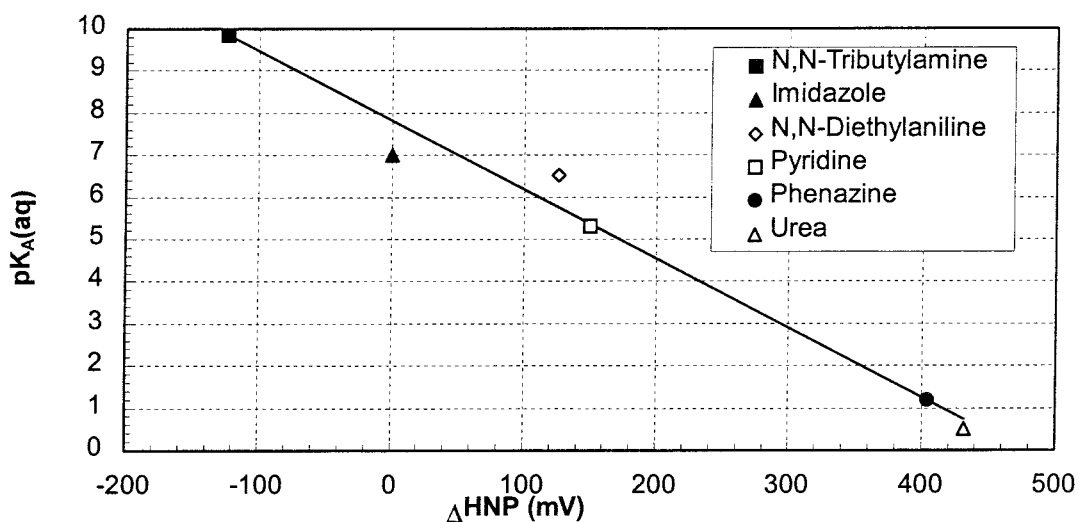


Figure 6. $pK_A(\text{aq})$ versus the ΔHNP in acetonitrile for some substances with known $pK_A(\text{aq})$ [2]. ΔHNP is compared to HNP of imidazole

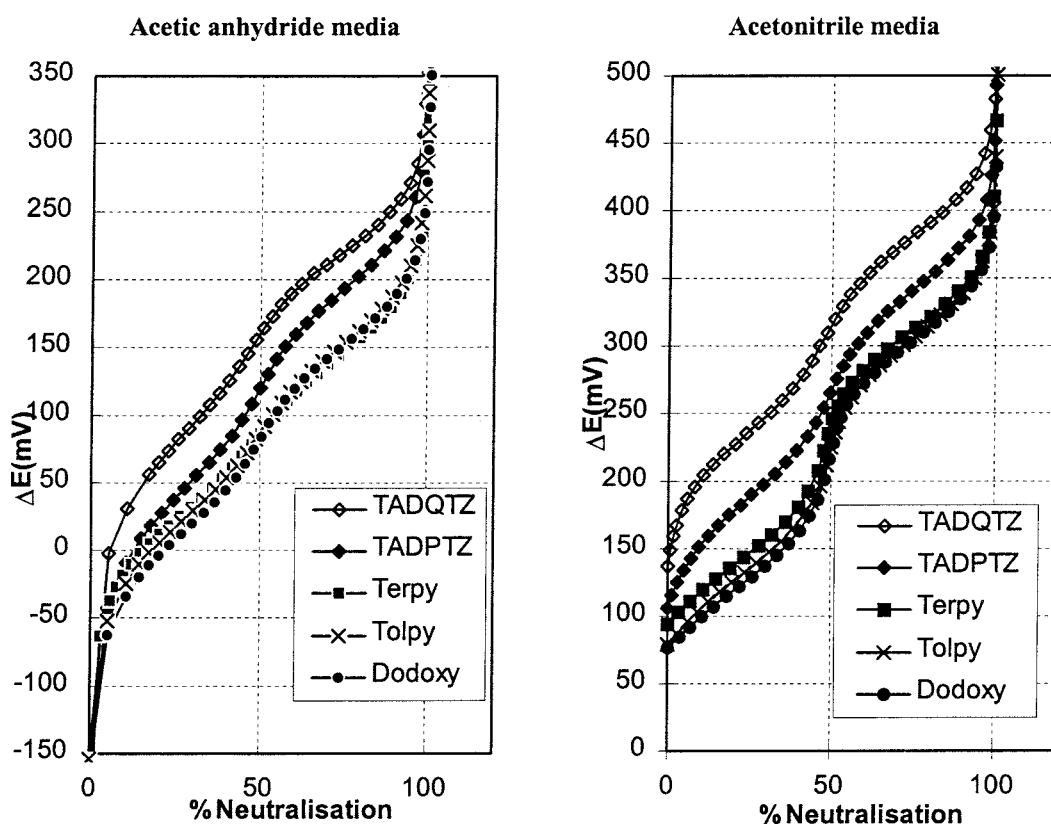
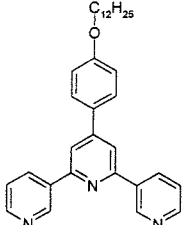
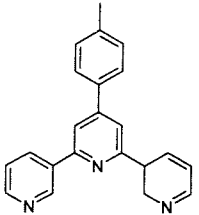
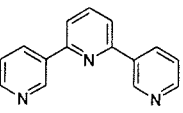
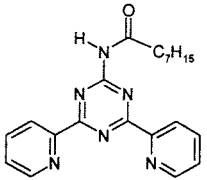
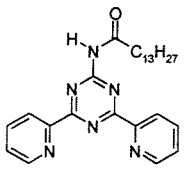
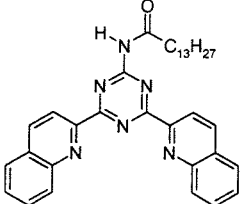
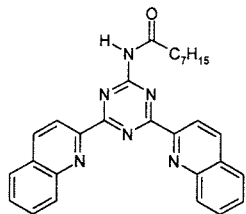


Figure 7. Titration curves for the investigated triazines and oligopyridines in acetic anhydride and acetonitrile media. 100% neutralisation refers to the second protonation.

Table 2 shows the experimentally determined ΔHNP (half neutralisation potential) values for the new triazine ligands and some of the previously investigated oligopyridines and triazines. The higher the ΔHNP , the less basic is the molecule. The relative basicity order in acetic anhydride media is basically the same as the order in

Table 2: Extraction data with 0.02M ligand and 1M HA in TBB and Δ HNP in acetic anhydride (Ac_2O) and acetonitrile (CH_3CN). $\Delta\text{HNP} = \text{HNP}_{\text{ligand}} - \text{HNP}_{\text{reference}}$ (*=interpolated values between two nitric acid concentrations)

Ligand	Name	ΔHNP (mV) $\text{Ac}_2\text{O}/\text{CH}_3\text{CN}$	D_{am} (0.01M HNO_3)	SF (0.02M HNO_3)
	Dodoxy	12/127	4.2	7.6
	Tolpy	22/138	2.8	8.8
	Terpy	30/156	13	7.2
	OADPTZ	33/190	287	10.5
	TADPTZ	45/187	359	8.2*
	TADQTZ	81/233	0.16	3.0*
	OADQTZ	81/215	0.09	3.4

acetonitrile. TADPTZ and OADPTZ showed a reverse order but the difference in ΔHNP is within the statistical error. A low basicity is expecting to give a high extraction and this is seen for the TADPTZ and OADPTZ ligands compared to the oligopyridines and also between terpyridine and the substituted terpyridines. The quinolinyl derivatives showed to be the least basic molecules and the extraction was therefore expected to be better than with the pyridyl derivatives. However, the quinolinyl derivatives showed considerably lower extraction than all other oligopyridines and triazines, as mentioned earlier, sterical hindrance might cause this big change in extraction. Further studies are needed to verify these correlations. The titration method in acetonitrile, using imidazole as an internal reference, proved to be satisfactory for determination of relative basicities and more ligands will be determined in the future.

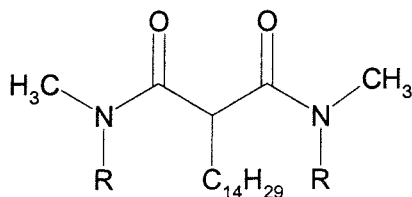
If the linear relation between $\text{pK}_A(\text{aq})$ and ΔHNP for the reference structures are used (Fig. 5-6), a pK_A can be calculated for the different ligands.

Table 1. Calculated pK_A for the different ligands using the relation in Fig.5-6.

Ligand	$\text{pK}_A(\text{Ac}_2\text{O})$	$\text{pK}_A(\text{CH}_3\text{CN})$
Dodoxy	6.02	5.74
Tolpy	5.82	5.56
Terpy	5.67	5.26
OADPTZ	5.61	4.70
TADPTZ	4.92	4.74
TADQTZ	4.64	4.01
OADQTZ	4.64	4.30

Malonamides

The basicity of some malonamides have been determined experimentally by non-aqueous titrations in acetic anhydride media, see Fig. 8. The higher the HNP (half-neutralisation potential) the less basic the molecule. The 4-chloro-phenyl substituted malonamide is thus the least basic malonamide and the cyclohexyl- and butyl substituted malonamide are the most basic ones.



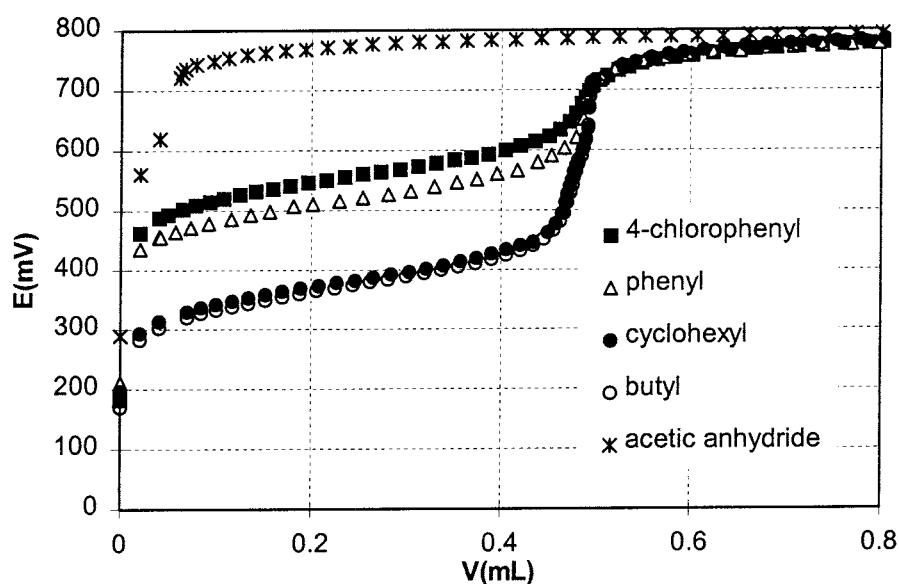


Figure 8. Titration with 0.1M HClO₄ in acetic acid, acetic anhydride media of four malonamides, (CH₃-NR-C=O)₂-C-C₁₄H₂₉, with different nitrogen substituents (R) and acetic anhydride.

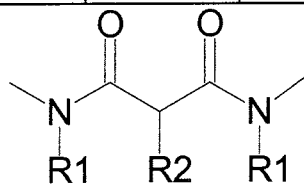
These experimentally obtained basicity data show the same relative order of basicity as the gas-phase basicities that was calculated with Gaussian 94, at Reading University. The gas-phase basicity is defined as the negative of the ΔG of the protonation reaction; $L + H^+ \leftrightarrow LH^+$

$$\Delta G_R = \Delta H_R - T\Delta S_R$$

The ΔH and ΔS terms can be obtained from frequency calculations preceded by geometry optimisation. The smaller the ΔG the more basic the molecule. The ΔG -data in Table 3 are ordered from the least basic to the most basic structure (the one with most negative ΔG). The long carbon chain at the central carbon (C₁₄H₂₉) was replaced by a hydrogen to minimise the computation time. The 2,6-dichlorophenyl derivative is (hopefully) being synthesised and will help to verify the relation between calculated and measured basicity.

Table 3. The difference free Gibbs energy for the protonation reaction of some different substituted malonamides (Gaussian94 HF/6-31G*, full geometry optimisation).

R ₁	R ₂	ΔG_R (kcal/mol)
4-Cl-phenyl	H	-215.30
phenyl	H	-228.56
2,6-diCl-phenyl	H	-229.35
cyclohexyl	H	-230.71



These basicity data is also consistent with earlier extraction studies which shows a decrease in metal extraction for the cyclohexyl and butyl substituted malonamides at high nitric acid concentration, see Fig. 9. This could be due to the higher basicity for these ligands and thus the competition between protons and metal for the binding site is more severe than for the less basic molecules. The 4-chloro-phenyl and phenyl derivatives don't show this decrease in extraction at high HNO_3 concentration. More calculations and measurement on new malonamides, e.g. with alkoxy groups on the central carbon, are in progress and are needed to verify the relation between calculated and experimental basicity and the correlation between basicity and extraction.

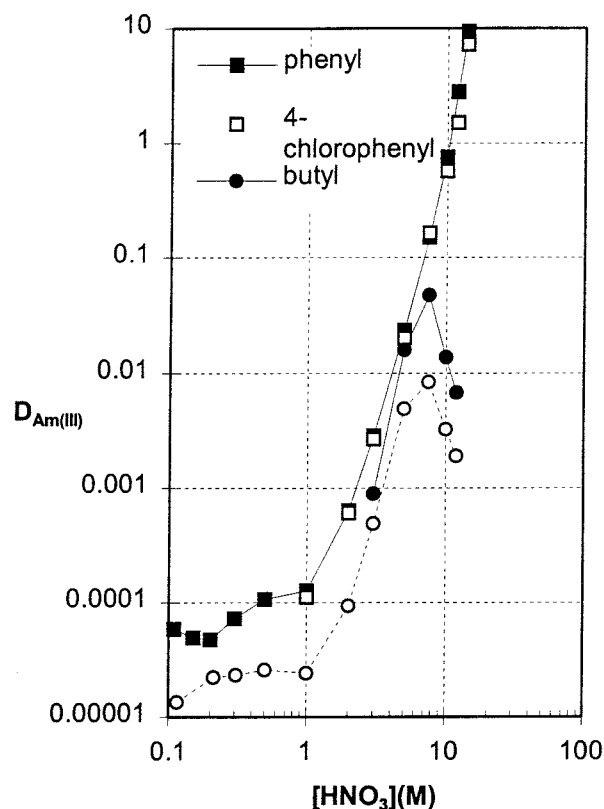


Figure 9. Extraction of Am(III) by 0.1M DMDCHTDMA, DMDPHTDMA, DMD(pCIPH)TDMA and DMDBTDMA in TBB

Terpyridine system

As been indicated in previous reports, the optimal concentration of 2-bromodecanoic acid (HA) in the synergistic mixture with terpyridine is about 3-5 times the concentration of terpyridine. Some complementary experiments were performed to find the different optimal concentrations concerning the best extraction and separation of trivalent actinides and lanthanides. The extraction shows a maximum at intermediate concentrations of HA when the concentration of terpyridine is kept constant, but the maximum is slightly moved to higher HA concentration when the concentration of terpyridine is increased, Fig. 10.

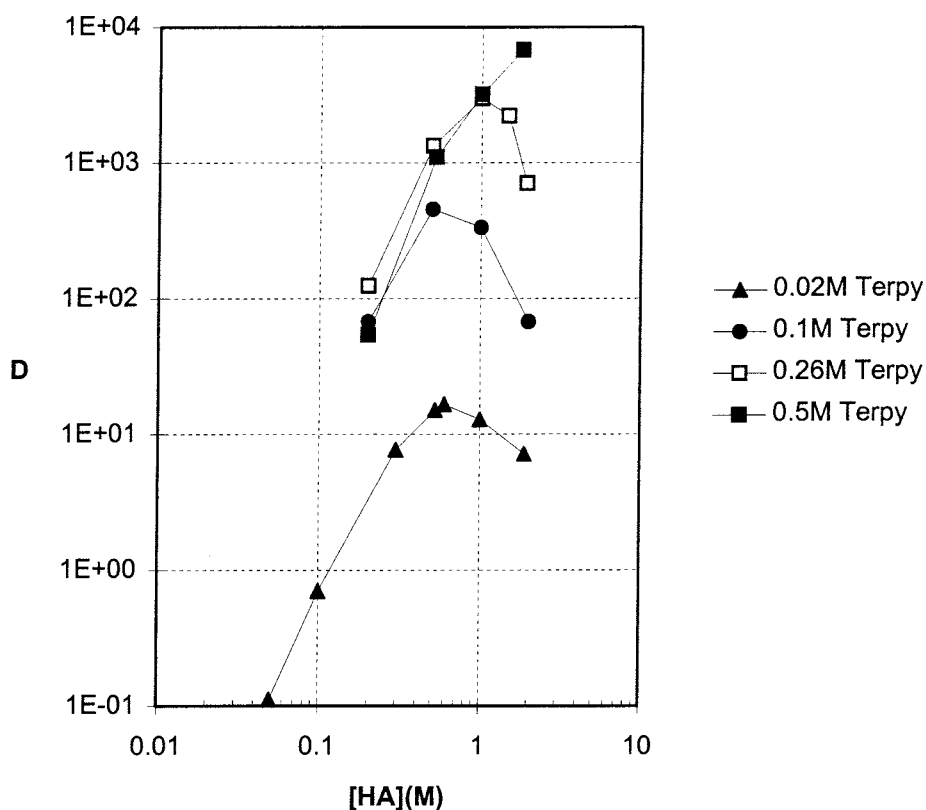


Figure 10. The dependence of the concentration of HA and terpyridine on the extraction of Am(III) at 0.01M HNO₃.

The 2-bromodecanoic acid concentration also influences the separation factor. The separation factor first increases when the concentration of 2-bromodecanoic acid is increased, but decreases again at very high HA concentrations. This decrease is only seen for 0.02M terpyridine, but the separation factor seems to level out for the other concentrations as well, see Fig. 11. The extraction with only HA might be important at these high concentrations of HA, compared to the terpyridine, and could cause the lower separation factors. The polarity of the solvent increases when the concentration of HA is increased which might also influence the separation. Extraction studies in decanol, a more polar diluent, showed lower separation factors compared to *tert*-butylbenzene. The pH at equilibrium in the aqueous phase after contact with these highly concentrated HA solutions might also have an effect and must be further investigated.

A synergistic mixture of 0.1M terpyridine and 0.5M 2-bromodecanoic acid in *tert*-butylbenzene was chosen as the operating point for the future process calculations for separation of actinides from the lanthanides. The acidity in the aqueous phase will be set at 0.1M initially. Two-phase titrations for this new synergistic mixture has been performed to be able to model the system in the process calculations (Fig.12).

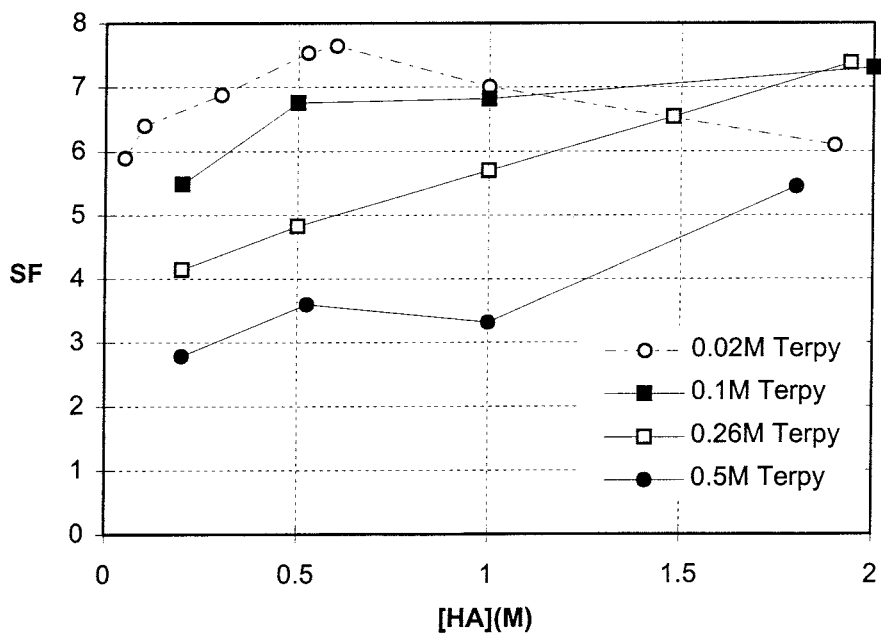


Figure 11. The dependence of the concentration of HA on the separation factor at 0.01M HNO₃.

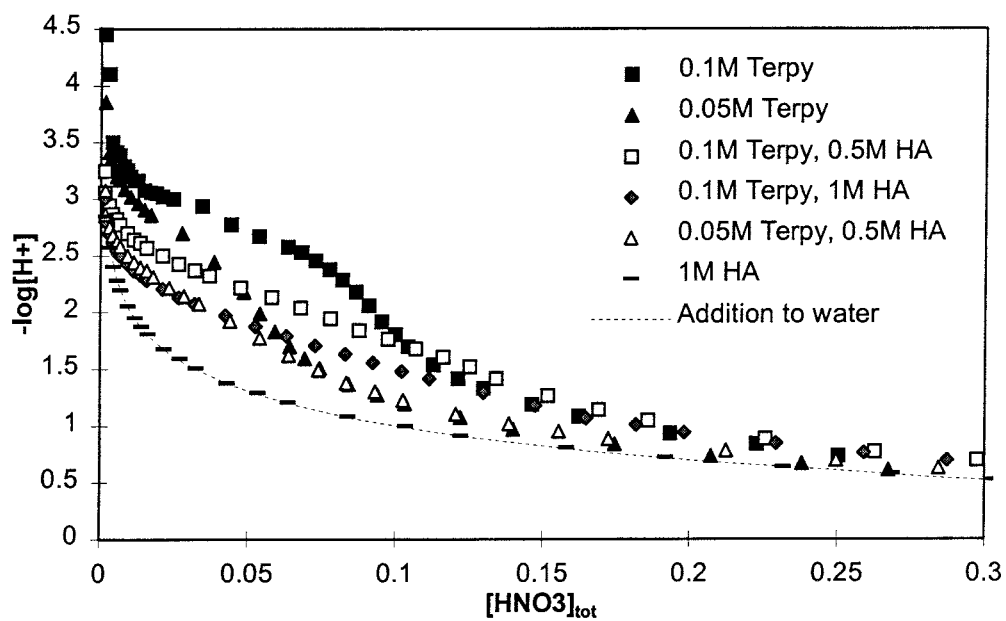


Figure 12. Values of $-\log[H^+]$ in the aqueous phase after different additions of HNO₃ when contacted with different mixtures of terpyridine and HA.

Future Work

Process calculations for the separation of trivalent actinides and lanthanides from 0.1M HNO₃ with the synergistic mixture of 0.1M terpyridine and 0.5M 2-bromodecanoic acid in *tert*-butylbenzene will be performed. Extraction studies and experimental basicity measurements with new ligands will continue and spectrophotometrical analysis will be considered to be used for determination of basicities.

References

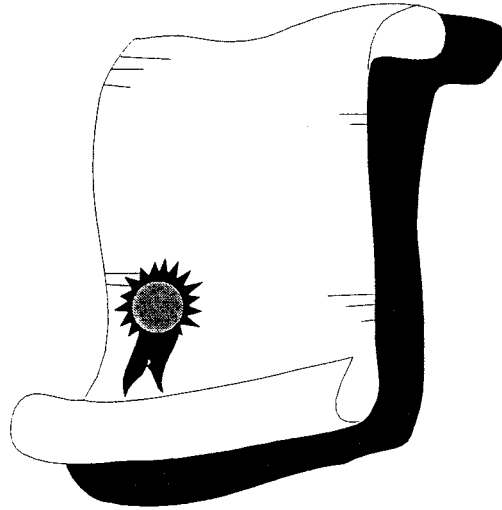
- [1] Streuli, C.A., *Anal. Chem.* vol. 30(5), 997, 1958
- [2] Fritz, J.S., *Anal. Chem.* vol. 25(3), 407, 1953
- [3] Chan, G.Y.S., Drew, M.G.B., Hudson, M.J., Iveson, P.B., Liljenzin, J.O., Skålberg, M., Spjuth, L. and Madic, C., *J. Chem. Soc., Dalton Trans.*, 1997, 649-660.

Appendix

VI

**Basicity and Extraction Studies of Ligands
for
Actinide/Lanthanide Separation**

**Göran Källvenius
1998**



MASTER OF SCIENCE THESIS, 20P

DEPARTMENT OF NUCLEAR CHEMISTRY
CHALMERS UNIVERSITY OF TECHNOLOGY
GÖTEBORG
SWEDEN
981103

Examiner: Prof. Jan-Olov Liljenzin
Supervisors: M.Sc. Lena Spjuth
M.Sc. Anders Landgren

Abstract

Nitrogen donor extractants (which coordinate to metals with nitrogen atoms), have shown good separation ability for trivalent actinides over lanthanides. The basicity of these reagents is considered to be of great importance for the extraction and was therefore investigated.

Non-aqueous titrations in acetonitrile and acetic anhydride has previously been used for titrations of weakly basic compounds. The method has been modified to be able to measure and compare the basicity for aromatic amines accurately.

Extraction tests have been performed on two new ligands. The basicity was determined for these new ligands and some previously studied ligands and attempts to correlate extraction data to the basicity was performed. There seems to be a correlation between the extraction and basicity; the lower the basicity the better metal extraction. However, no obvious correlation between separation factors and basicity was found.

Contents

1. Introduction	1
1.1.1. Background	1
1.1.2. What has been done?	1
1.1.3. Problems	2
1.1.4. Ligands	2
2. Theory	3
2.1. Metal extraction	3
2.1.1. Distribution ratio	3
2.1.2. Error estimation	3
2.1.3. Extraction mechanism	4
2.2. Non-aqueous titrations	5
2.2.1. Titration media	5
2.2.2. Reactions between titrand and acetic anhydride	5
2.2.3. Limitations for the use of acetic anhydride	6
3. Experimental	7
3.1. Experimental material	7
3.1.1. Reagents	7
3.1.2. Radionuclides	7
3.1.3. Apparatus	7
3.2. Performance	7
3.2.1. Procedure for extraction experiments	8
3.2.2. Procedure for basicity titrations	8
3.3. Ligands	9
4. Results	11
4.1. Extraction studies	11
4.2. Evaluation of different non-aqueous titration systems	12
4.3. Results of the titrations	13
4.3.1. General	14
4.3.2. Influence on HNP from 2-bromodecanoic acid	16
4.3.3. Basicity-extraction behavior	16
4.3.4. Basicity and separation factors	17
5. Conclusions	19
6. Further investigations	20
7. Acknowledgments	20
8. References	21

1. INTRODUCTION

1.1.1 Background

In advanced reprocessing of spent nuclear fuel, separation of trivalent actinides An(III) from lanthanides Ln(III) have become of great importance for reducing the radiotoxicity of the nuclear waste. By decreasing the radiotoxicity the need of expensive deep geological repositories is reduced. Instead it would be possible to store the waste in near surface sites.

The spent nuclear fuel contains actinides, lanthanides and other fission products. The aim is to separate the actinides, and if possible, some long-lived fission products from the rest of the fission products and then convert them to more short-lived nuclides by neutron irradiations. This conversion is called transmutation. The difficult step in the separation is to separate the trivalent actinides from the lanthanides because they are chemically very similar. The lanthanides are necessary to remove since they have high cross sections for neutron absorption and would otherwise make the transmutation process ineffective. In fact, it would be quite unrealistic without this separation.

During the transmutation process, energy will be produced which partly will finance the costs of a transmutation plant. The alternative to transmutation is to store the unprocessed waste deep in the bedrock and make sure it stays there for a very long time.

In order to create a separation process a number of extracting reagents have to be developed. To minimise the volume of the secondary waste in the reprocessing process new reagents should be completely incinerable. From this follows that the reagents should only consist of the elements carbon, hydrogen, nitrogen and oxygen. This is called the CHON-principle.

1.1.2 What has been done?

The partitioning is today planned to be performed in three successive steps:

- Separation of U and Pu
- Co-extraction of actinides and lanthanides
- Separation of trivalent actinides from lanthanides

The first task, to separate uranium and plutonium from the spent fuel, is realised by the PUREX process [CHO 95]. A modified process using N,N-dialkylamides, which are CHON-reagents, has been proposed [CON 88]. Actinides and lanthanides can thereafter be co-extracted for example as in the TRUEX process [CHO 95], which uses phosphorus reagents, or as in the DIAMEX process. The DIAMEX process makes use of malonamides as reagents, which are CHON-reagents, and the malonamide molecule is now being improved to give optimal extraction ability.

For the actinide/lanthanide separation nitrogen ligands have been suggested. This work concerns this last separation step.

1.1.3 Problems

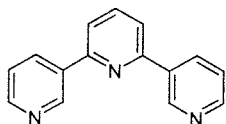
The problem with the trivalent actinide/lanthanide separation originates from similarity in charge and radii which makes them chemically almost identical. However, there are differences that can be used to develop a separation process. It has been shown that ligands with soft donor atoms (P, N, S) have higher affinity to An(III) than to Ln(III). Hence complexes containing soft donors such as nitrogen then become more stable with actinides than with lanthanides.

Up to date quite a few ligands with nitrogen as donors have been investigated. It would be attractive to find a more systematic way of searching for new ligands.

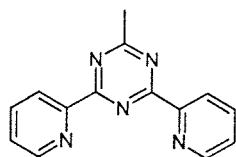
1.1.4 Ligands

The ligands that have been studied are of two basic types. They are the oligopyridines and the triazines.

The oligopyridines have the following common structure element:



The triazines are built up from the structure:



For both ligands the metal coordinates to the nitrogens in the cavity between the aromatic rings.

The extraction and the separation properties are dependent of the ligands' basicity [NIG 92]. Nonaqueous titrations were therefore performed to determine the basicity of the ligands and to relate it to the metal extraction. The extraction and separation properties of two new ligands have also been studied in this work.

2. THEORY

2.1 Metal extraction

2.1.1 Distribution ratio

The distribution ratio, D_M , for a metal, M, between two immiscible liquids is defined as

$$D_M = \frac{[M]_{org}}{[M]_{aq}} \quad (2.1.1)$$

where $[M]_{org}$ and $[M]_{aq}$ are the equilibrium concentrations of the metal in the organic and the aqueous phase respectively

For a successful separation it is crucial that the distribution ratios differ from each other. The separation factor, S_F , between species 1 and 2 is defined as:

$$S_F = \frac{D_{M1}}{D_{M2}} \quad (2.1.2)$$

The distribution ratio is easily determined if radioactive nuclides are used. If the phase volumes in the extractions are equal the ratio can be written as:

$$D_M = \frac{(R_{org} - R_{0,org}) / V_{org}}{(R_{aq} - R_{0,aq}) / V_{aq}}, \quad (2.1.2)$$

V_{org} and V_{aq} are the withdrawn volumes of each phase. This assumes equal detector efficiency for the organic and the aqueous phase. R and R_0 are the count rates for the sample and the background respectively.

2.1.2 Error estimation

Since radioactive decay is a random process there will always be a statistical uncertainty in the measurements. This uncertainty propagates through the calculations to the distribution ratio. One can derive the following expression for the statistical standard deviation for the distribution ratio:

$$\sigma_D = D_M \sqrt{\frac{R_{aq} / t_{aq} + R_{0,aq} / t_{0,aq}}{(R_{aq} - R_{0,aq})^2} + \frac{R_{org} / t_{org} + R_{0,org} / t_{0,org}}{(R_{org} - R_{0,org})^2}} \quad (2.1.3)$$

If the background and the sample is measured at the same time and if the total of counts is used instead of the count rates one gets the following expression:

$$\sigma_D = D_M \sqrt{\frac{(2 \times GROSS_{org} - NET_{org})}{(NET_{org})^2} + \frac{(2 \times GROSS_{aq} - NET_{aq})}{(NET_{aq})^2}}, \quad (2.1.4)$$

GROSS and NET are peak areas with background subtracted for the latter. With 95% certainty the true D_M -value is within $1.96 \sigma_D$ from the calculated value.

Except from the statistical uncertainty there are other sources of errors. At high D-values the aqueous phase is easily contaminated by highly radioactive organic phase, since it is removed after the organic phase. This means that the D-value could be underestimated at high D-values. Another source of error is the pipetting error but that is probably insignificant compared to the contamination error.

2.1.3 Extraction mechanism

The main criteria for extracting metal ions from an aqueous to an organic phase are that the formed complex must be uncharged and lipophilic enough to be soluble in the organic phase.

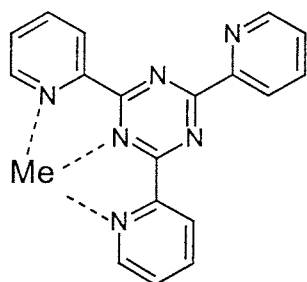
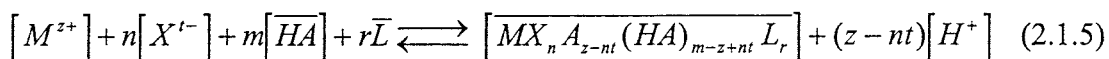


Figure 2.1 Structure of TPTZ, with metal in the major cavity

TPTZ is an example of a reagent that have the ability to separate An(III) from Ln(III). A lipophilic anion, like 2-bromodecanoic acid has to be used to make the complex uncharged. The metal ion coordinates to the three nitrogens in the major cavity in TPTZ (Fig 2.1). TPTZ, which is very similar to the ligands investigated in this work, is suggested to extract according to the mechanism [VIT 84]:



If extracted from a HNO_3 solution then $[H^+] = [NO_3^-]$ and $t=1$. If K_{ex} is the reaction constant the following expression is valid, assuming that the formed ligand complexes are completely insoluble in the aqueous phase. This is not true but a good approximation:

$$\log D = \log K_{ex} - z \times \log[H^+] + m \times \log[\overline{HA}] + r \times \log[\overline{L}] \quad (2.1.6)$$

Thus the ionic charge of the metal specie can be found from the slope of the relationship between $\log D$ and $\log [H^+]$. This assumes that the ligand concentration is constant which might not be correct in this system since the ligands can form adducts with HA. The equilibrium concentration of H^+ must be known. However, due to small sample volumes this was not determined. The initial and equilibrium concentration of H^+ was therefore assumed to be the same, which might be almost true.

2.2 Non-aqueous titrations

2.2.1 Titration media

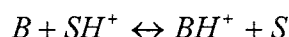
Since all the ligands used were aromatic amines, which are almost insoluble in water and too weak bases to be titrated in water, non-aqueous solvents were used.

Two different solvents were studied; acetic anhydride and acetonitrile. Acetic anhydride was chosen because earlier studies had shown it effective for titrating very weak bases [DAV 58, STR 58]. Acetonitrile is a good medium for differential titrations of amines [STR 58], though it has the disadvantage that it is poisonous. The main reason for the differentiating effect are the weak basic and acidic properties of acetonitrile [COE 62]. The titrand used was perchloric acid. Perchloric acid is the only acid that is completely dissociated in acetonitrile.

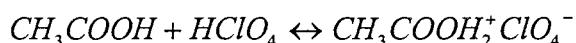
2.2.2 Reactions between titrand and acetic anhydride

In combination with acetic anhydride perchloric acid forms more acidic species which makes it possible to titrate very weak bases [DAV 58].

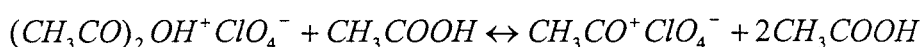
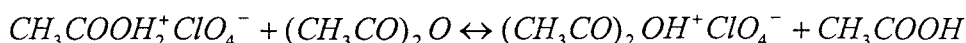
The equilibrium for a titration of a weak base, B, in a solvent, S, can be represented as:



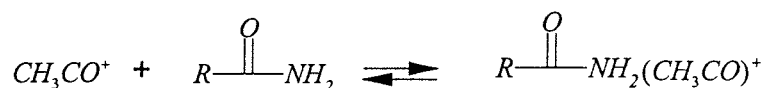
When perchloric acid in acetic acid the following reaction will occur:



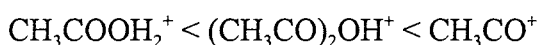
Further reaction with acetic anhydride establishes the following equilibrium:



At high acetic anhydride concentrations, which was the case, the acetyl ion becomes the predominant acidic species. The titrating reaction becomes:



Studies of acylation reactions has indicated that the acetyl ion is the most acidic specie and the other species are in the order [DAV 58]:



(the perchlorate anion is omitted here to simplify)

2.2.3 Limitations to the use of acetic anhydride

Titration in acetic anhydride to determine basicity can only be used for tertiary or aromatic amines. Secondary and primary amines reacts with acetic anhydride and forms acetylates. The titration will then only give the basicity of the acetylated species, and the method will only be useful for quantitative determinations. But since all the ligands used in this work were aromatic amines the method was suitable.

3. EXPERIMENTAL

3.1 Experimental material

3.1.1 Reagents

All ligands used in the experiments were synthesised at the *University of Reading*, UK, except for terpyridine. Anhydrous pyridine 99.8% as well as 2,2':6,2''-terpyridine (Terpy) (98%) obtained from *Aldrich*. Other chemicals were Tert-Butylbenzene (TBB) (99 %) [*Acros*], 2-bromodecanoic acid (98 %) [*Fluka*], acetic acid (99-100 %) and acetic anhydride (97 %) [*J.T. Baker*]. The perchloric acid (70-72%) and the acetonitrile (98%) used were manufactured by *Merck*.

3.1.2 Radionuclides

The nuclides used were the following:

^{241}Am : α -emitter, $t_{1/2}=432.6$ y, $E_{\gamma}=59.5$ keV, ~ 30 kBq/extraction was added

$^{152,154}\text{Eu}$: 152: β -emitters (β^+ and β^-) 152: $t_{1/2}=13.3$ y, $E_{\gamma}=121.8$ keV
154: $t_{1/2}=8.8$ y, $E_{\gamma}=123$ keV

^{147}Pm : β -emitter, $t_{1/2}=2.62$ y

All nuclides were dissolved in 0.6-0.9 M HNO_3

3.1.3 Apparatus

^{241}Am and ^{152}Eu were measured on a HPGe detector from *ORTEC* and ^{147}Pm was measured on a liquid scintillation detector of model 1219 Rackbeta from *Wallac*.

The basicity titrations were performed potentiometrically using an ABU 91 Auto Burette from *Radiometer Copenhagen* connected to a PC. The PC software used was written by Anna-Maria Jacobsson and modified by Göran Källvenius both at the Department of Nuclear Chemistry, Chalmers.

For the pH measurements a pHG201 (*Radiometer Copenhagen*) glass electrode and a REF251 (*Radiometer Copenhagen*) reference electrode, which is a Ag/AgCl electrode with a double liquid junction, were used. The lower reservoir was filled with 0.1 M LiClO_4 in the solvent used. LiClO_4 was used since it has a good solubility in acetic anhydride and acetonitrile. In the upper reservoir the saturated KCl solution was replaced with 2 M NaCl to avoid precipitation of KClO_4 at the porous pin.

3.2 Performance

3.2.1 Procedure for extraction experiments

The organic phase in the experiments consisted of 0.02 M ligand and 1 M 2-bromodecanoic acid in TBB. The aqueous phase was prepared by adding the appropriate amount of 0.5 M HNO₃ and radionuclides in HNO₃ to a test tube and then filling up to 1 ml with Milli-Q grade water. The water phase was then left to stand for a few minutes to equilibrate. 1 ml of the organic phase was added and the phases were mixed in the test tubes by vigorous shaking for 5 minutes. They were then separated by centrifugation at 4500 rpm for 5 minutes. The phases were then removed from the test tubes by pipetting.

Am- and Eu-extractions were performed in the same experiment. The amount withdrawn of each phase depends on the acid concentration. For the concentration interval 0.008-0.12 M HNO₃ it was varying from 0.4 to 0.05 ml for the aqueous phase and from 0.1 to 0.8 ml for the organic phase. The lower the acid concentration the larger the amount of aqueous phase and smaller the amount of organic phase. This was done since the D-values and thus the count rates were greatly dependent of the acid concentration. The γ -intensities at 54.5 keV and 121.8 keV was measured for ²⁴¹Am and ¹⁵²Eu respectively. The measurements continued until a reasonable small statistical error was achieved.

¹⁴⁷Pm extractions were made in separate experiments. The procedure was the same as for the Am/Eu extraction. Each sample was measured for 1 minute.

3.2.2 Procedure for basicity titrations

The titrand used was 0.1 M HClO₄ in anhydrous acetic acid. It was prepared by dissolving 0.9 ml perchloric acid (70-72%) in acetic acid. 2.5 ml of acetic anhydride was added and the solution was diluted to 100 ml. The solution was left to stand over night before use.

At each titration about 25 to 50 μ mol of the ligand was used, and about 40 to 50 ml solvent was added. Most ligands were very difficult to dissolve directly in the titration media. Instead they were first dissolved into 0.25 M 2-bromodecanoic acid in TBB to a concentration of 0.02 M before they were dissolved in the titration media. A titration curve for each ligand was performed and the equivalence points and the HNP:s (half neutralisation potential) in millivolts were noted. The values were compared with a reference substance. In the case of acetic anhydride, pyridine was used as an external standard and in the case of acetonitrile, imidazole was used as an internal standard. In acetic anhydride the standard was external because acetic anhydride proved to be quite poor in differentiating between equally strong bases.

3.3 Ligands

The structures of the two new ligands are presented below. Two ligands with similar structure, but with a carbon tail of only 8 carbons, has been investigated before. The longer carbon chain is supposed to give higher solubility in the organic phase and lower solubility in the aqueous phase, and therefore better extraction.

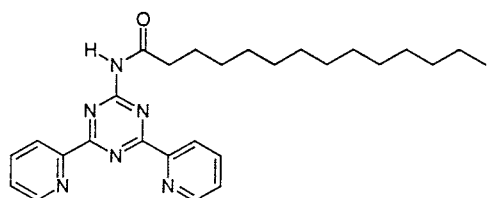


Figure 3.1 4-tetradecanoyl amino-2,6 di(2-pyridyl) 1,3,5 triazine (TADPTZ)

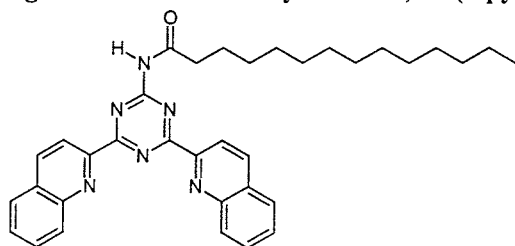


Figure 3.2 4-tetradecanoyl amino-2,6 di(2-quinolinyl)3,5 triazine (TADQTZ)

For comparison a few old ligands were included in the basicity titrations. They are presented here

Triazines:

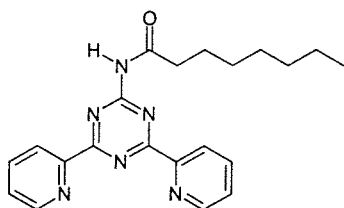


Figure 3.3 4-octanoyl amino-2,6 di(2-pyridyl) 1,3,5 triazine (OADPTZ)

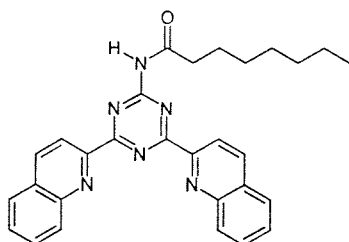


Figure 3.4 4-octanoyl amino-2,6 di(2-quinolinyl)3,5 triazine (OADQTZ)

Oligopyridines:

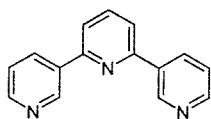


Figure 3.5 2,2':6,2''-terpyridine (*Terpy*)

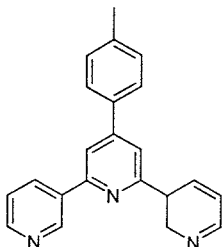


Figure 3.6 4'-tolyl-2,2':6,2''-terpyridine (*Tolpy*)

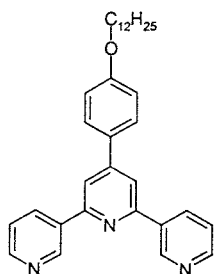


Figure 3.7 4'-(4-dodecyloxyphenyl)-2,2':6,2''-terpyridine (*Dodoxy*)

4. RESULTS

4.1 Extraction studies

TADPTZ showed good extraction ability and the separation factor was around 8. TADQ TZ on the other hand had an extraction factor less than unity for all nitric acid concentrations investigated, and a separation factor around 3 (Fig 4.1). As seen in the figure this extraction is mainly due to HA itself. The relative statistical errors for the D-values were calculated for the TADPTZ ligand. The errors were 1-4 % for Eu- and 3-8 % for the Am-extraction with a 95 % confidence interval (calculated from eq 2.1.4).

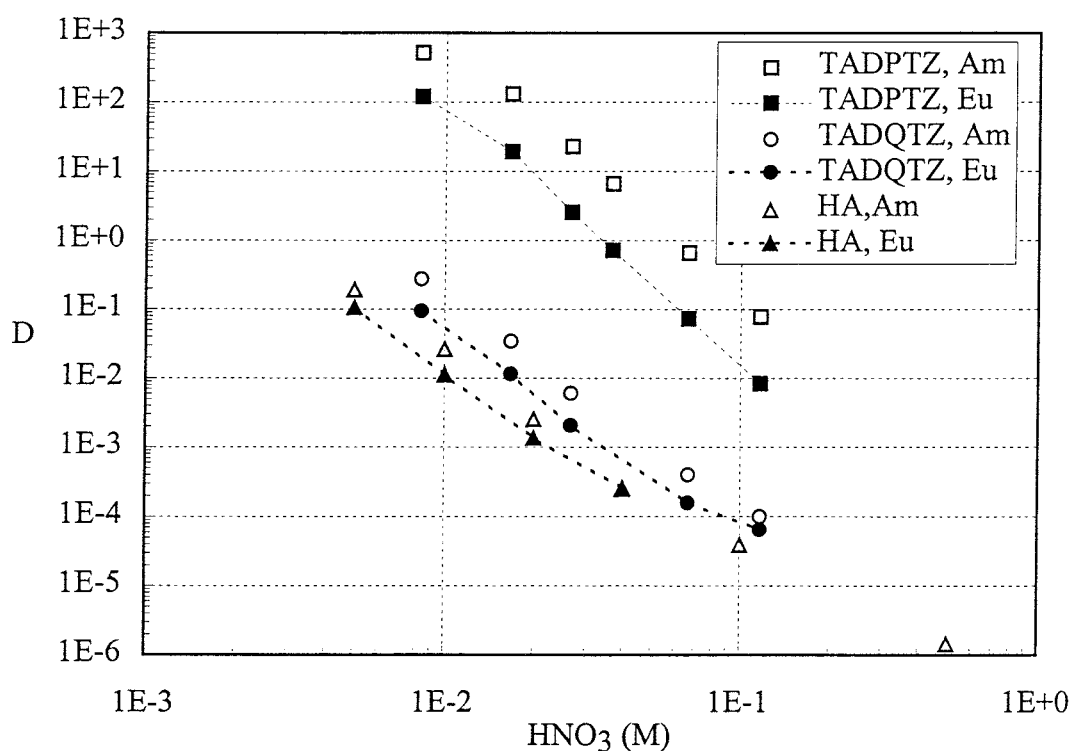


Figure 4.1 Extraction curves for the tested ligands and pure 2-bromodecanoic acid. All experiments with 0.02 M of ligand and 1.0 M 2-bromodecanoic acid

The extraction behaviour of the two new ligands is similar to previously studied triazines (Appendix A). The extraction is very dependent on nitric acid concentration. At low concentrations (less than 0.01 M) high D-values are obtained but at higher nitric acid concentration (more than 0.02 M) no significant extraction takes place. The extension of the length of the carbon chain from 8 to 14 carbons doesn't seem to have any significant influence on the extraction. It could be expected that a longer carbon chain would extract better due to higher solubility in the organic phase. The

extraction with TADPTZ, which has 14 carbons in the carbon chain, is however only slightly better.

Equation (2.1.6) can be rewritten as

$$\log D = A - B \times \log[HNO_3]$$

where $A = \log K_{ex} + m \times \log[\overline{HA}] + r \times \log[\overline{L}]$ and B is the ionic charge of the metal.

The expected value of B is 3 since that is the stable ionic charge of the metal used in the given solutions. Most ligands had B:s between 3 and 3.5 except for TADPTZ which got very close to 4.. One explanation for this is that the ligands get protonated as the acid concentration increases i.e. the ligand extracts HNO₃, and thus B seems to increase. On the other hand contamination of the aqueous phase with the organic one tend to push B in the other direction, especially at high D-value which correspond to low acid concentration. How much, will depend on how accurate each experiment is performed and that will probably vary, and then also the observed value of B.

At high D-values the deviation from equation (2.1.6) was significant. A probably cause for this is contamination of the aqueous phase as mentioned above.

4.2 Evaluation of different non-aqueous titration systems

To evaluate the two titration systems used, compounds with known pK_A(aq) were titrated in the two different solvents. To eliminate the effect of electrode drifting a reference substance (pyridine in Ac₂O and imidazole in acetonitrile) was titrated at the same time. The half neutralisation potential (HNP) for the ligand was compared with the HNP of the reference to get a ΔHNP as seen in **Fig 4.2** and **Fig 4.3**

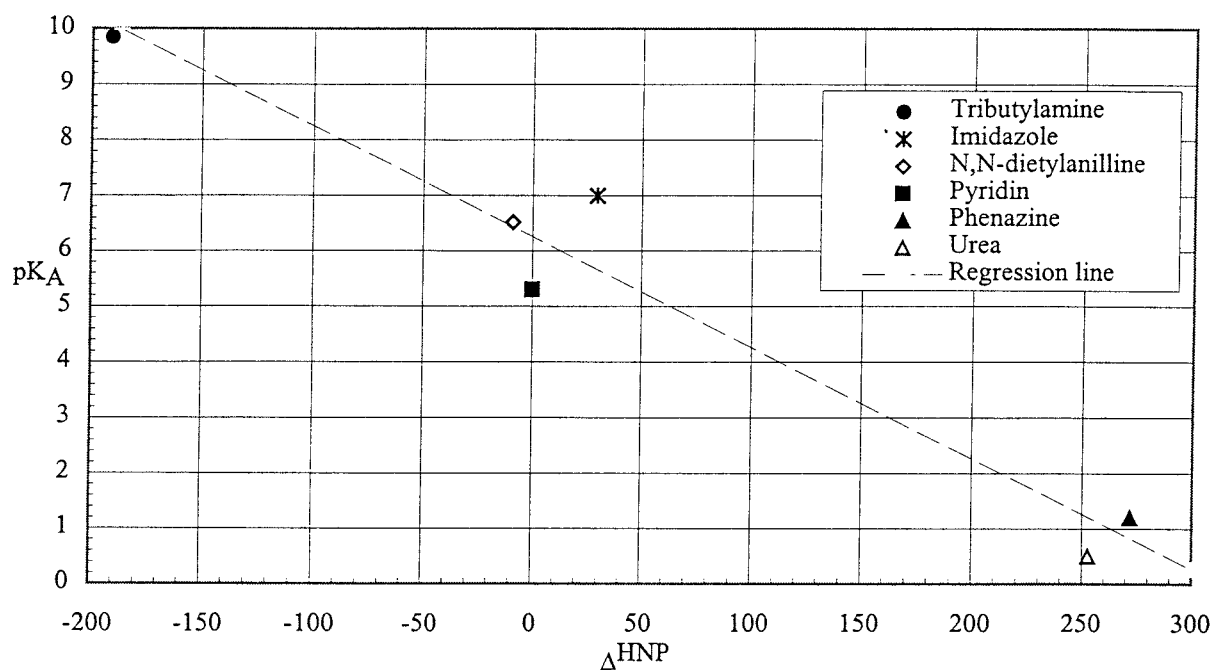


Figure 4.2. ΔHNP in acetic anhydride plotted against $pK_A(H_2O)$. Slope ≈ -50 mV/ pK_A

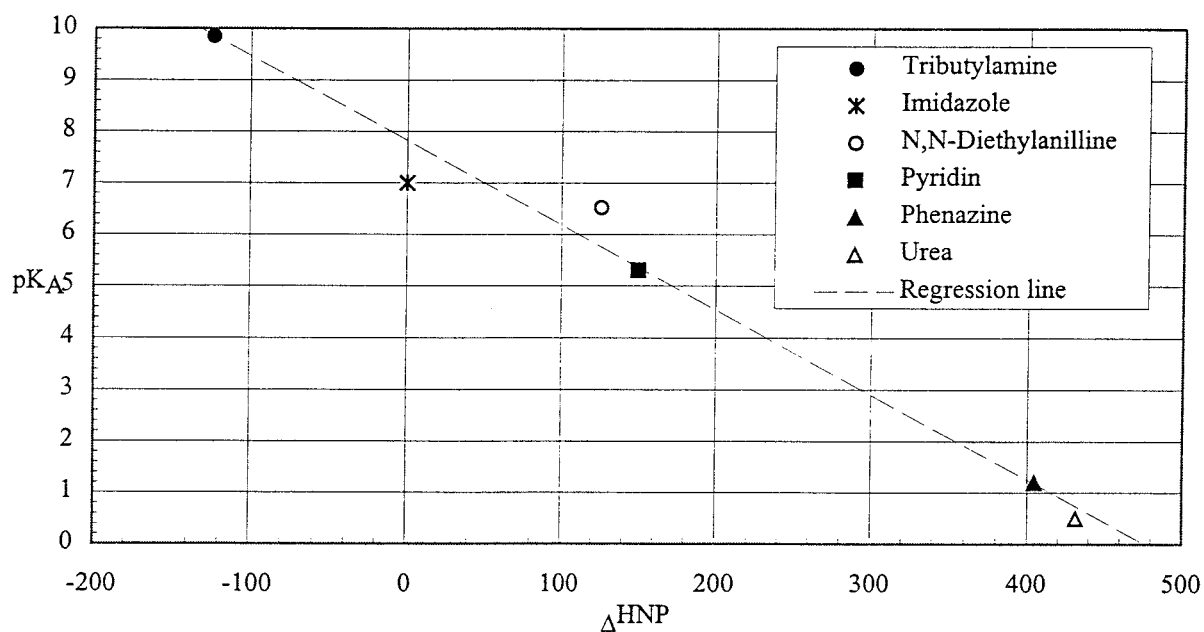


Figure 4.3. ΔHNP in acetonitrile plotted against $pK_A(H_2O)$. Slope ≈ -61 mV/ pK_A

The slope in the pK_A - ΔHNP relation is slightly higher in acetonitrile. This makes the differentiation between similar substances easier in this media.

If the linear relation between $pK_A(aq)$ and ΔHNP for the reference structures are used a pK_A can be calculated for the different ligands. The result is shown in **Table 4.1** below.

Table 4.1. Calculated values for ligands in water.

Ligand	pK _A (Ac ₂ O)	pK _A (CH ₃ CN)
Dodoxy	6.02	5.74
Tolpy	5.82	5.56
Terpy	5.67	5.26
OADPTZ	5.61	4.70
TADPTZ	4.92	4.74
TADQTZ	4.64	4.01
OADQTZ	4.64	4.30

4.3 Results of the titrations

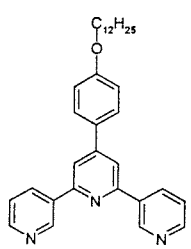
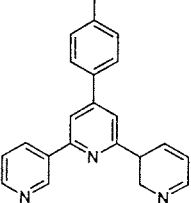
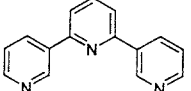
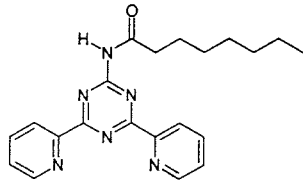
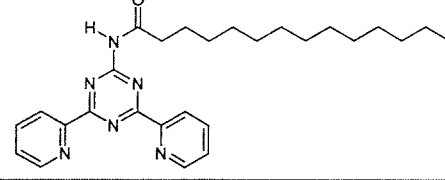
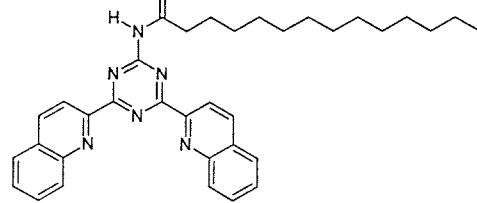
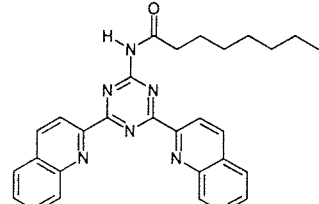
4.3.1. General

A better separation of the HNP values from the basicity titrations is obtained in acetonitrile. The difference between the most acid and basic ligand is 106 mV in acetonitrile compared with only 69 mV in acetic anhydride (Table 4.2). The better separation can also be seen Fig 4.4 below. The equivalence point is also easier to identify in acetonitrile. The volume is given as percent of neutralisation with the second protonation as 100 %. The potential is the measured potential with HNP for the reference subtracted.

As seen in the tables and diagrams below the relative order of basicity is basically the same in both solvents. The order of the OADPTZ and the TADPTZ ligands is reversed, though. The only difference between these ligands is the length of the carbon chain which is not expected to affect the basicity. The small differences in potential is probably within the limits of the statistical error for the measurements

Table 4.2: $\Delta\text{HNP} = \text{HNP}_{\text{ligand}} - \text{HNP}_{\text{ref}}$ Ref(Ac_2O)=pyridine Ref(CH_3CN)=imidazole

* Interpolated values Extraction data at 0.02M $[\text{HNO}_3]$ with 0.02M ligand and 1M HA in TBB.

Ligand	Name	ΔHNP (mV) Ac_2O	ΔHNP (mV) CH_3CN	D_{Am} (0.01M HNO_3)	S_{F} (0.02M HNO_3)
	Dodoxy	12	127	4.2	7.6
	Tolpy	22	138	2.8	8.8
	Terpy	30	165	13	7.2
	OADPTZ	33	190	287.3	10.5
	TADPTZ	45	187	358.9	7.5*
	TADQ TZ	81	233	0.16	3.0*
	OADQ TZ	81	215	0.09	3.4

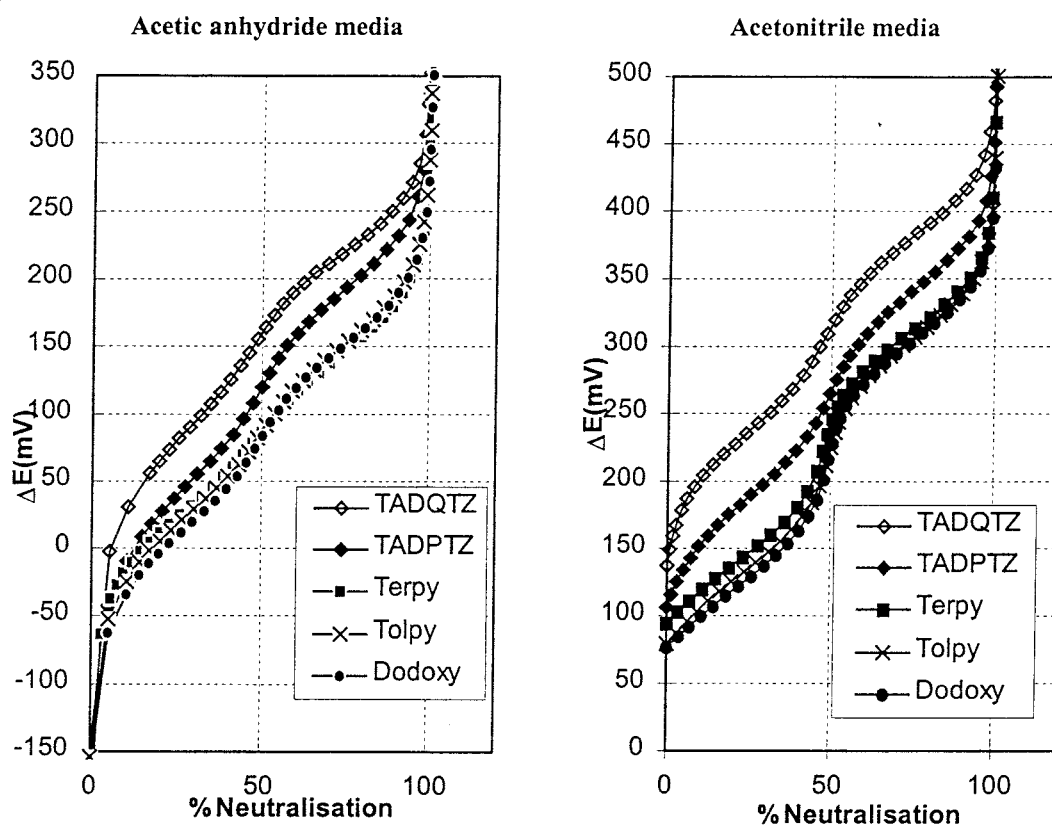


Figure 4.1. Titration curves for the investigated triazines and oligopyridines in acetic anhydride and acetonitrile media. 100% neutralisation refers to the second protonation.

4.3.2. Influence of 2-bromodecanoic acid

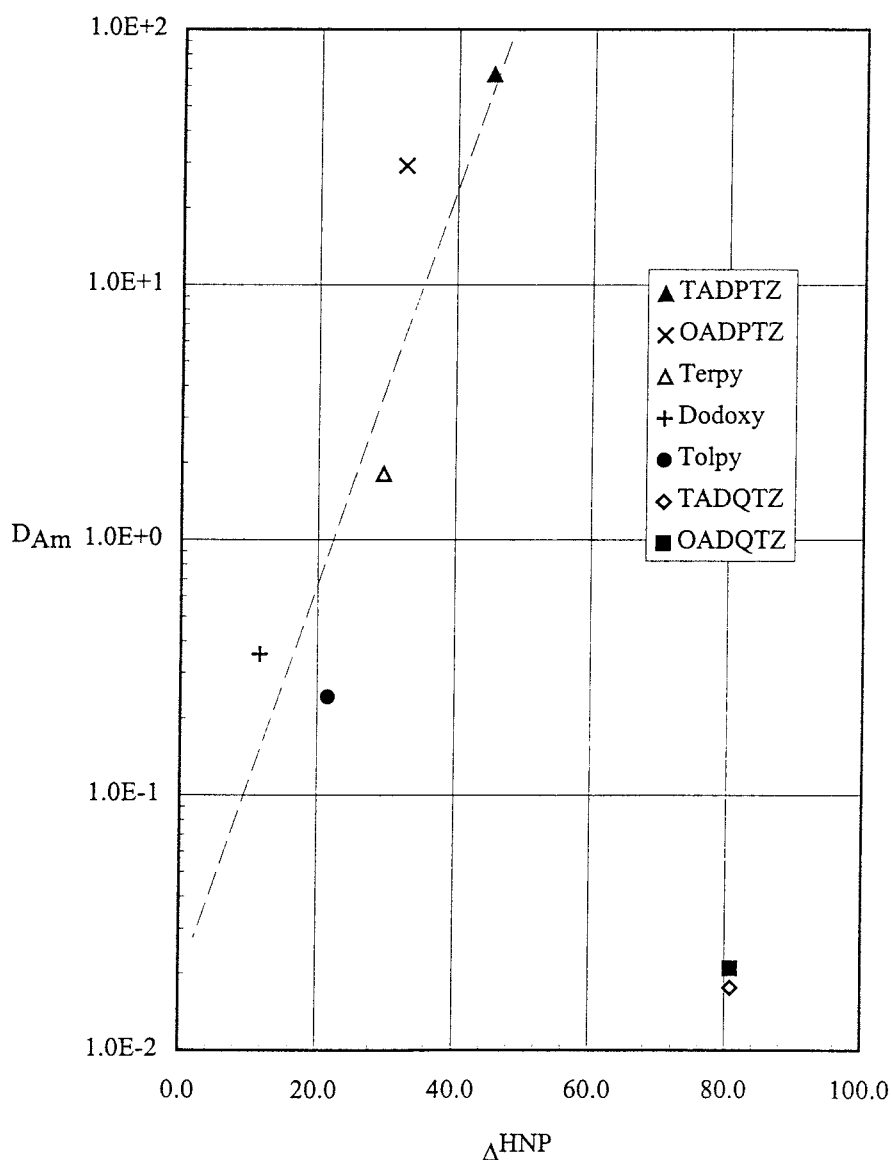
In acetic anhydride, titrations with the few soluble ligands indicated that the addition of 2-bromodecanoic had no effect on the measurements. In acetonitrile on the other hand, the addition of 2-bromodecanoic acid (HA) tended to increase the starting potential of the titration and HNP for the reference used, imidazole, was therefore different when different amount of "HA" was added.. This effect should be studied further, but since the concentration was practically held constant during the experiment the relative order in basicity should be correct.

4.3.3 Basicity-extraction behavior

There seems to be a linear relation between the logarithm of the D-values and the basicity measured as HNP. This could be due to the fact that metal ions compete with protons for the binding sites in the ligand. The lower the basicity, the more likely it is that a metal ion occupies the site instead of a proton. If this was a general rule it would have made the quinolinyl derivatives the best extractants, but they showed the lowest extraction of all investigated ligands. A reason for this could be that the ligand is sterically hindered. Molecule modelling might be used to study this further.

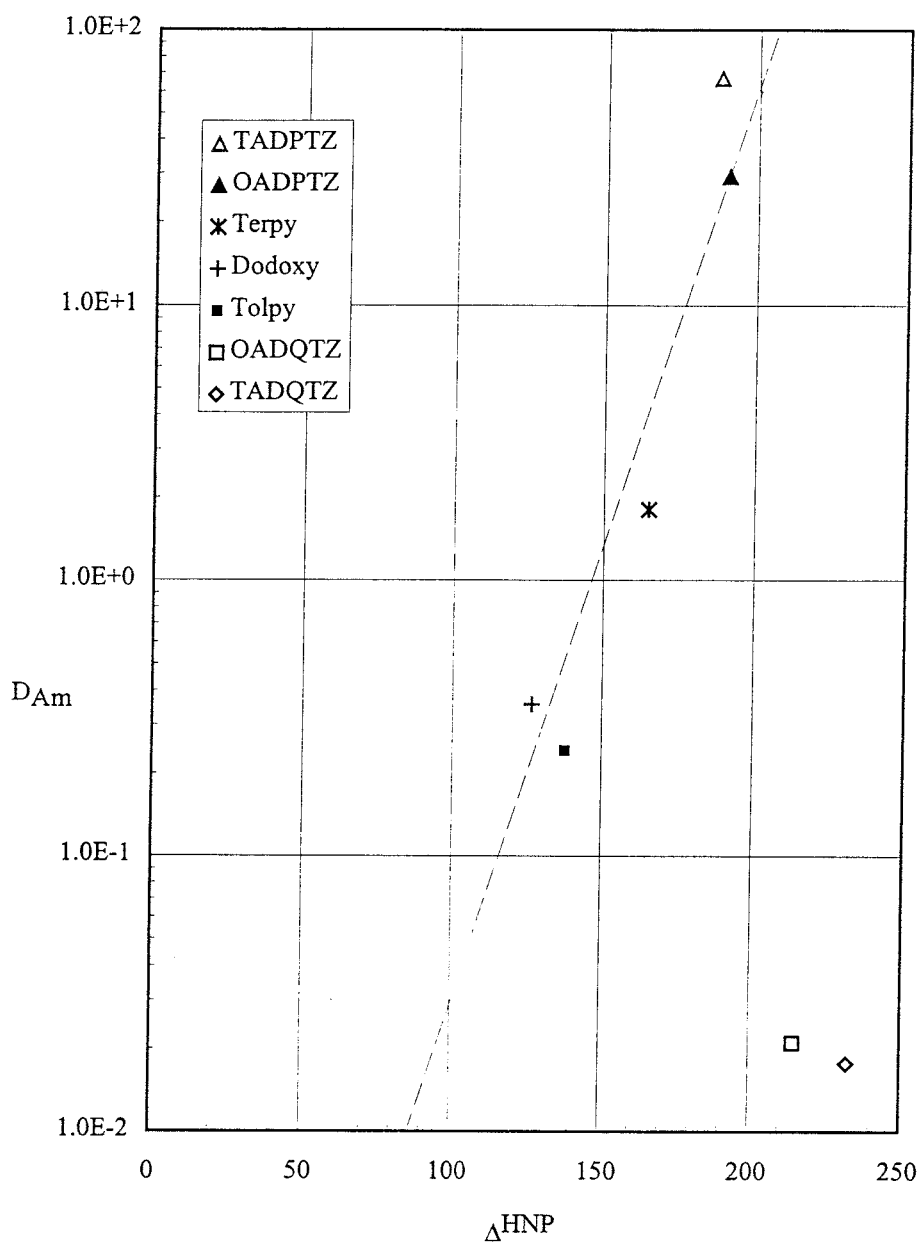
4.3.4 Basicity and separation factors

It is hard to draw any conclusions about the relation between basicity and the separation factor. No obvious correlation seems to exist. Perhaps such a correlation will reveal itself if more ligands are tested with a broader range of basicity. Worth noticing is that the quinolinyl derivatives have lower separation factors than the other ligands.



Americium extraction at $[HNO_3]=0.02M$ compared with basicity in acetic anhydride.

$$\Delta HNP = HNP_{\text{ligand}} - HNP_{\text{pyridine}}$$



Americium extraction at $[HNO_3]=0.02M$ compared with basicity in acetonitrile.

$$\Delta HNP = HNP_{\text{ligand}} - HNP_{\text{imidazole}}$$

5. Conclusions

This work has shown acetonitrile to be good media for basicity differentiation of weak aromatic amines. Compared to the method with acetic anhydride it shows better separation in HNP:s and more distinct equivalence points. It is also possible that this method could be used for primary and secondary amines since there will be no problems with acetylation.

The way of dissolving the substances is not satisfying. The ligands in this work had too low solubilities to dissolve directly in acetonitrile and was therefore dissolved by an addition of 2-bromodecanoic acid. This affected the starting potential, and thus the HNP of the reference substance used in a way that was dependent of the 2-bromodecanoic acid concentration. If the 2-bromodecanoic acid is not replaced, a correlation between its' concentration and the HNP of the reference should be found.

6 Further investigations

A primary interest should be to investigate more ligands with more varying basicity. That would make data for the correlation between extraction and basicity more certain. It would also reveal if there is any correlation between the separation factor and the basicity.

This work also leaves a few interesting questions unanswered.

- Why do the quinolinyll derivatives give such a low extraction? Sterical hinders? If so, is it possible to make a similar molecule without those problems?
- How does the addition of 2-bromodecanoic acid affect the measured value of the basicity in acetonitrile? Is it possible to calculate what HNP would be without 2-bromodecanoic acid?
- How should the ligands be modified to be able to extract at lower pH?

7. Acknowledgments

As a Ms.Sci student it is not easy to know what is expected from you when you do your first “real” work.. Fortunately I had a lot of people to help me out.

First of all I want to thank my supervisor Lena Spjuth. She was always there to help me with experimental problems, report writing tips or a good mood if that was what was needed.

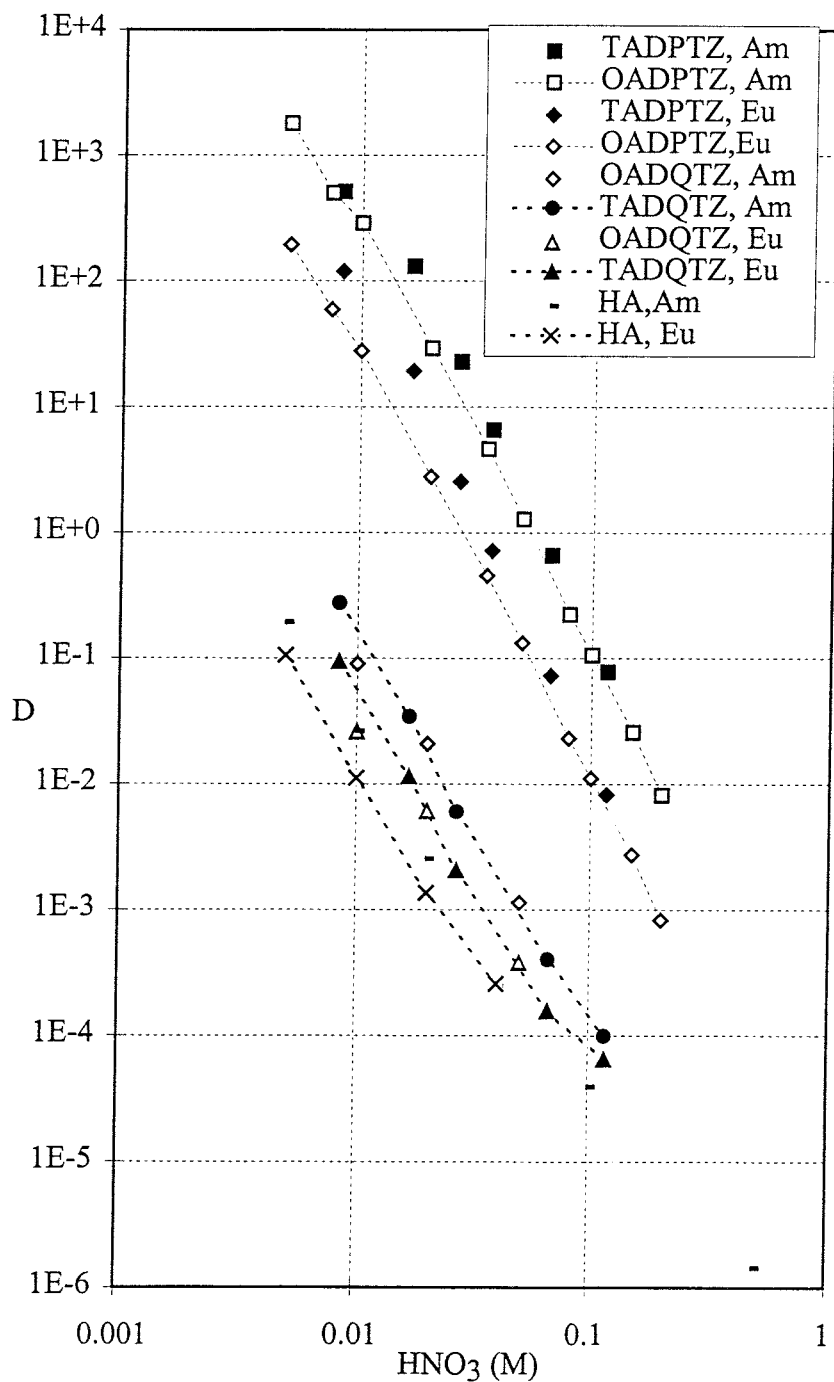
I also want to express my gratitude to Anders Landgren for his help with nasty computer programs as well as lunch company and Anna-Maria Jacobson for helping me with the software modifications in her titration program.

At last I want to thank all the staff at the Department of Nuclear Chemistry, Chalmers, for always being helpful and kind and therefore made my time as a diploma worker a pleasant experience.

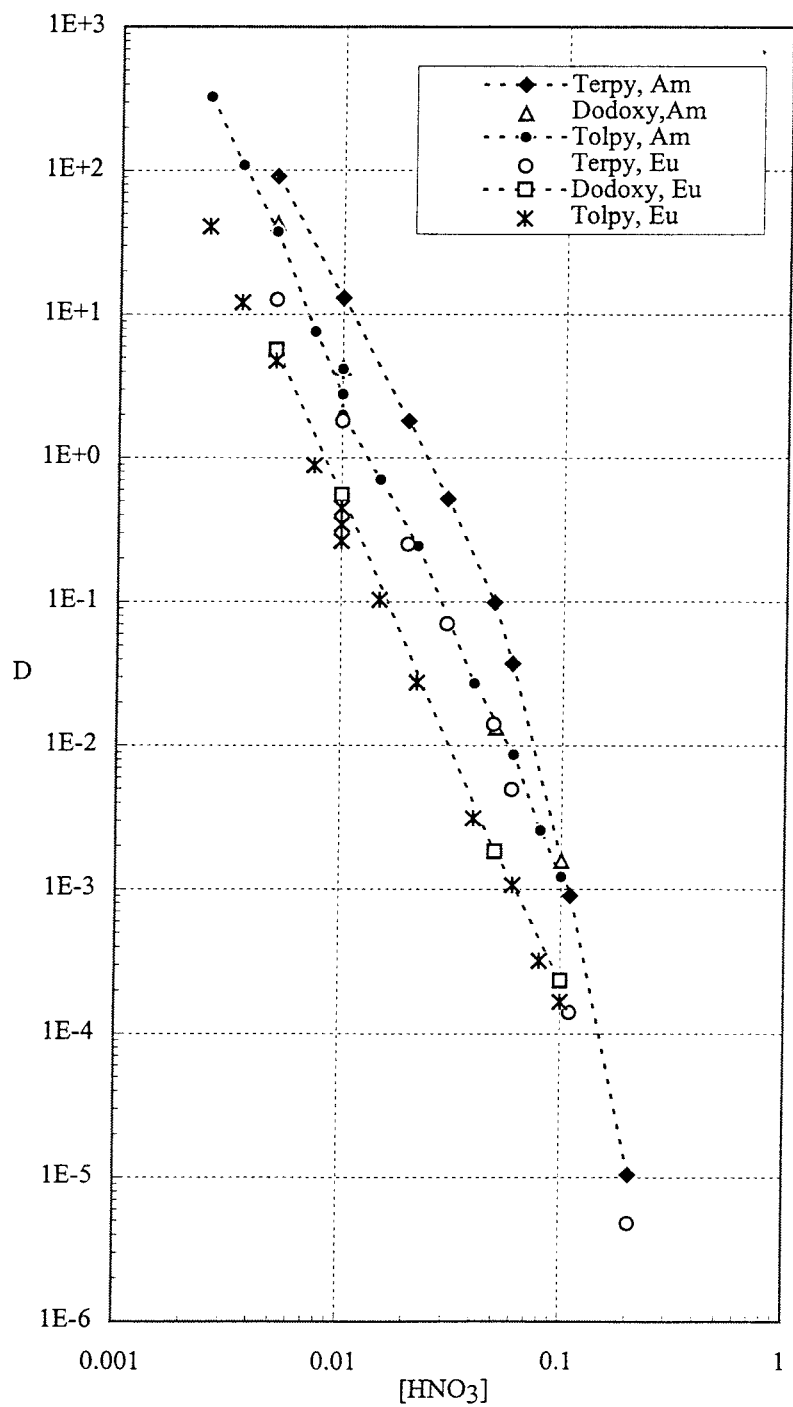
8. References

- [CHO 95] G.Choppin, J.Rydberg, J.O. Liljenzin, *Radiochemistry and nuclear chemistry* **1995**
- [CON 88] N.Condamines, C. Musikas, *The extraction by N,N Dialkylamides I. HNO₃ and Other Inorganic Acids*, Solvent Extr. Ion Exch. 6(6), 1007-10034, **1988**
- [DAV 58] David C. Wimer, *Potentiometric determination of amides in acetic anhydride*, An.Chem, **1958**, vol 30
- [DUT 84] P.K. Dutta and R.J. Holland, *Acid-base characteristics of petroleum asphaltenes as studied by non-aqueous potentiometric titrations*, FUEL, **1984**, vol 63
- [NIG 92] Nigond, L., Thèse de Doctorat D'Université de Clermont Ferrand II, **1992**, CEA-R-5610
- [STR 58] C.A. Streuli, *Basic Behavior of molecules an ions in acetic acid* An.Chem, **1958**, vol 30
- [VIT 84] P. Vitorge, *Complexation de lanthanides et d' actinides trivalent par la tripyridyltriazine applications en extraction liquide-liquide*, Report **CEA-R-5270**, CEA Centre d'Etudes Nuclearies de Fontenoy-aux-Roses, 92(France), **1984**

Appendix A - Extraction curves



**Extraction with -TZ derivates from TBB to water.
All experiments with 0.02 M of ligand and 1.0 M 2-bromodecanoic acid**



Extraction with oligopyridines from TBB to water.
 All experiments with 0.02 M of ligand and 1.0 M 2-bromodecanoic acid

Appendix

VII

Travel Report

UK Macrocyclic and Supramolecular Chemistry Group Conference
Nottingham, UK, January 5-6 1998
Lena Spjuth

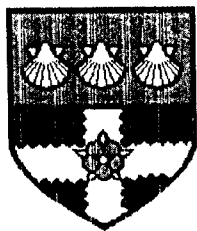
As a start of my 3-months visit to the University of Reading and my new "career" in synthesising new extractants, I attended a conference in Nottingham concerning macrocyclic and supramolecular chemistry. One group of extractants that we are interested in has a macrocyclic structure with several pyridine groups attached to each other. These nitrogen-donor ligands show selectivity for trivalent actinides over lanthanides

At the conference, we presented the poster: "Metal-Ion Complexation Studies Involving A Novel Heterocyclic Nitrogen Donor Ligand", *M.G.B. Drew, J.O. Halvarsson, M.J. Hudson, P.B. Iveson, L. Spjuth and M.L. Russell.*

The conference concerned many different topics concerning macrocycles and supramolecules.

- Synthesis of new macrocyclic extractants.
- Self-assembly of macrocycles to mimic properties that are found in photosynthetic organisms.
- Using supramolecular self-assemblies with metal ions to exploit the hydrogen bonding that exists in nature, e.g. holding DNA strands together.
- Supramolecular receptors for cations and neutral molecules for use in molecular switches and sensors.
- Studies of interactions of cation peptide complexes with DNA.
- Synthesis of synthetic receptors for recognition of protein surfaces (e.g. antibodies)
- Phosphorescent pH and anion sensors using lanthanide complexed with macrocycles.

Enclosed: Copies of the poster presented.

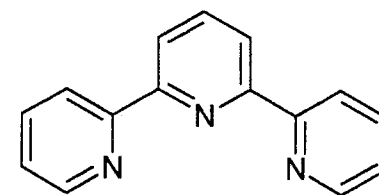


Metal-Ion Complexation Studies Involving A Novel Heterocyclic Nitrogen Donor Ligand

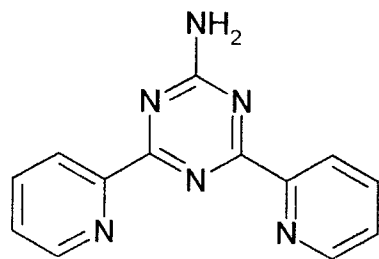
M. G. B. Drew, J. O. Halvarsson, M. J. Hudson, P. B. Iveson, L. Spjuth and M. L. Russell
Department of Chemistry, Whiteknights, University of Reading, Reading, RG6 6AD

Ligands of Interest

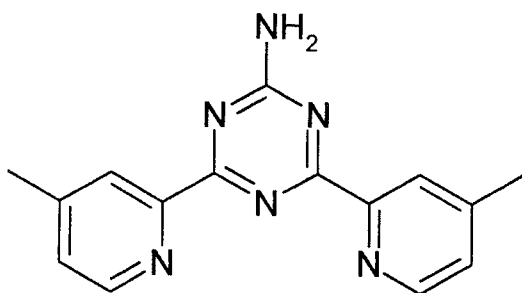
Ligands which contain the central terpyridyl cavity are of interest for complexation studies.¹



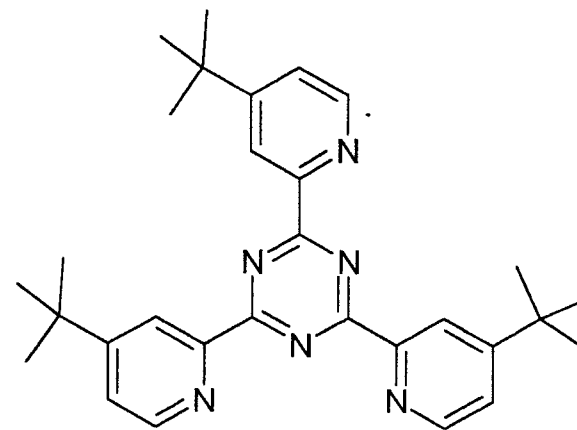
2,2':6'',2-terpyridine



4-amino-2,6-bis(2-pyridyl)-1,3,5-triazine²



4-amino-2,6-bis(4-methyl-2-pyridyl)-1,3,5-triazine



2,4,6-tris(4-tert-butyl-2-pyridyl)-1,3,5-triazine³

Lanthanide-Heterocycle Complexes.

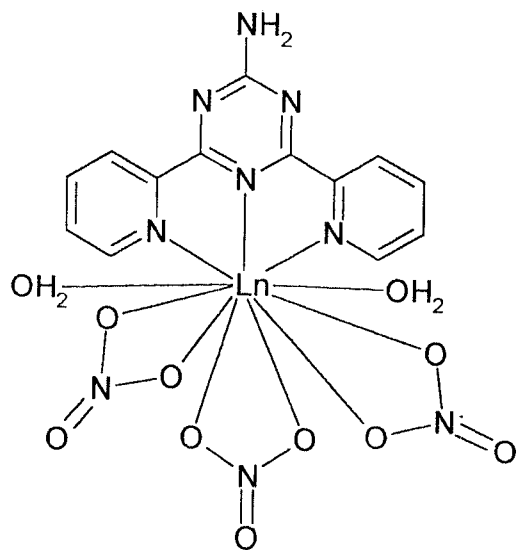
The lanthanide series of elements were chosen for study due to their steady decrease in ionic radii.

Key Features of Lanthanide Complexes.

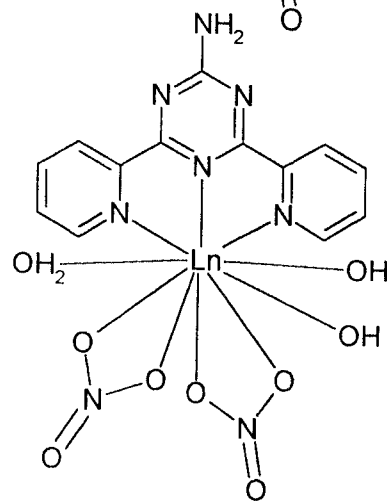
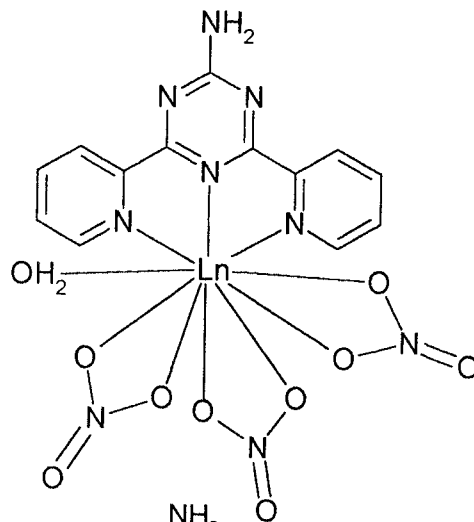
- Four of the lanthanides have two structures - lanthanum, neodymium, samarium and ytterbium.
- The coordination numbers of the complexes are 11, for the largest trivalent ion - lanthanum, through to 9 for the smallest - lutetium.
- In all cases the coordination consists of the ligand bound to the metal ion, with nitrate and water molecules to fill the coordination sphere of the metal ion.
- For the 11 coordinate lanthanum structure, the lanthanum is outside the terpyridyl cavity. All the other lanthanides are within the cavity.
- The second ytterbium structure, contains a monodentate nitrate ion. This structure is also, that possessed by the yttrium trivalent ion.

Structure of Lanthanide Ligand Complexes

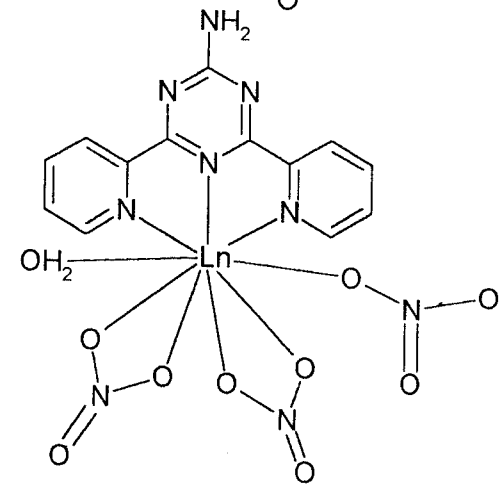
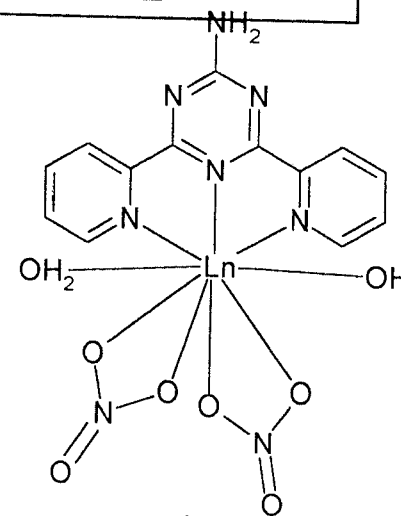
There are 5 distinct structural types.



11 Coordinate

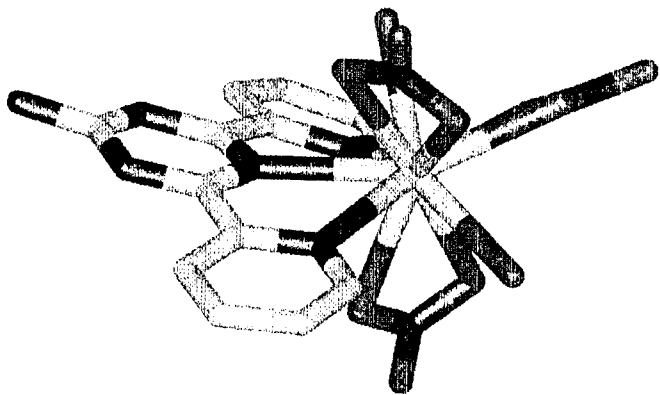


10 Coordinate

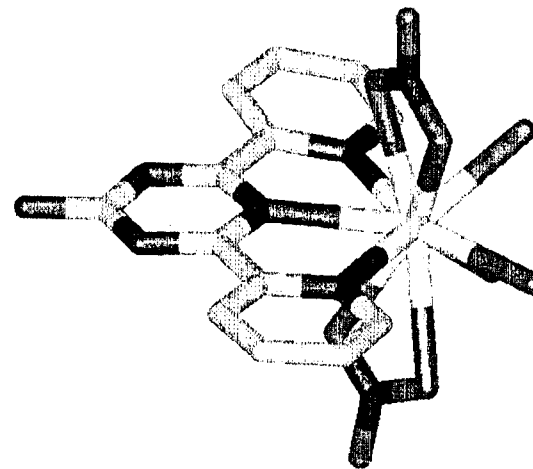


9 Coordinate

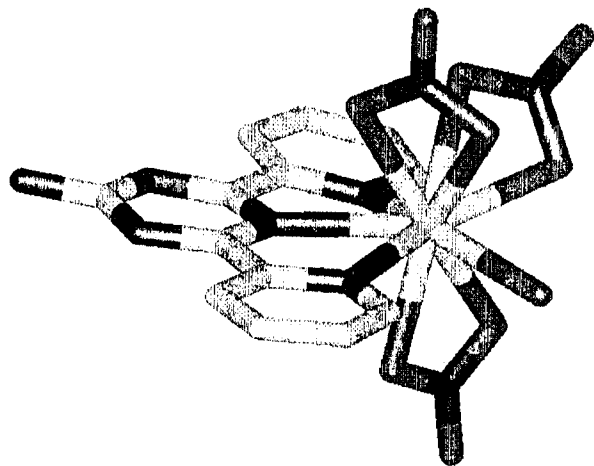
Lanthanide Structures I



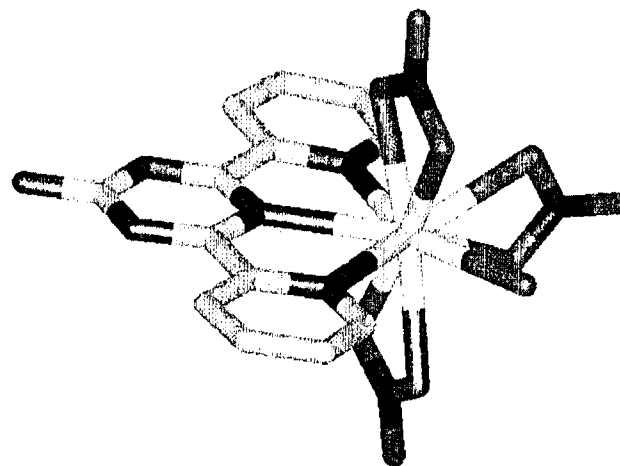
11 Coordinate Lanthanum



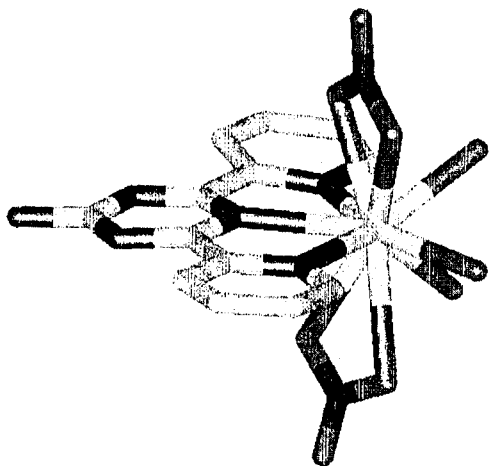
10 Coordinate Neodymium



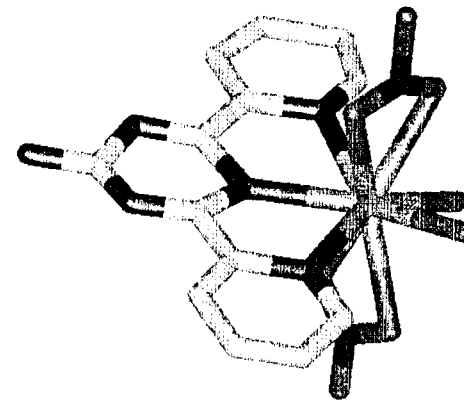
10 Coordinate Lanthanum



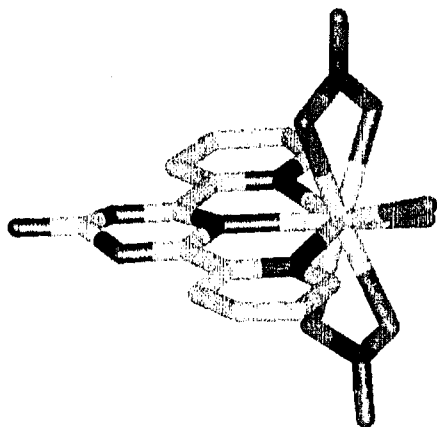
Lanthanide Structures II



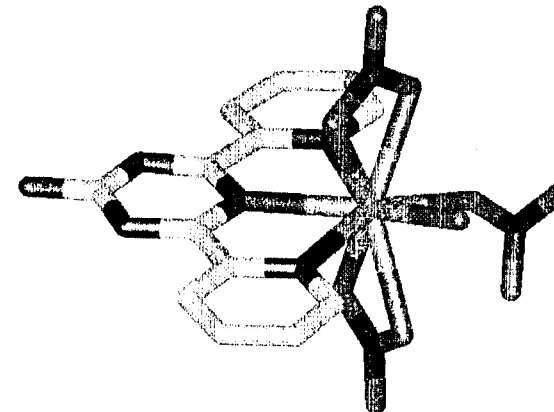
10 Coordinate Samarium



9 Coordinate Ytterbium

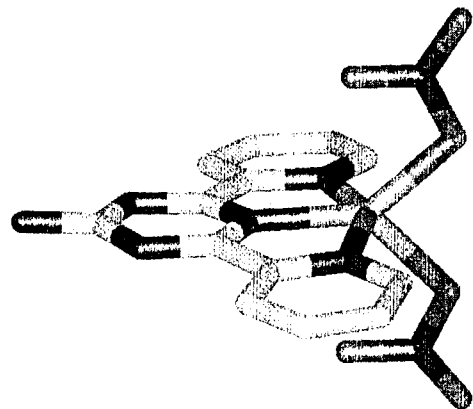


9 Coordinate Gadolinium

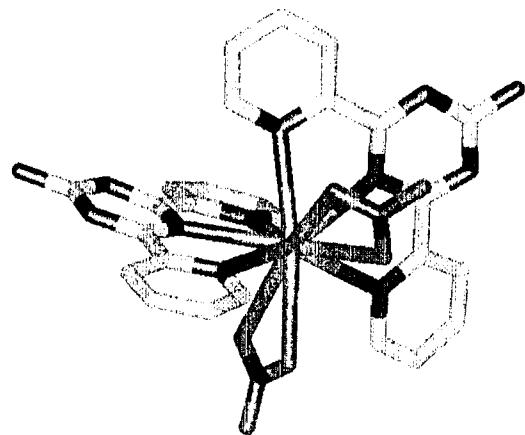


9 Coordinate Ytterbium
- monodentate nitrate

Zinc and Nickel Complex Structures.



Zinc Complex



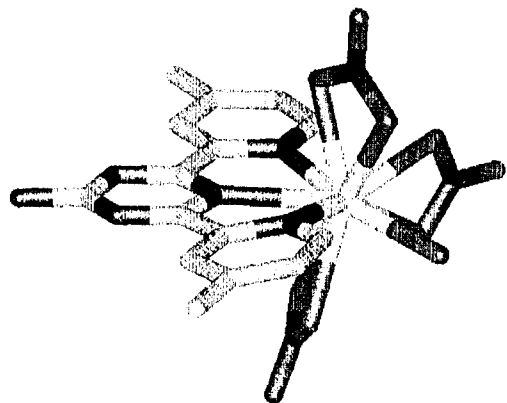
Nickel Complex

Some other elements, apart from the lanthanides were investigated.

Key Features of Both Structures.

- The zinc structure has two monodentate nitrates, with secondary axial interactions. This is typical of known zinc crystal structures.
- The nickel complex contains two ligands and two bidentate nitrates.

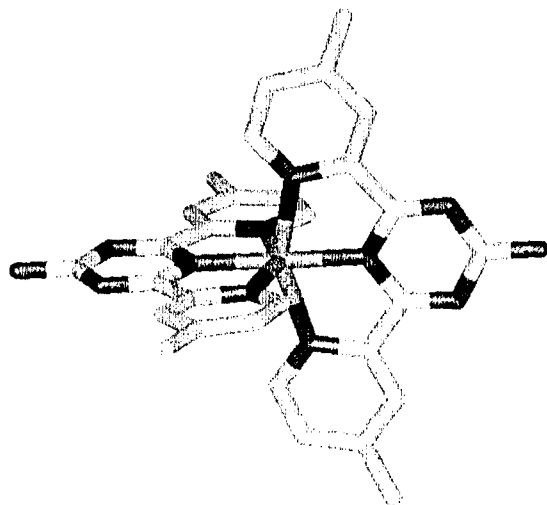
Neodymium and Lead Complex Structures.



Neodymium Complex

The main ligand was changed slightly, by substitution at the four position on the pyridyl rings.

This should produce a better ligand, by analogy with pyridine and 4-methyl pyridine.



Lead Complex

Key Features of Both Structures.

- The neodymium structure is isomorphous with that of the previous ligand.
- The lead complex is unusual as it contains two ligands and no other coordinating species. The coordination polyhedra is that of a distorted octahedron.

Conclusion

The structures for the majority of the lanthanide complexes have been determined and there is a definite trend between the size of the metal ion and the structure adopted.

Several other, non-f block, elements have been investigated and their structures determined.

A second ligand has been compared with the previously determined ligand and the structure obtained is identical.

References

1. E. C. Constable. *Advances in Inorganic Chemistry*, 1986, 30, 69.
2. F. H. Case, *J. Am. Chem. Soc.*, 1959, 905.
3. P. Byers, G. Y. S. Chan, M. G. B. Drew, M. J. Hudson, *Polyhedron*, 1996, 15, 2845.

Acknowledgements

We are grateful for the financial support from the European Union Nuclear Fission Safety Programme Task 2 (Contract F12W-CT91-0112).

Support also came from the EPSRC and the University of Reading for funding for the Image-Plate system.

Appendix VIII

Travel Report

Department of Chemistry, University of Reading, UK

January 4 - March 31, 1998

Lena Spjuth

There is a close collaboration between the participants in the European contract (NEWPART FI41-CT-96-0010) and there is a continuous exchange of new extractants and personnel between the different participants.

At the University of Reading, new extractants are synthesised and the co-ordination chemistry of these new ligands is studied by crystallography and molecular modelling. I spent 3 months at the University of Reading to learn more about molecular modelling and to synthesise new extractants for actinide/lanthanide selective extraction.

The objective of the work was to study the influence of different malonamide structures on the metal extraction. It has earlier been shown that a low basicity of a ligand results in a good metal extraction and we therefore wanted to investigate whether the basicity could be accurately calculated using a quantum chemical approach. *Ab initio* calculations with the Gaussian 94 software were used.

We investigated if any calculated parameter (charge density, dipolemoment, different energies etc.) could be related to the experimental extraction ability. We found a good agreement between calculated gas-phase basicity (ΔG for the protonation reaction) and experimentally determined basicities. The ligand with the lowest basicity also showed the highest metal extraction, which was expected.

After calculating the basicities of several new malonamide structures we chose one of the new structures with low basicity which we thought had potential to give an enhanced metal extraction compared to previously studied ligands. This molecule was synthesised and experimental studies at Chalmers showed it to be a good extractant and the experimental basicity was as low as expected from the calculations.

Basicity calculations of new malonamides are under progress and will help to verify the correlation between calculated and experimental basicity and between basicity and metal extraction.